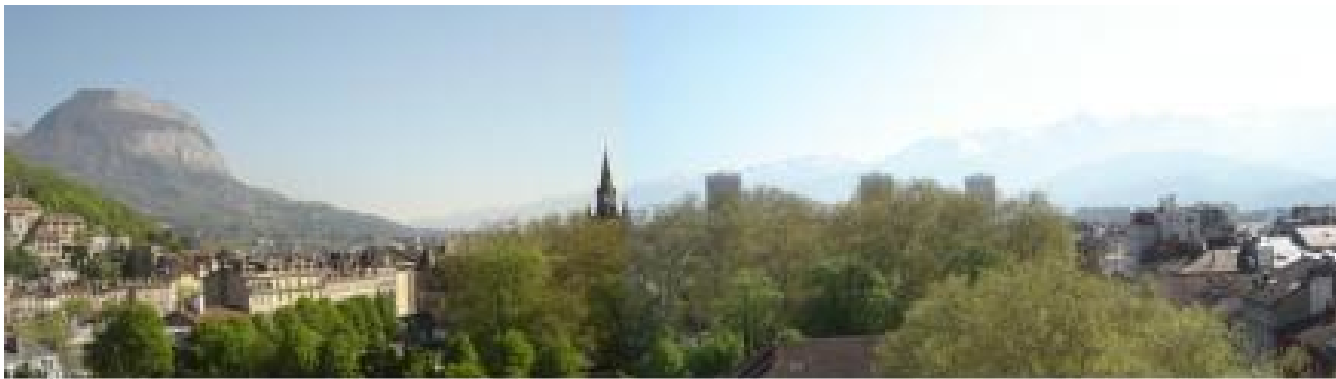


# Mise au point de la calorimétrie au Run II de l'expérience DØ et mesure de la masse du boson W

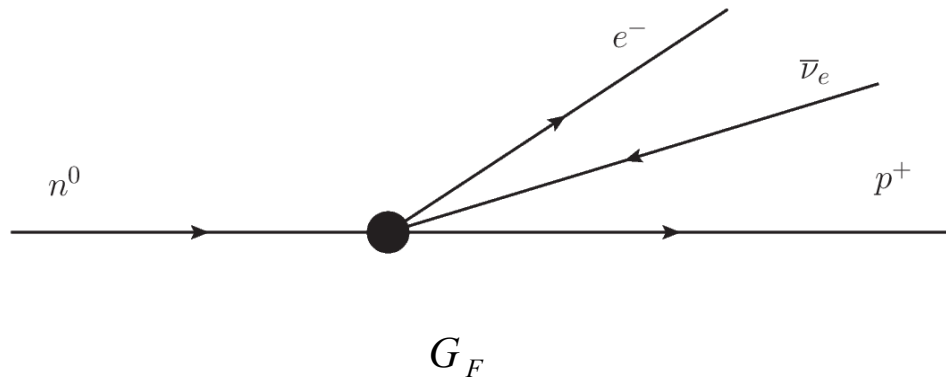
**Jan Stark**

Laboratoire de Physique Subatomique et de Cosmologie  
Grenoble, France



Soutenance HDR, Grenoble, 19 février 2013

# Weak interaction: some history



$\beta$  decay appeared to violate energy conservation  
(Chadwick, 1914)

Neutrino hypothesis  
(Pauli, 1930)

First theory of weak interaction: contact interaction  
(Fermi, 1935)

$SU(2) \times U(1)$  gauge theory, unified “electroweak interaction”  
predicts weak force mediated by heavy particles: W and Z bosons  
(Glashow, Weinberg, Salam, 1960s)

Discovery of the W and Z bosons  
(At CERN Sp $\bar{p}$ S collider, 1983)

$$M_W = \sqrt{\frac{\pi \alpha}{\sqrt{2} G_F}} \frac{1}{\sin \theta_W}$$

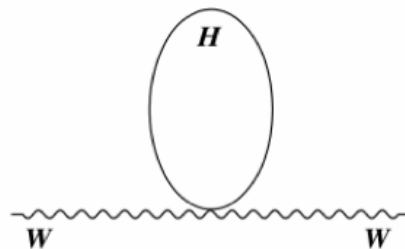
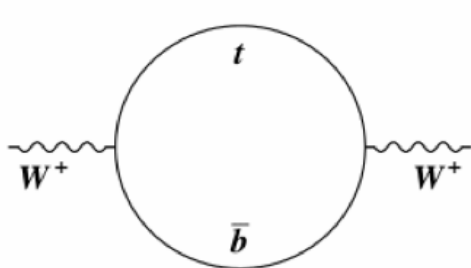
$$\sin^2 \theta_W = 1 - (M_W / M_Z)^2$$

# W boson mass

Today's measurements are precise enough to **test the electroweak theory at the loop level**. At higher orders (including loop diagrams), the equation from the previous slide needs to be modified:

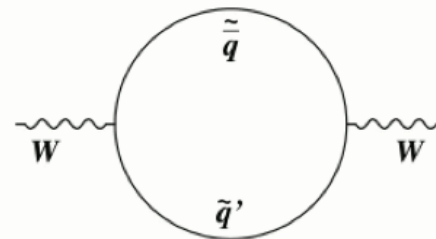
$$M_W = \sqrt{\frac{\pi \alpha}{\sqrt{2} G_F} \frac{1}{\sin \theta_W \sqrt{1 - \Delta r}}}$$

**Radiative corrections ( $\Delta r$ )** depend on  $M_t$  as  $\sim M_t^2$  and on  $M_H$  as  $\sim \log M_H$ . They include diagrams like these:

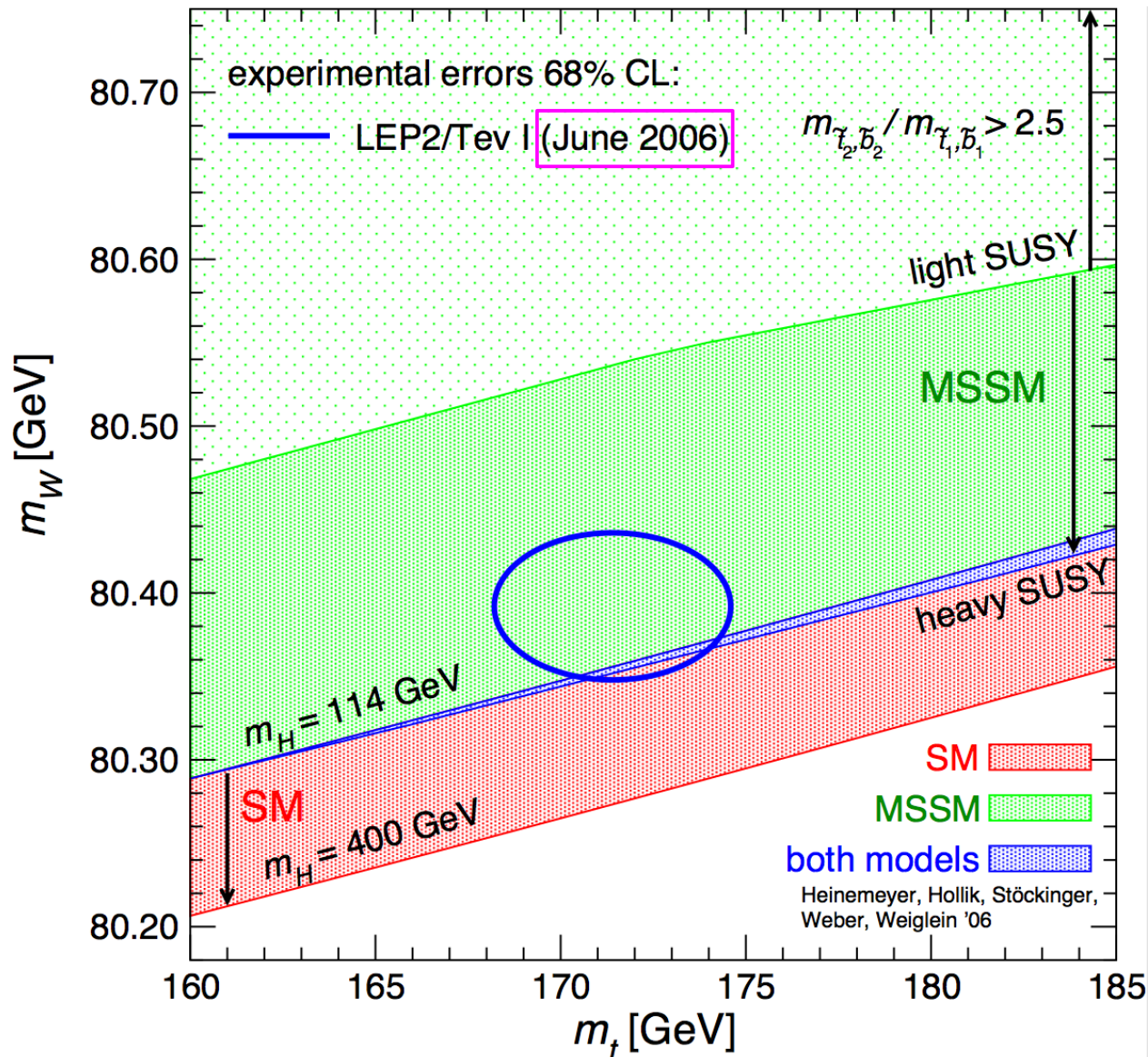


Precise measurements of  $M_W$  and  $M_t$  constrain SM Higgs mass.

Additional contributions to  $\Delta r$  arise in various extensions to the Standard Model, **e.g. in SUSY**:



# Motivation



For equal contribution to the Higgs mass uncertainty need:

$$\Delta m_W \approx 0.006 \Delta m_t.$$

Current (2013) Tevatron average:

$$\Delta m_t = 0.94 \text{ GeV} \quad (\text{arXiv:1207.1069})$$

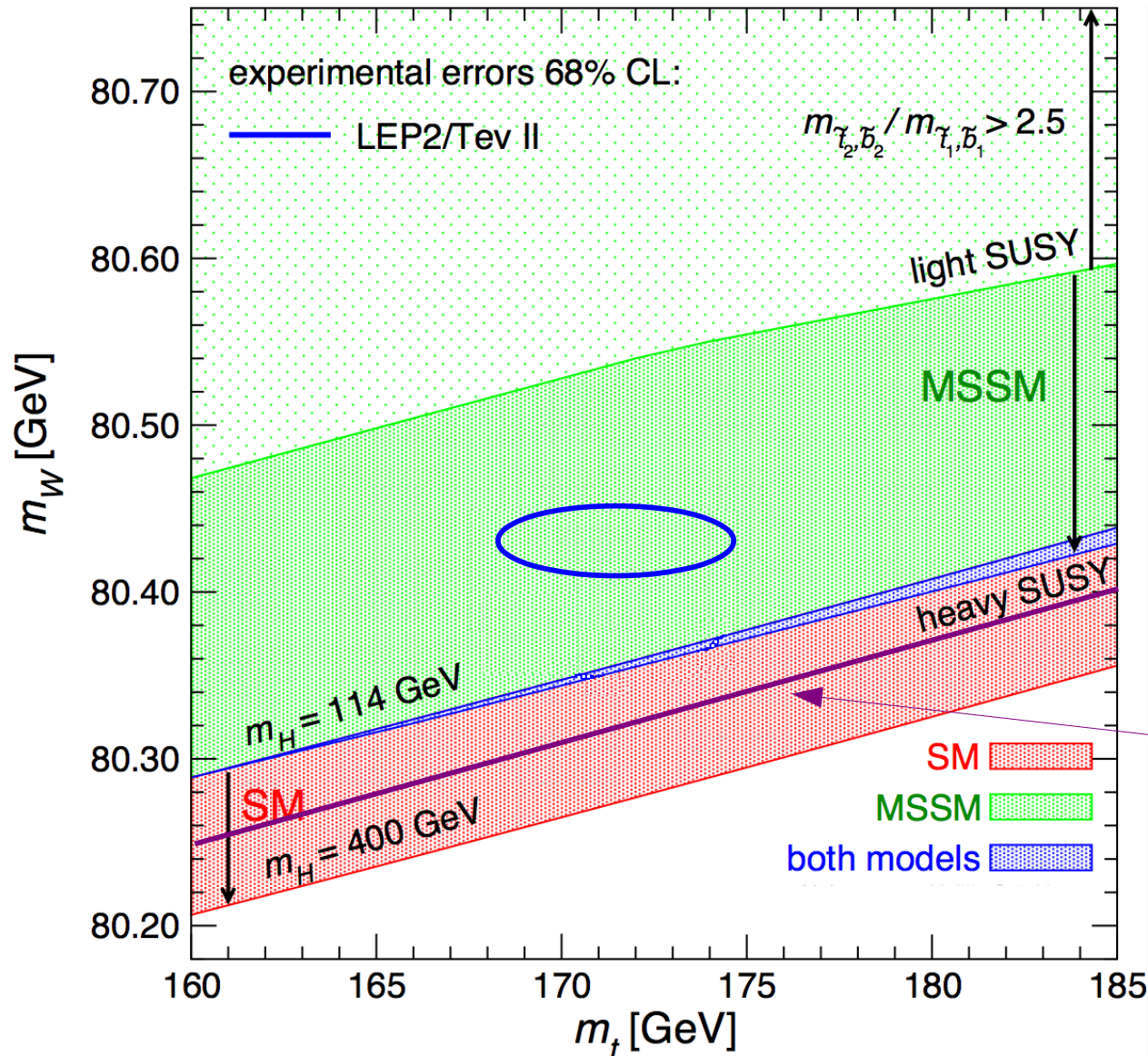
$$\Rightarrow \text{would need: } \Delta m_W = 5 \text{ MeV}$$

$$\text{Before Run II had: } \Delta m_W = 30 \text{ MeV}$$

At this point, *i.e.* after all the precise top mass measurements from the Tevatron, the limiting factor here is  $\Delta m_W$ , not  $\Delta m_t$ .



# At the start of Run II: a possible scenario for 2012

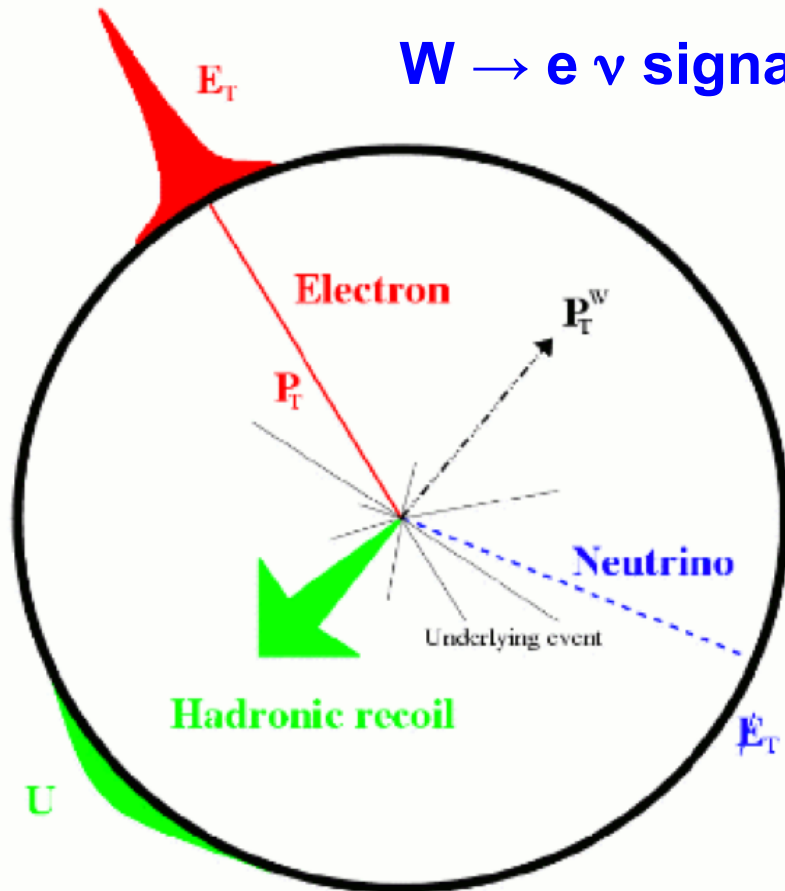


Hypothetical

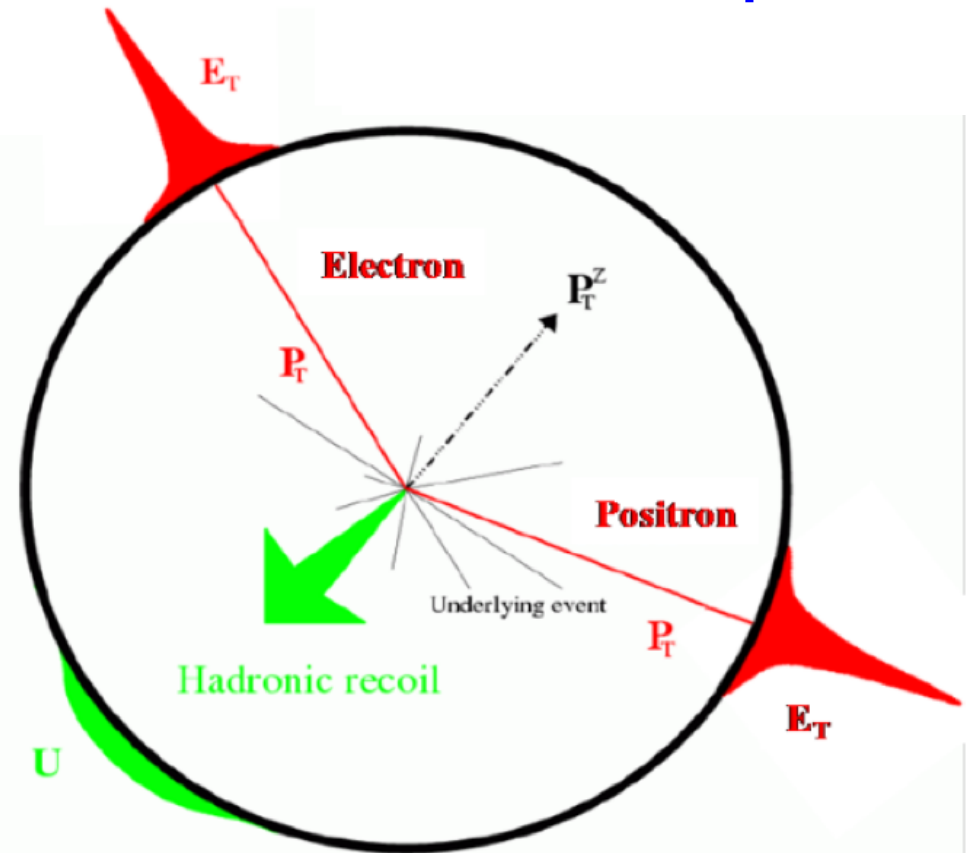
Direct observation  
at LHC and/or Tevatron

# W mass: measurement method

$W \rightarrow e \nu$  signal



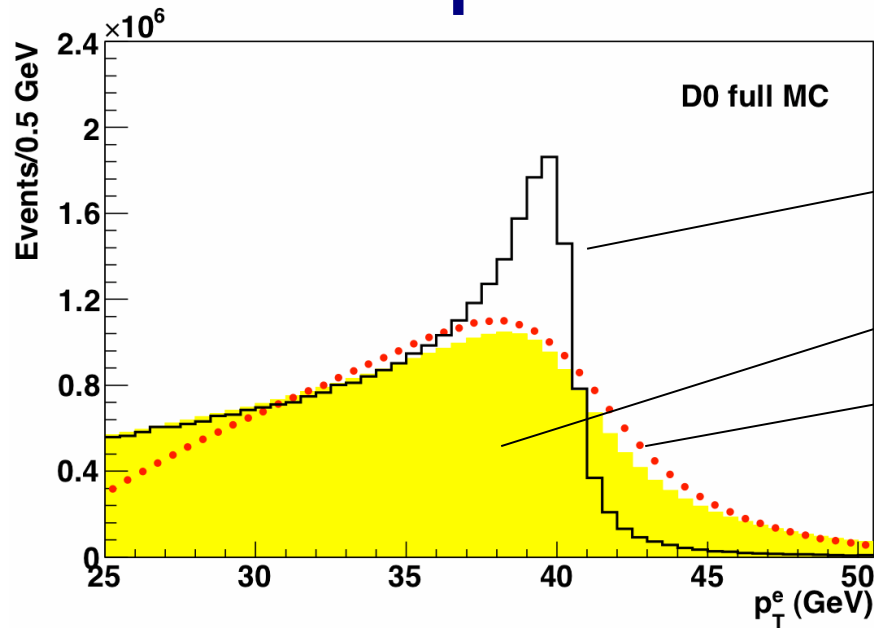
$Z \rightarrow e e$  events provide critical control sample



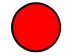


In a nutshell: measure two objects in the detector:

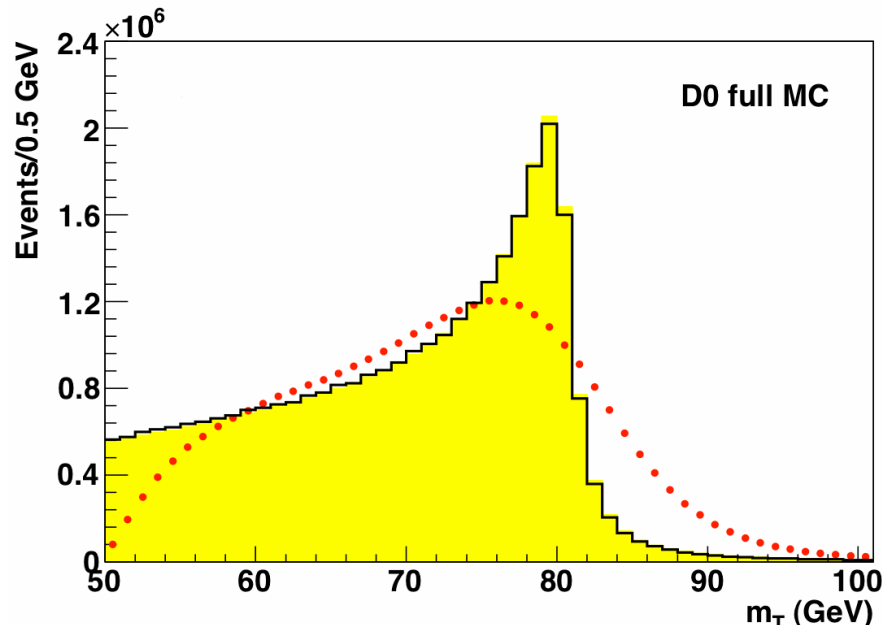
- Lepton (in our case an electron), need energy measurement with 0.1 per-mil precision (!!)
- Hadronic recoil, need ~1 % precision

# Experimental observables



 No  $p_T(W)$   
  $p_T(W)$  included  
 Detector Effects added

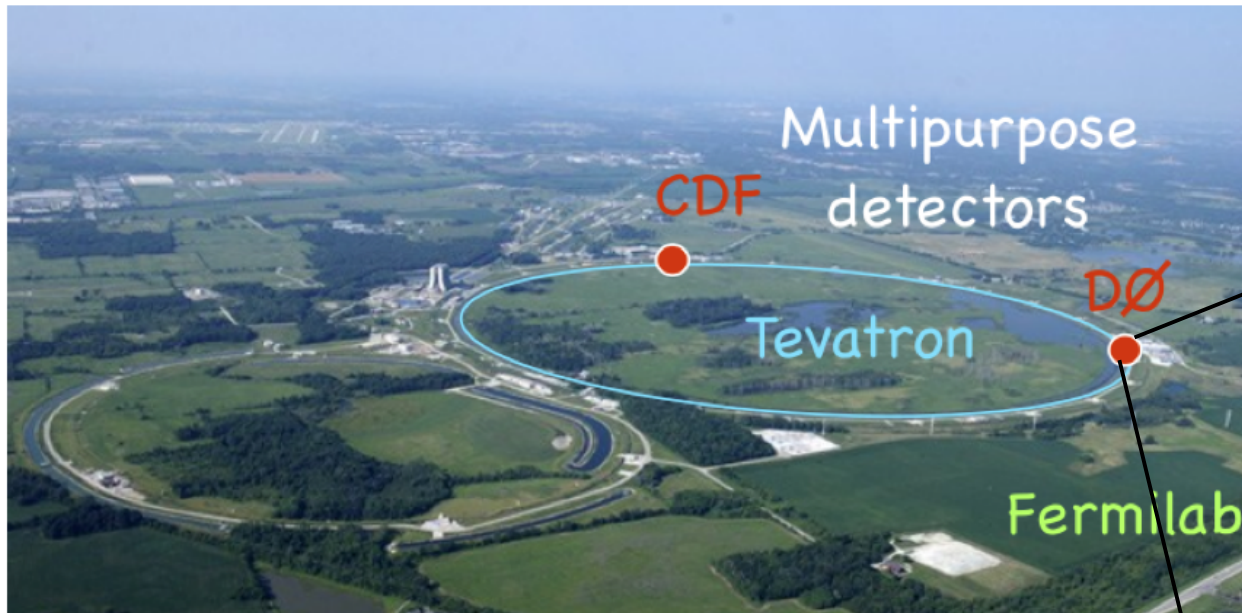
$p_T^e$  most affected by  $p_T(W)$



$$m_T = \sqrt{2 p_T^e E_T (1 - \cos \Delta \phi)}$$

$m_T$  most affected by measurement of recoil transverse momentum

# Fermilab

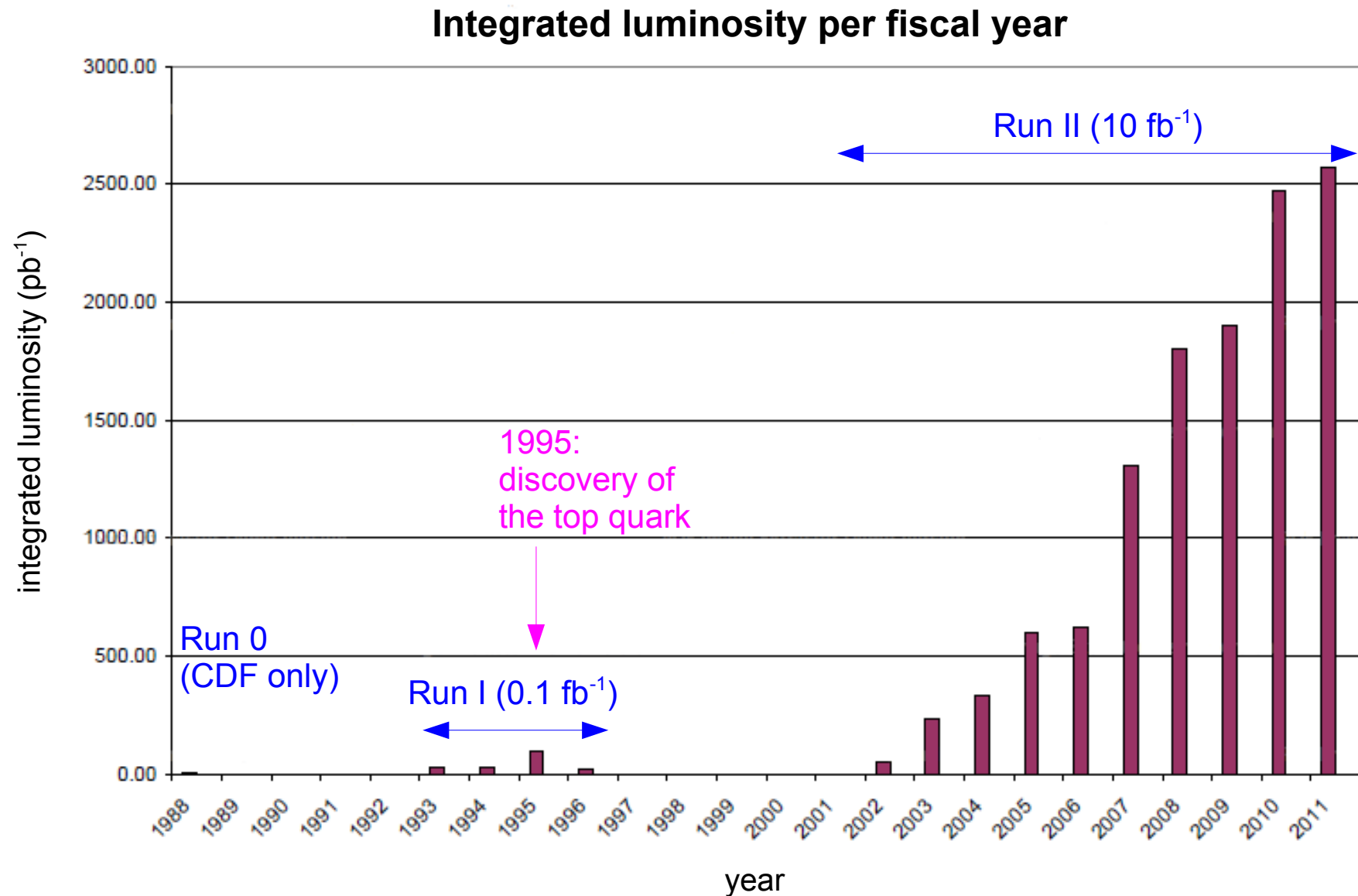


Tevatron collider at Fermilab near Chicago:  
proton-antiproton collisions at 2 TeV.

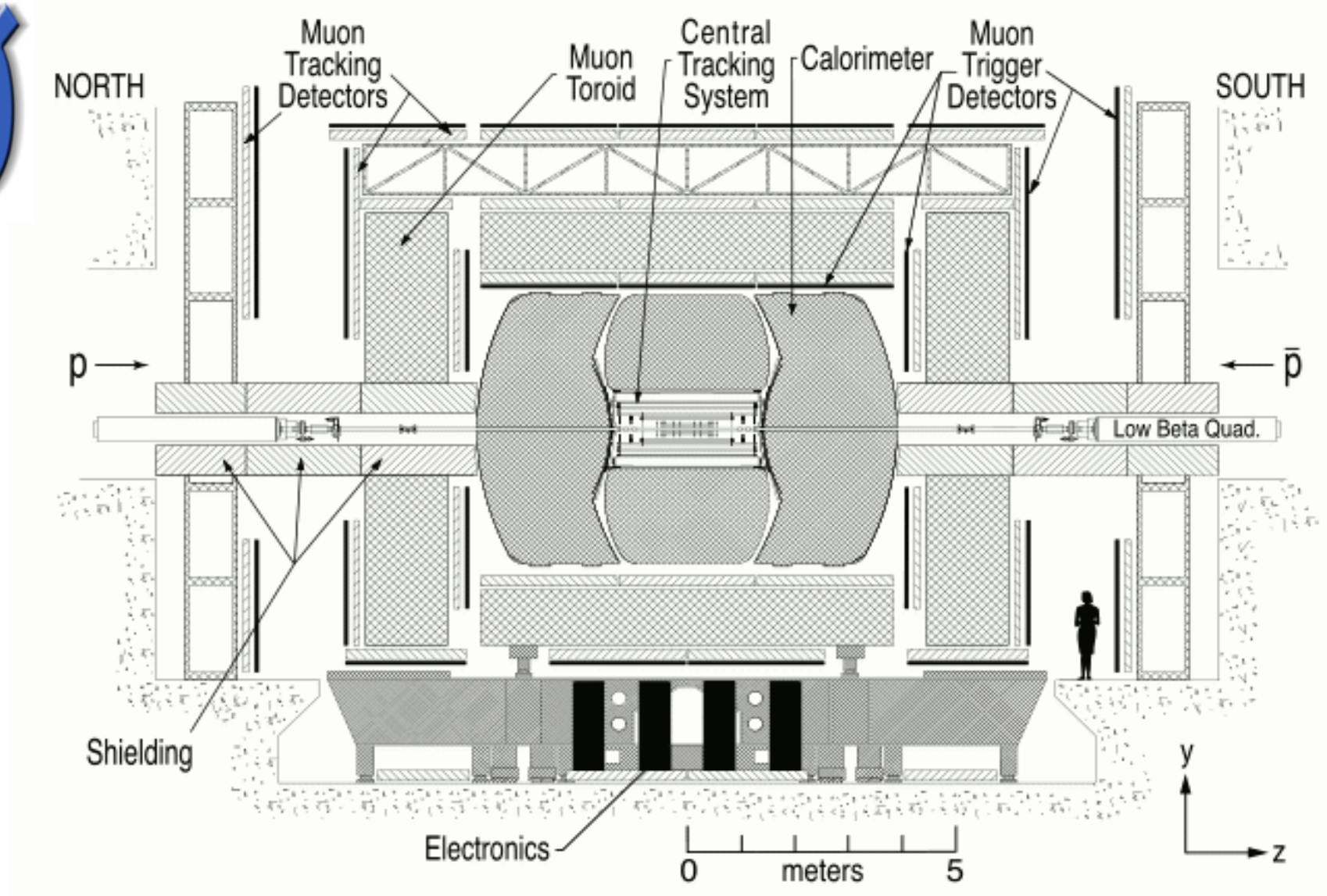




# Data taking periods



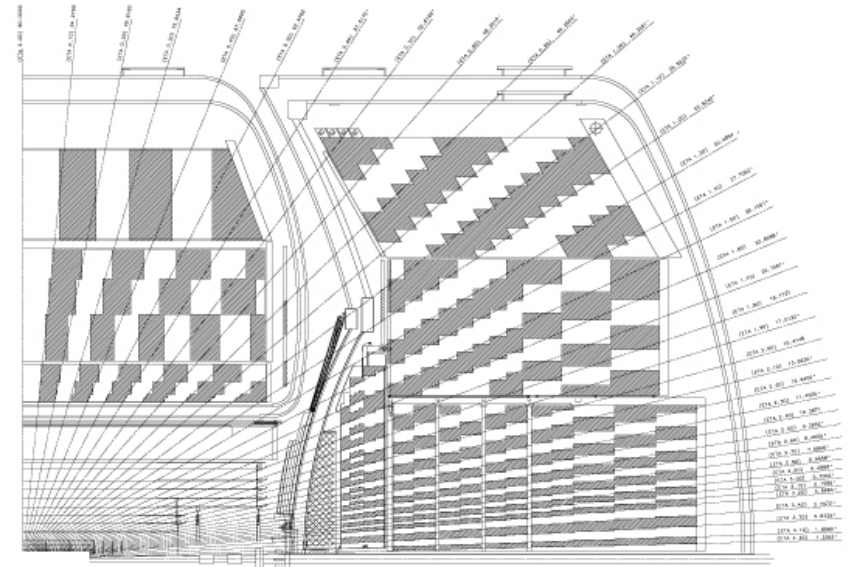
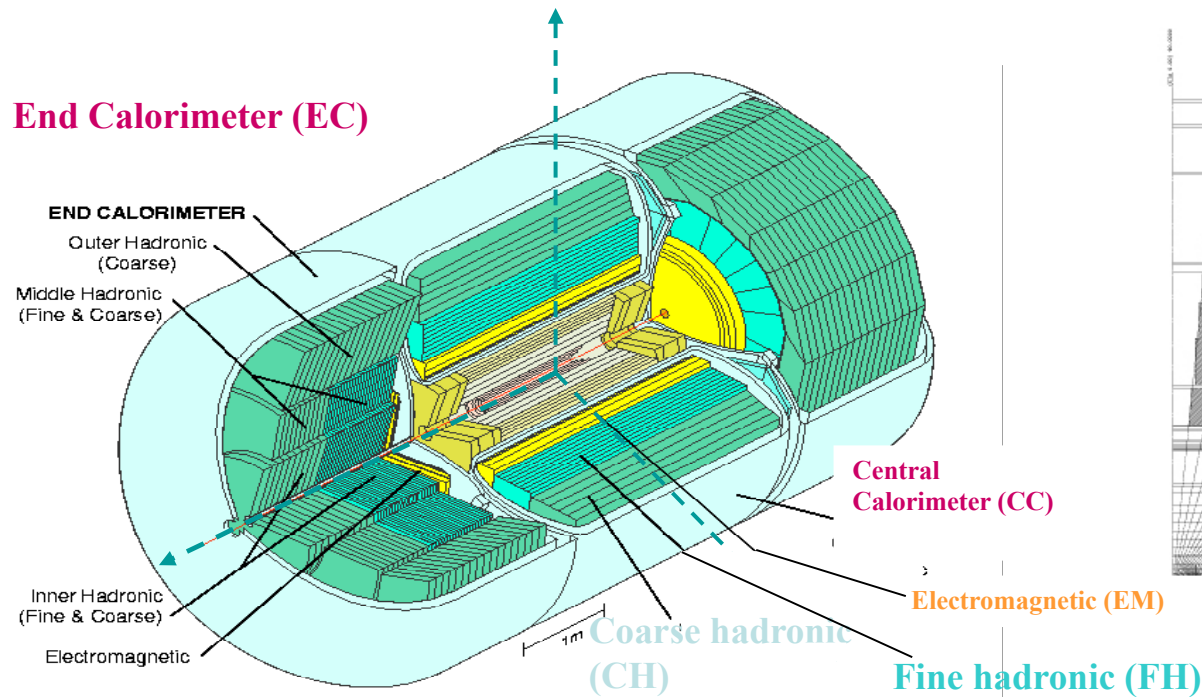
# The upgraded DØ detector





# Overview of the calorimeter

## End Calorimeter (EC)



46000 cells

50 dead channels

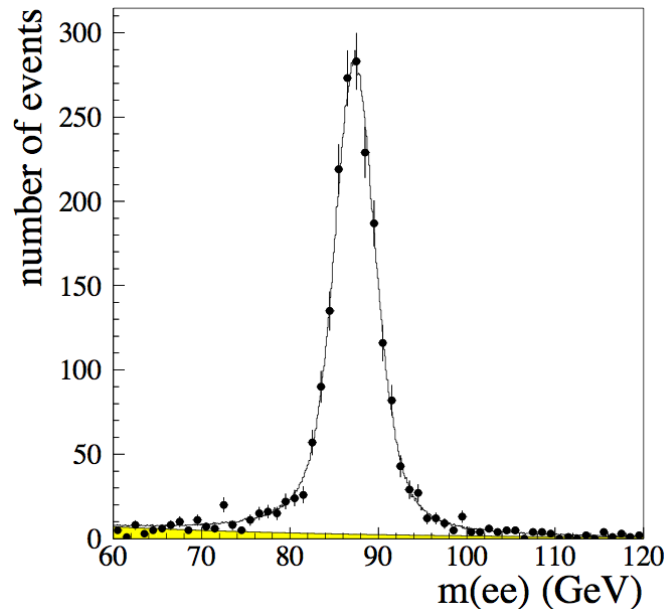
- Liquid argon active medium and (mostly) uranium absorber
- Hermetic with full coverage :  $|\eta| < 4$
- Segmentation (towers):  $\Delta\eta \times \Delta\phi = 0.1 \times 0.1$   
(0.05x0.05 in third EM layer, near shower maximum)

# Calorimeter performance: Run I vs. Run II

## Run I

constant term in electron

energy resolution:  $C = (1.15^{+0.27}_{-0.36}) \%$

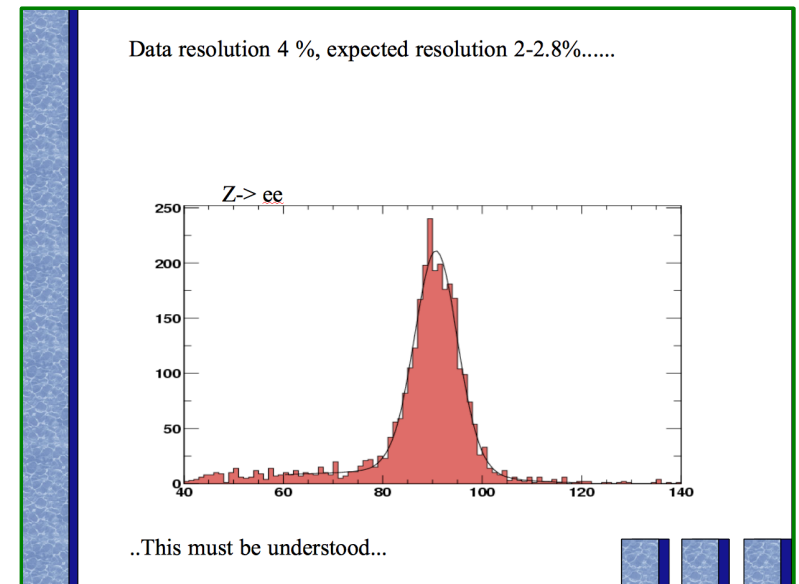


## Run II

J. Zhu, D0 note 4323 (2003):

$C = (3.73 \pm 0.28) \%$

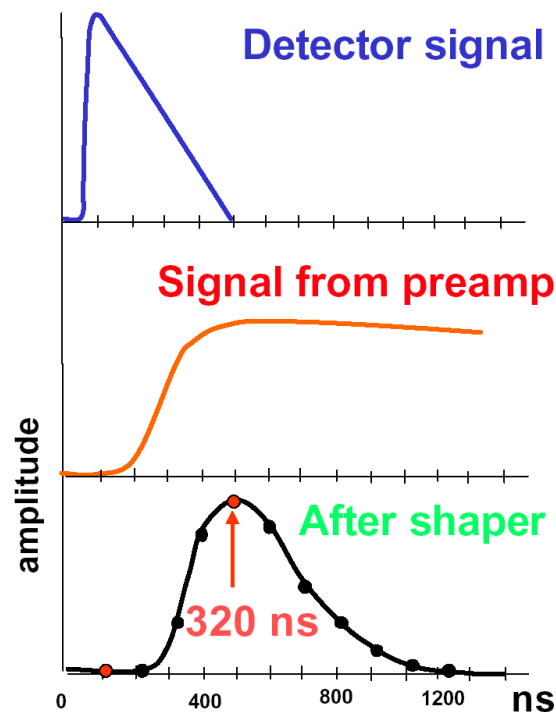
S. Söldner-Rembold, plenary talk at  
D0 Workshop in Beaune (summer 2003):



From the plenary talk of the convener of the  
Electroweak group at the same workshop:

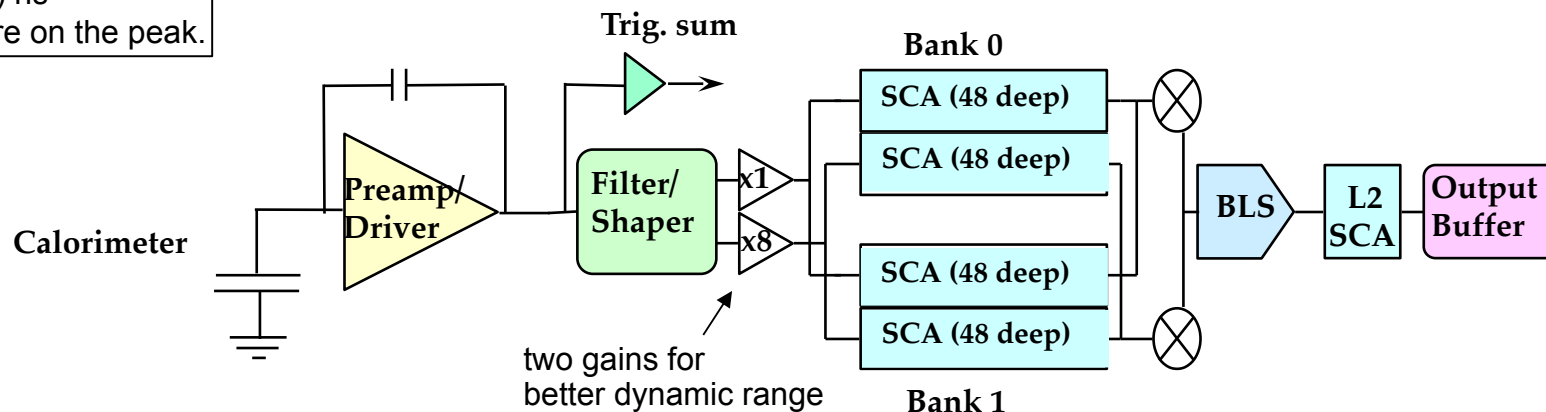
“With the current calorimeter performance  
we are NOT going to measure  
the W mass with DØ”

# New readout electronics

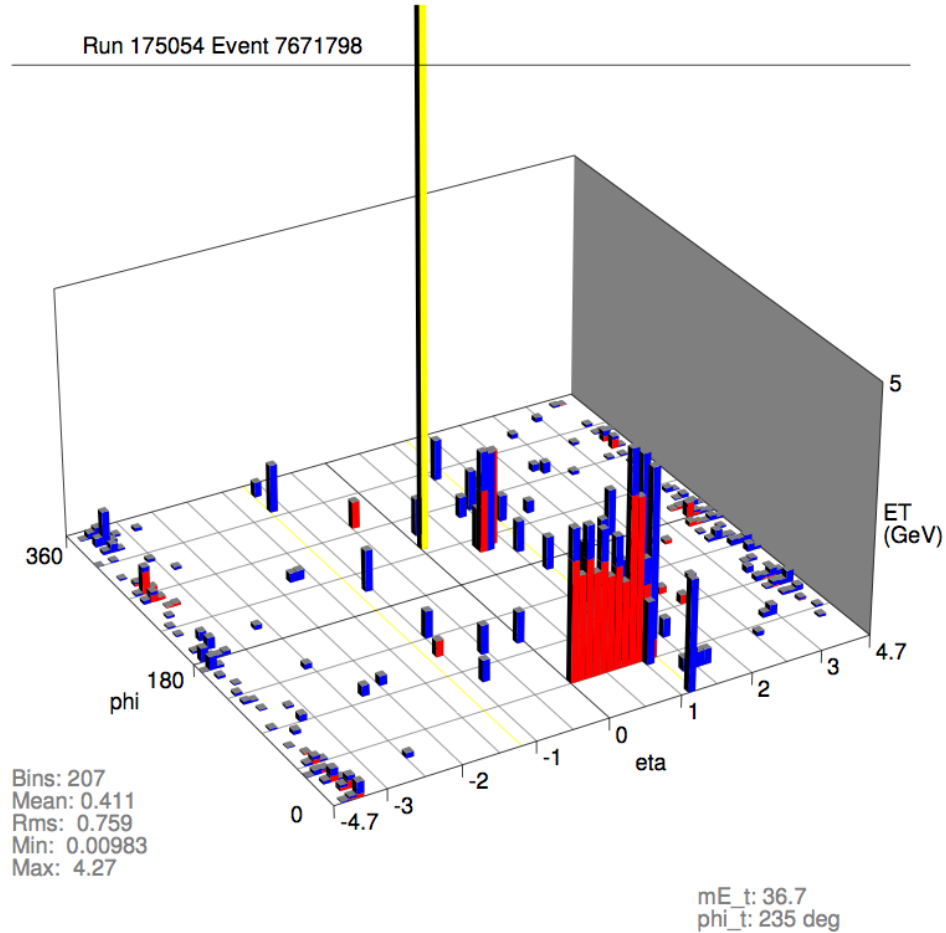


Have ability to sample and record the shaped signal also at  $(320 \pm 120)$  ns to make sure we are on the peak.

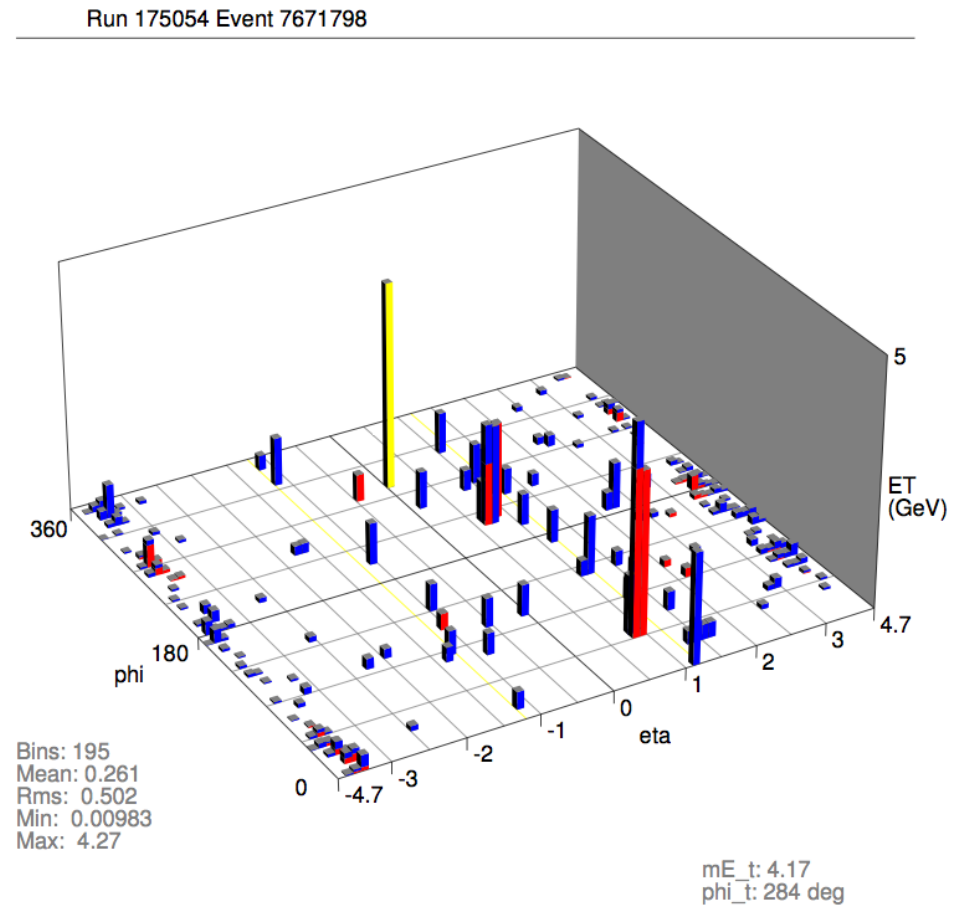
- Detector signal  $\sim 450$  ns long (bunch crossing time: 396 ns)
- Charge preamplifiers
- BLS (baseline subtraction) boards
  - short shaping of  $\sim 2/3$  of integrated signal
  - signal sampled and stored every 132 ns in analog buffers (SCA) waiting for L1 trigger
  - samples retrieved on L1 accept, then baseline subtraction to remove pile-up and low frequency noise
  - signal retrieved after L2 accept
- Digitisation



# “Energy sharing problem”



Before correction



After correction

# Gain calibration: strategy

## Factorise into two parts:

- calibration of the calorimeter electronics,
- calibration of the device itself.

## Electronics calibrated using pulsters.

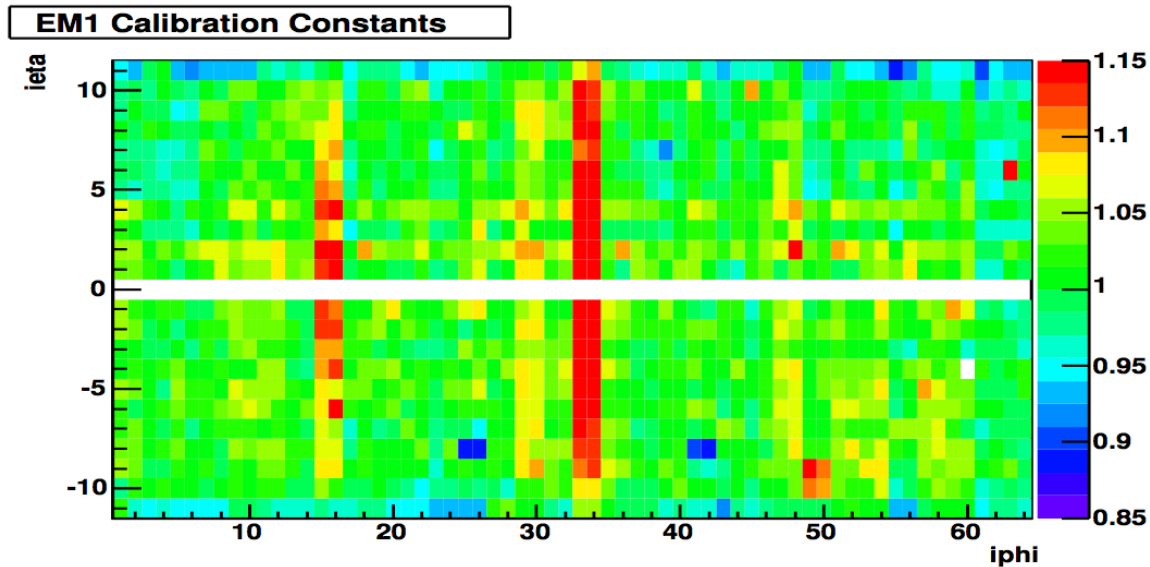
## Calibration of the device itself:

Determine **energy scale** (i.e. multiplicative correction factor), **ideally per cell**.

Use **phi intercalibration** to “beat down the number of degrees of freedom” as much as possible.

Use  $Z \rightarrow e^+ e^-$  to get access to the remaining degrees of freedom, as well as the absolute scale.

# Gain calibration: results and impact

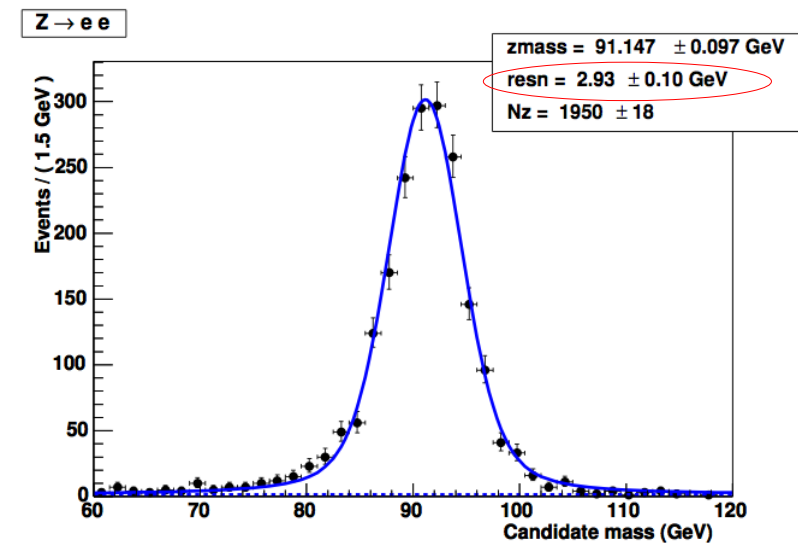
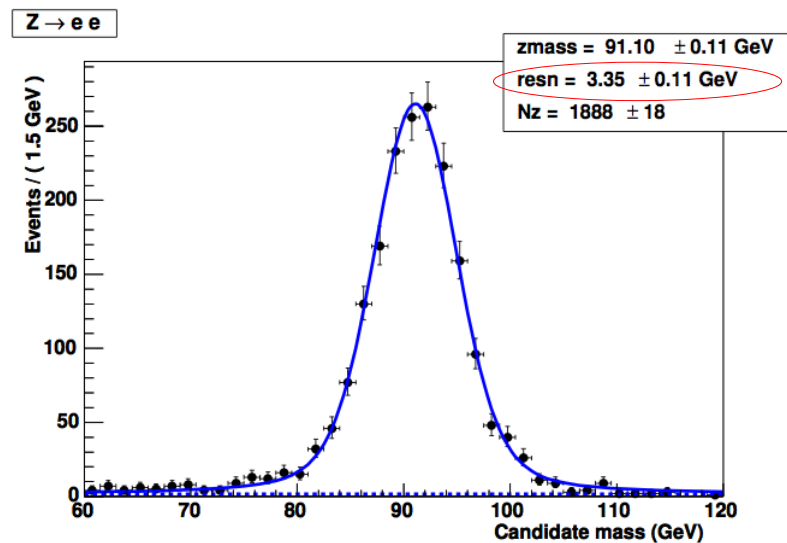


## Example of results:

intercalibration constants  
in first layer of CC-EM.

Same  $Z \rightarrow e e$  before  
and after calibration.

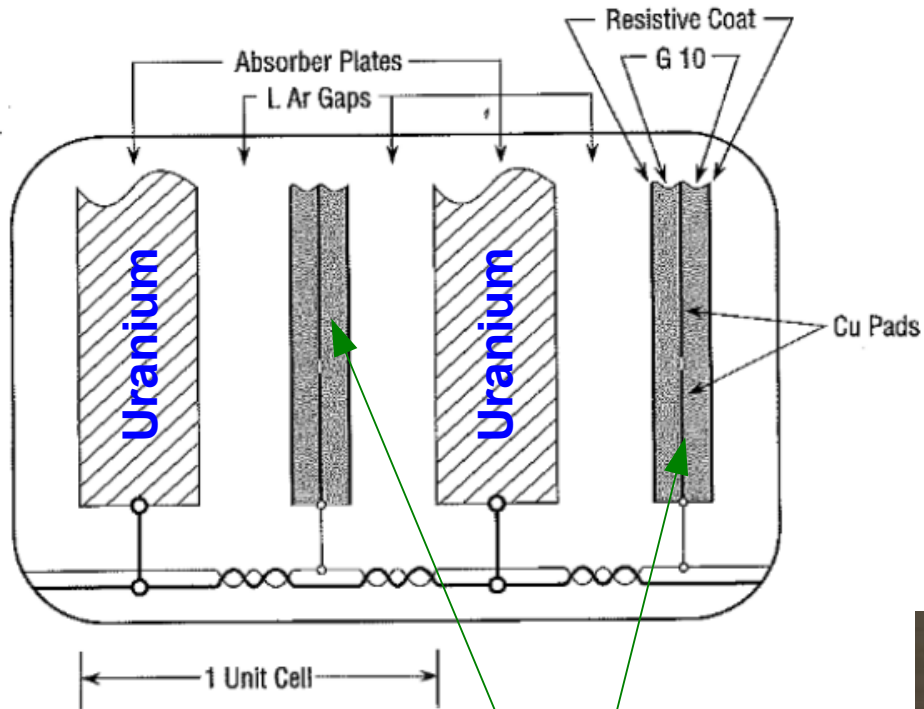
See improvement  
in mass resolution !





# Origin of large mis-calibrations

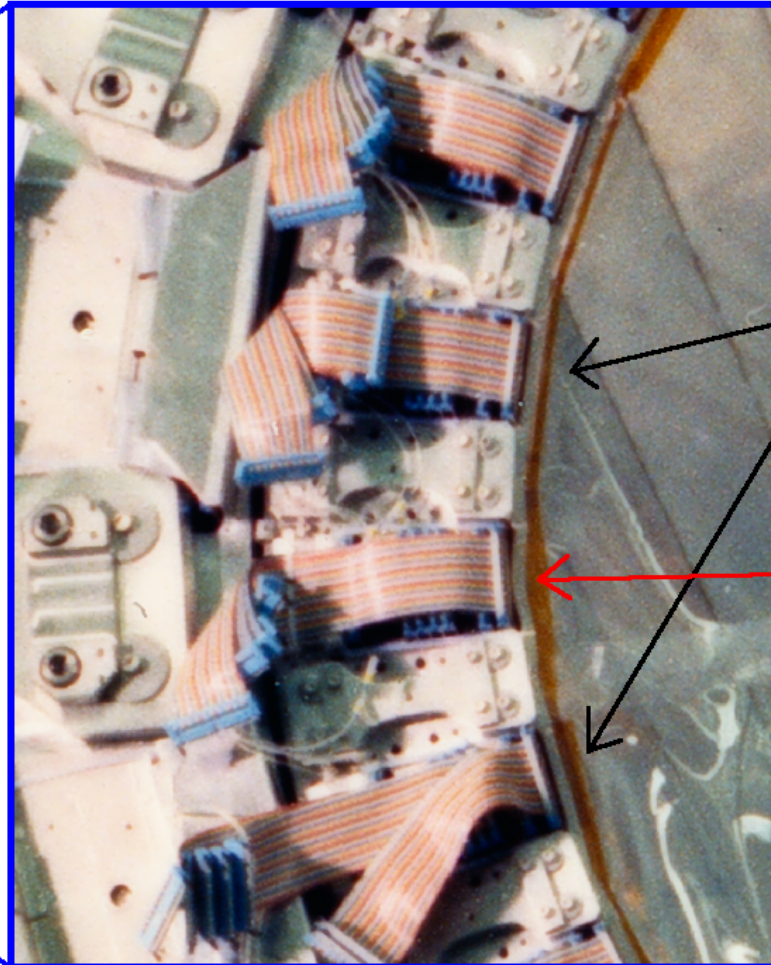
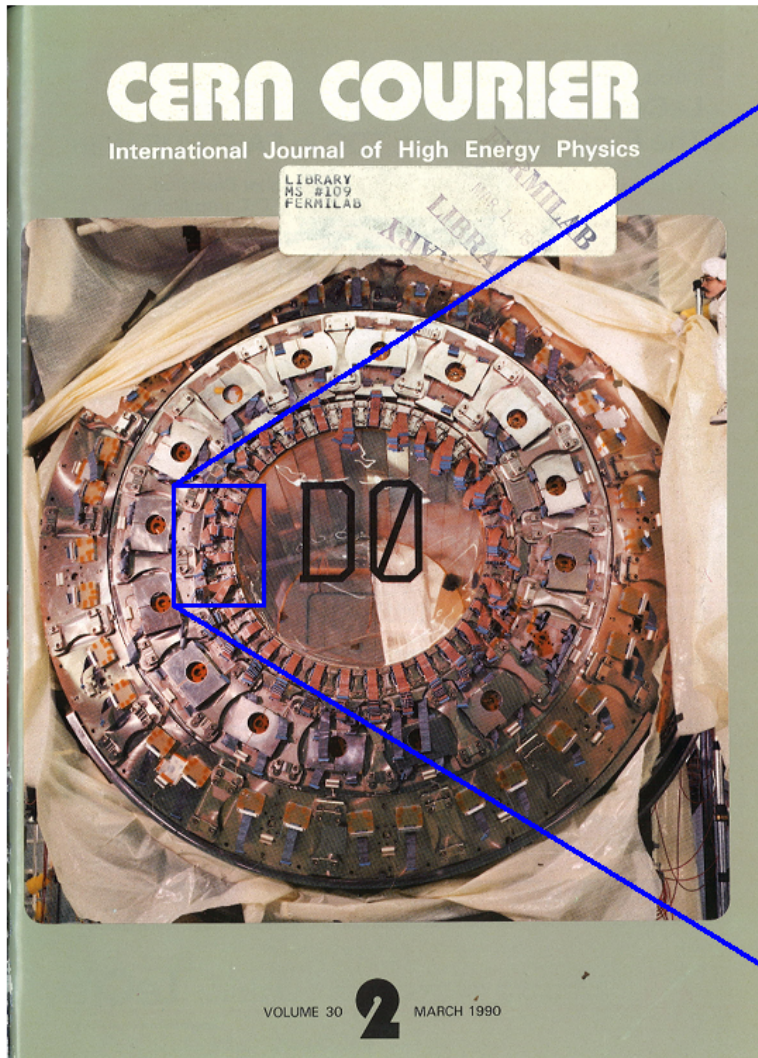
## Unit cell of the calorimeter readout:



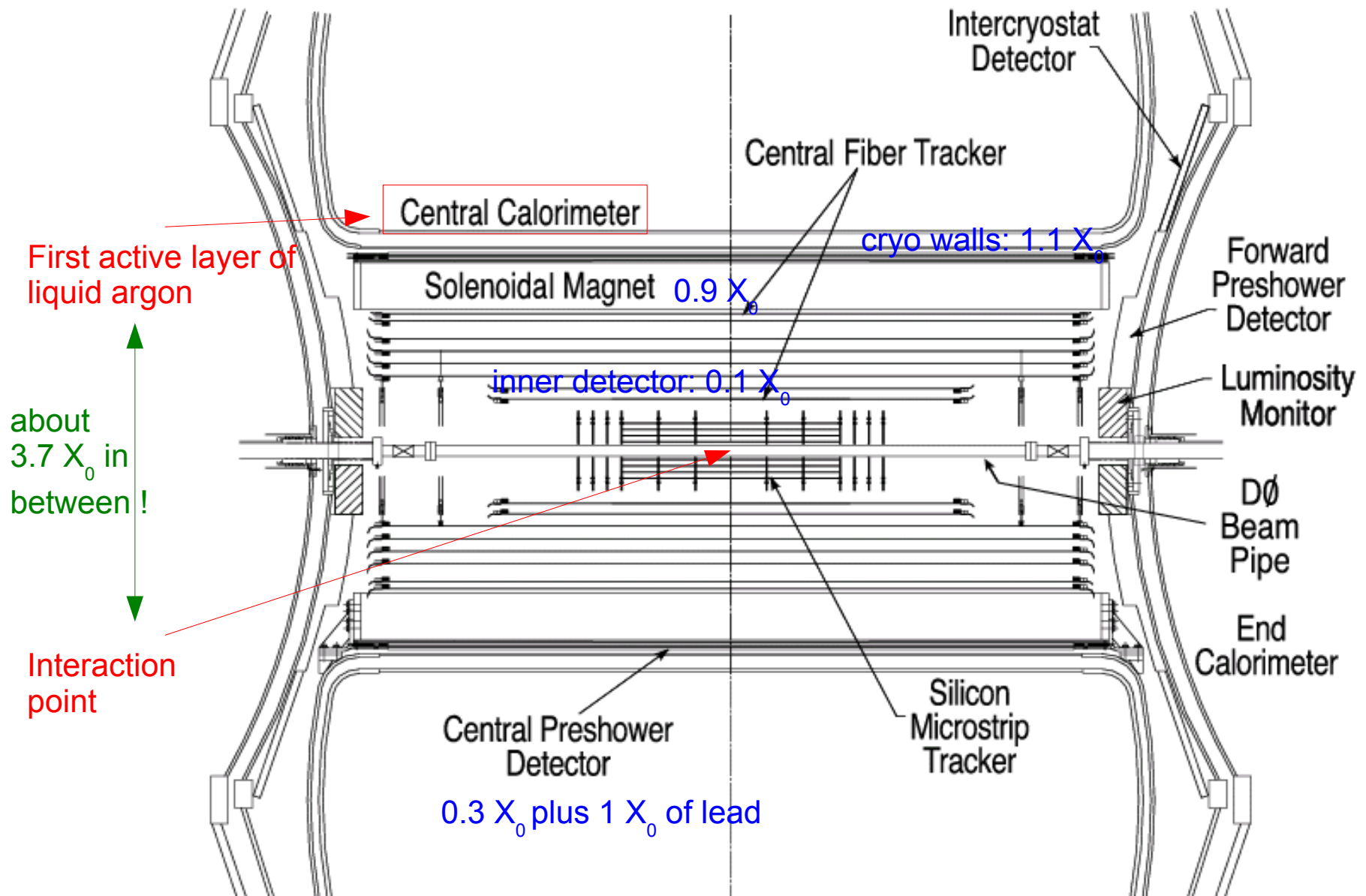
Signal board



# Origin of large “outliers”



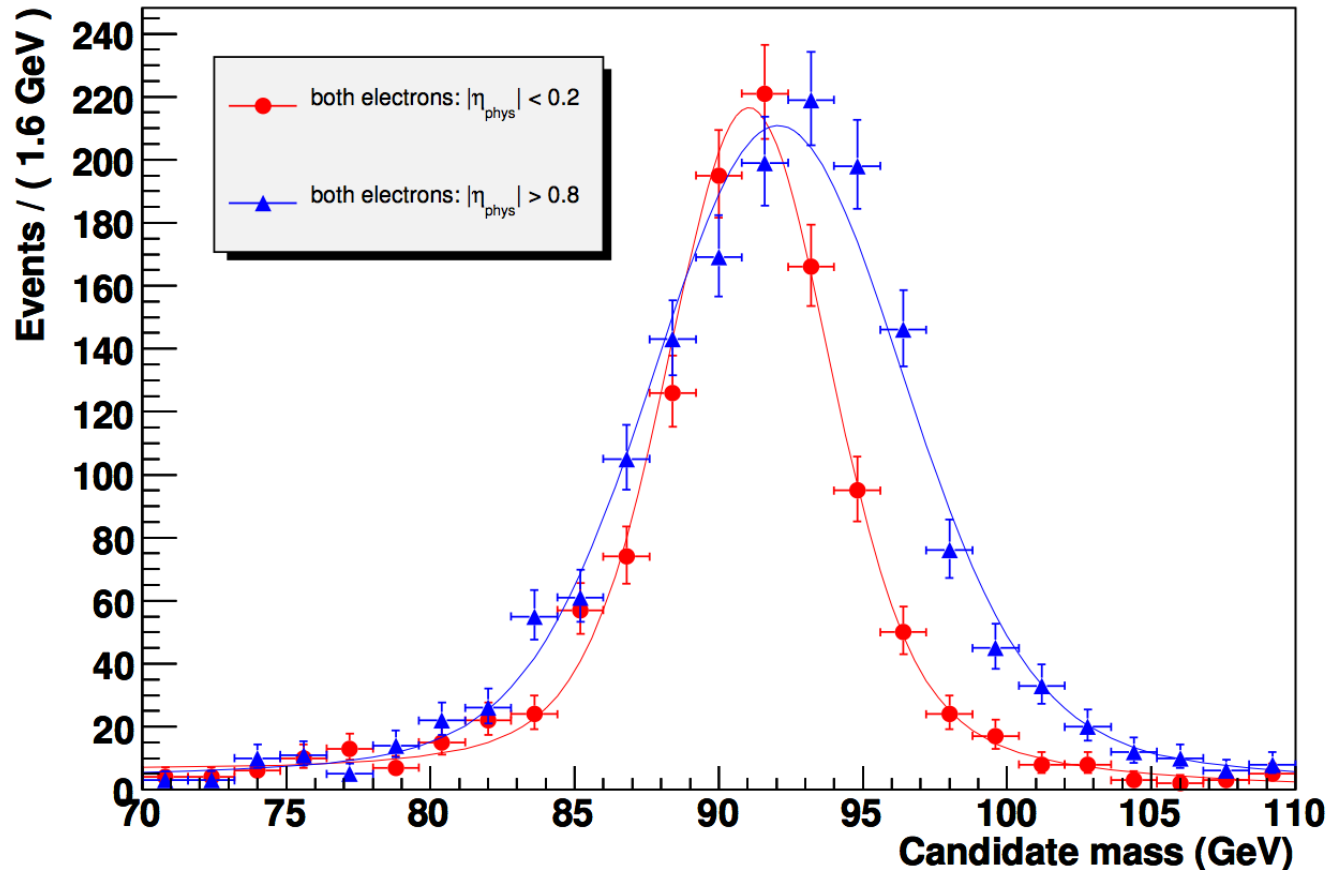
# Keep in mind: the CAL is not alone !





# Impact of uninstrumented material

$Z \rightarrow e e$  (both electrons in Central Cryostat)



**Two different subsets of CC-CC sample:**

- both electrons at  
~ normal incidence  
on dead material
- both electrons at  
very non-normal  
angle of incidence

Observations:

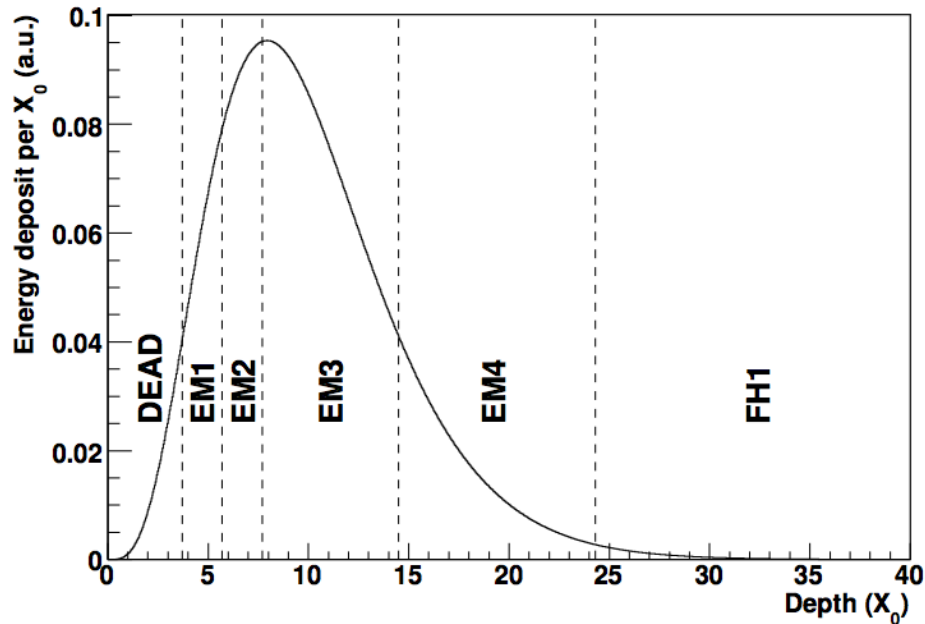
- The width of the two peaks is very different.
- The peak positions are not in the same place.

# How we sample showers in Run II

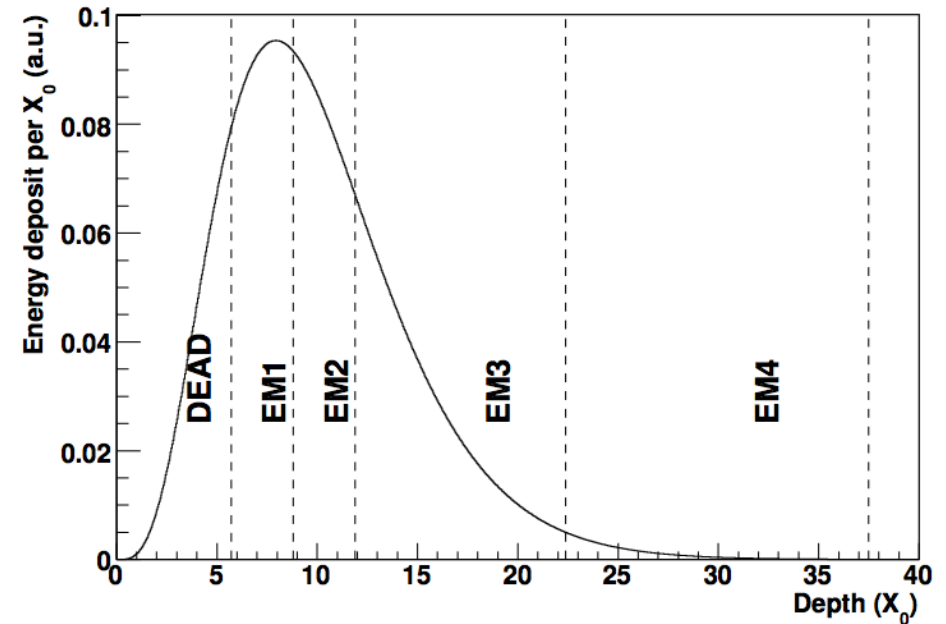
Average shower profile of an 45 GeV electron.

The positions of the readout sections of the D0 central calorimeter are indicated, for **two different angles of incidence**.

$\eta_{\text{phys}} = 0$



$\eta_{\text{phys}} = 1$



# Shower fluctuations !

On the previous slide, we have discussed the **average shower profile**.

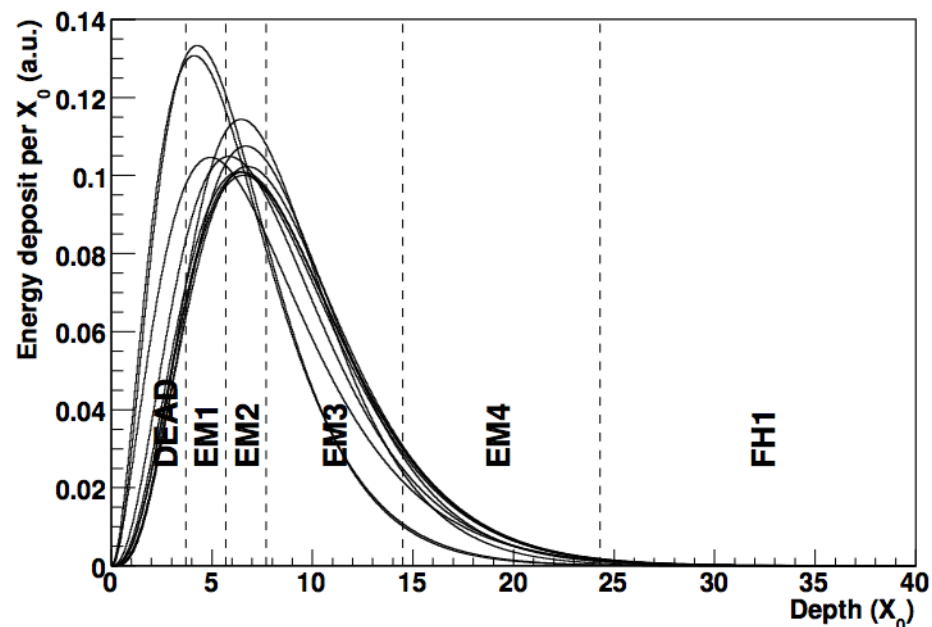
To illustrate the importance of **fluctuations**, we now show ten showers, generated using the GFlash parameterisation.

The fraction of energy lost in the dead region fluctuates from one shower to another.

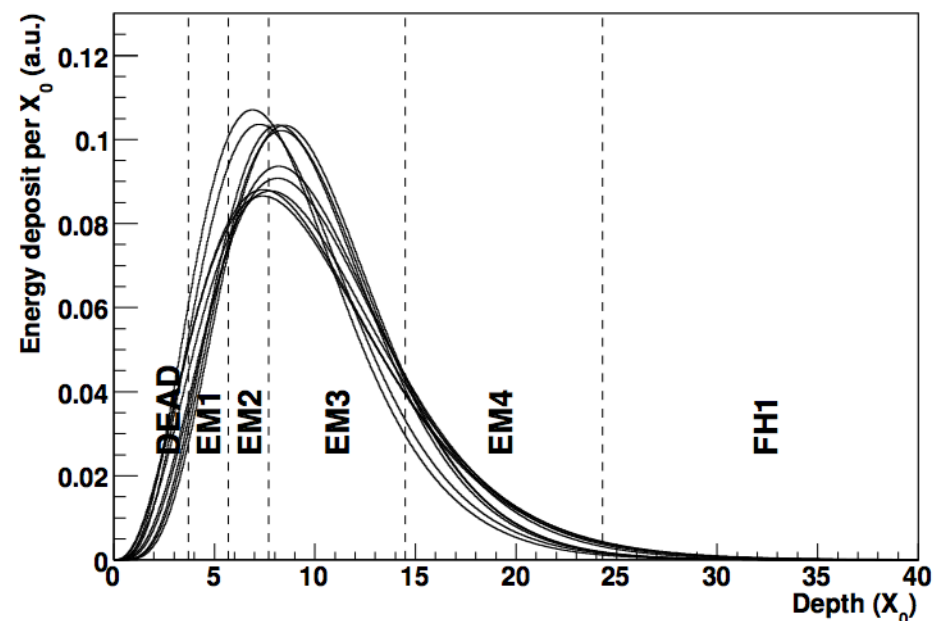
Fluctuations are larger at **low electron energy** than at **high energy**.

Fluctuations are larger at non-normal incidence than at normal incidence.

$E = 5 \text{ GeV}$        $\eta_{\text{phys}} = 0$



$E = 45 \text{ GeV}$        $\eta_{\text{phys}} = 0$

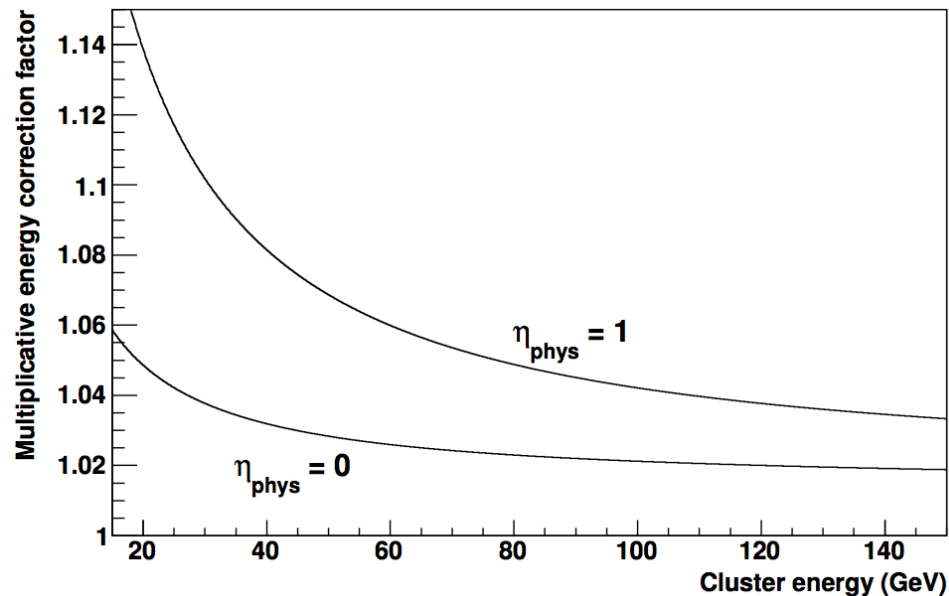




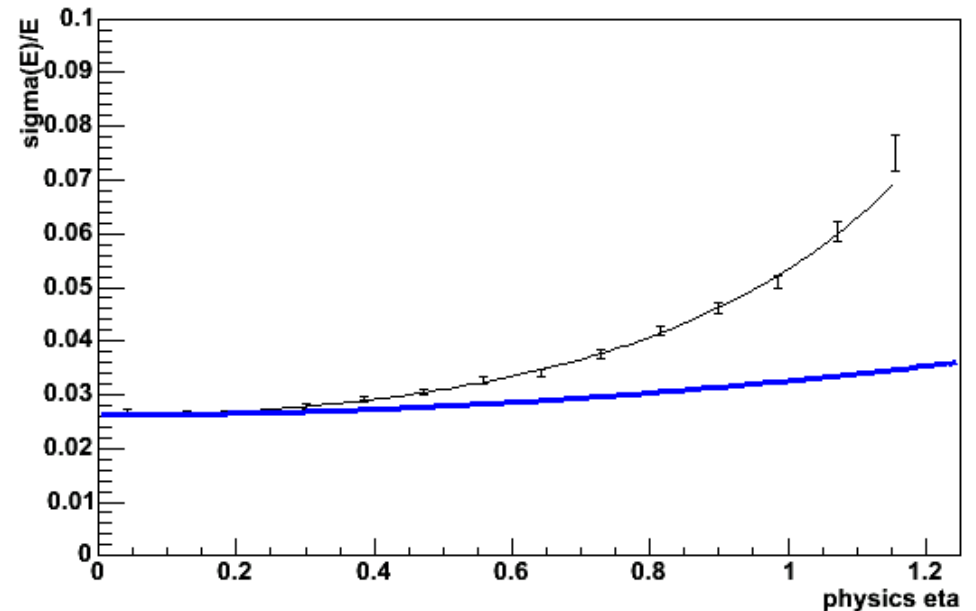
# Consequences

Correction factor:

reconstructed cluster energy  
→ electron energy

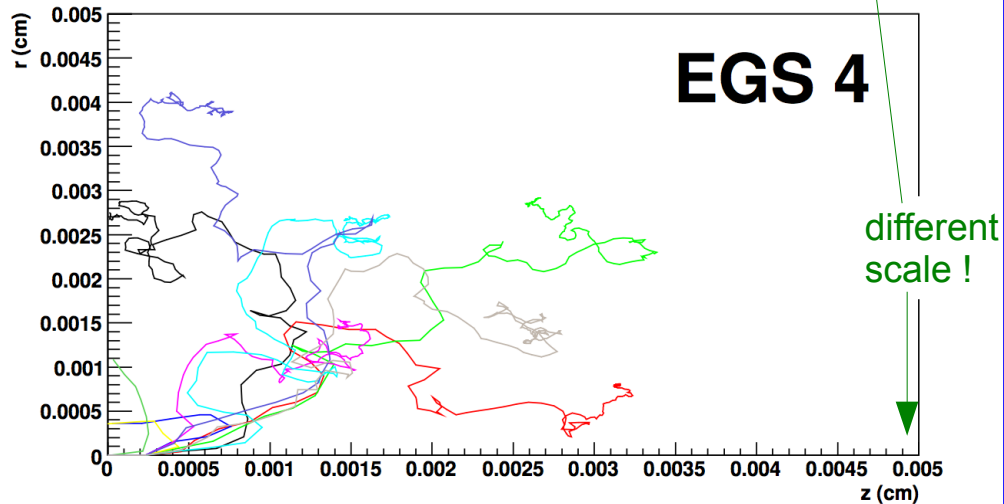
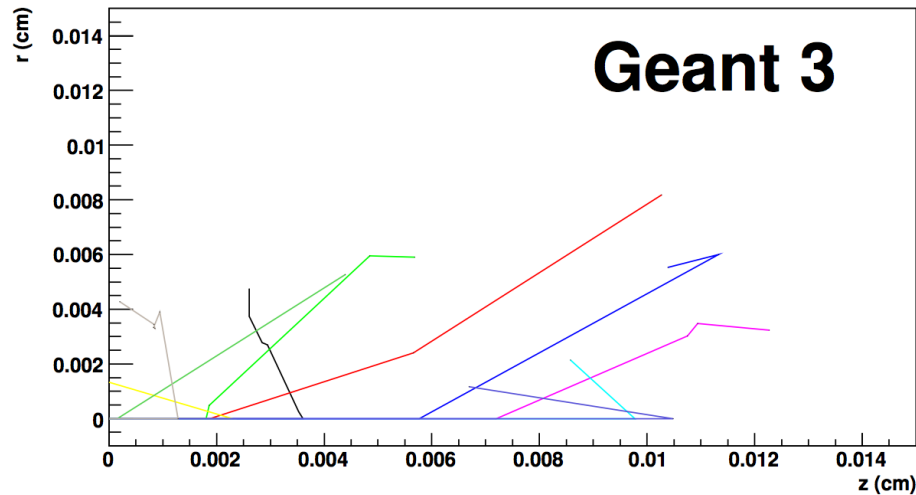


Fractional energy resolution  
as a function of angle of incidence  
(electrons with  $E = 45$  GeV)



Need precise first-principles simulations to determine the energy correction factors and a model of the sampling fluctuations.

# Geant 3

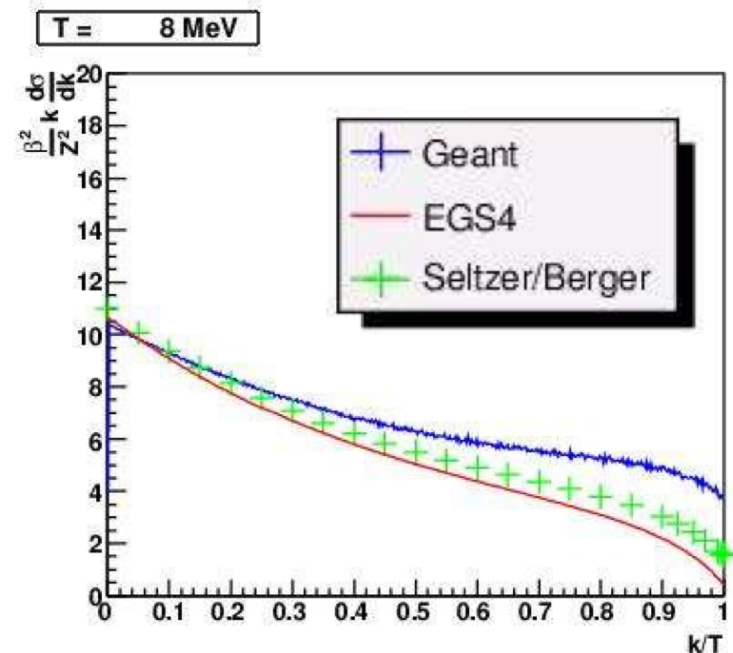


Simulated tracks of 400 keV electrons in uranium.

Identified various issues in Geant and the in the interface between D0 software and Geant.

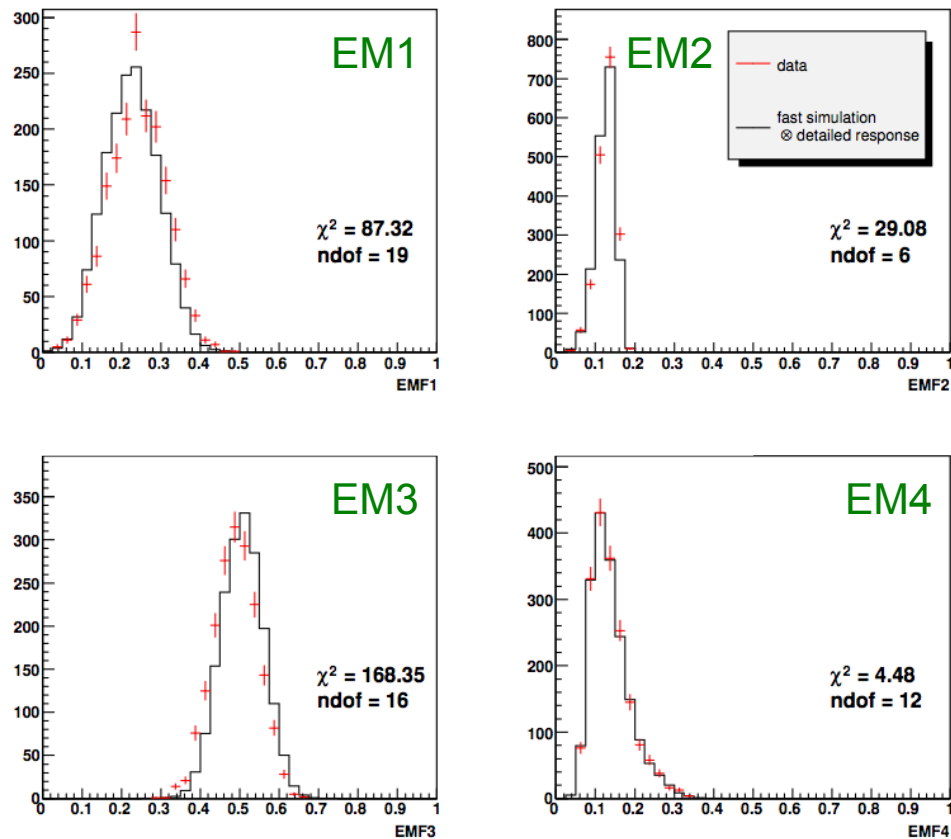
Key tool:  
comparisons between Geant 3 and EGS 4

Bremsstrahlung cross-section for electrons in uranium:

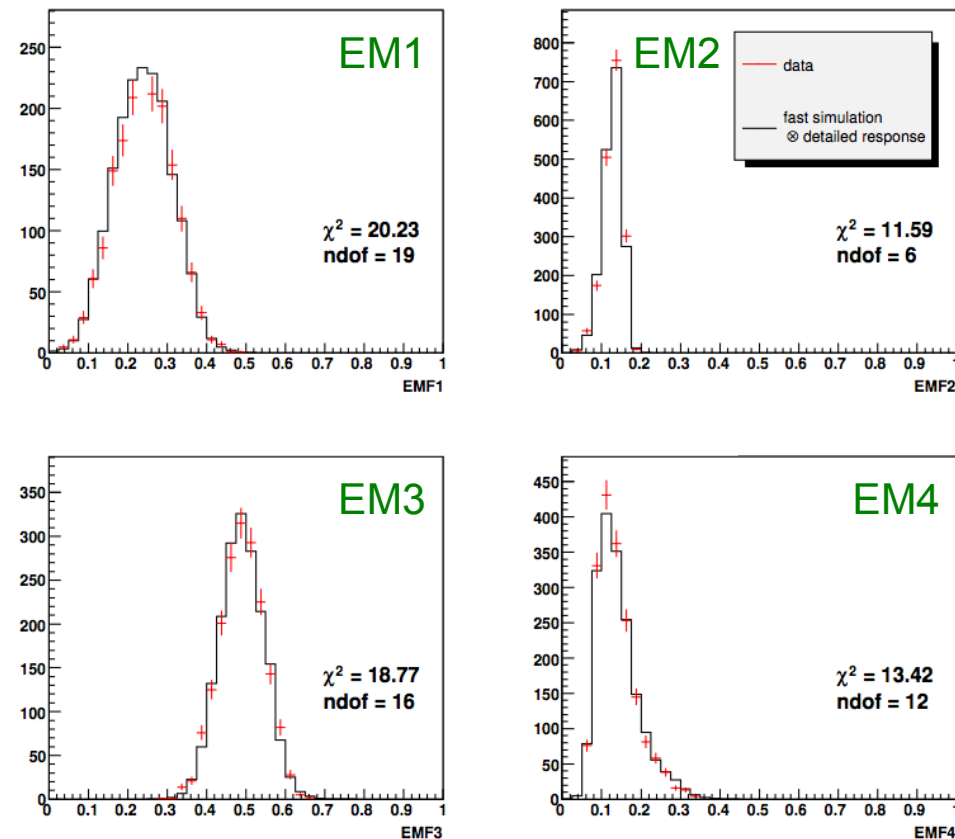


# Material tune

Before adjustment of material model



After adjustment



Conclusion: need to add  $(0.1633 \pm 0.0095) X_0$  of dead material on top of the “first-principles accounting” in the detailed simulation of the DØ detector.

# Calorimeter: stability of effective HV

## Unit cell of the calorimeter readout:

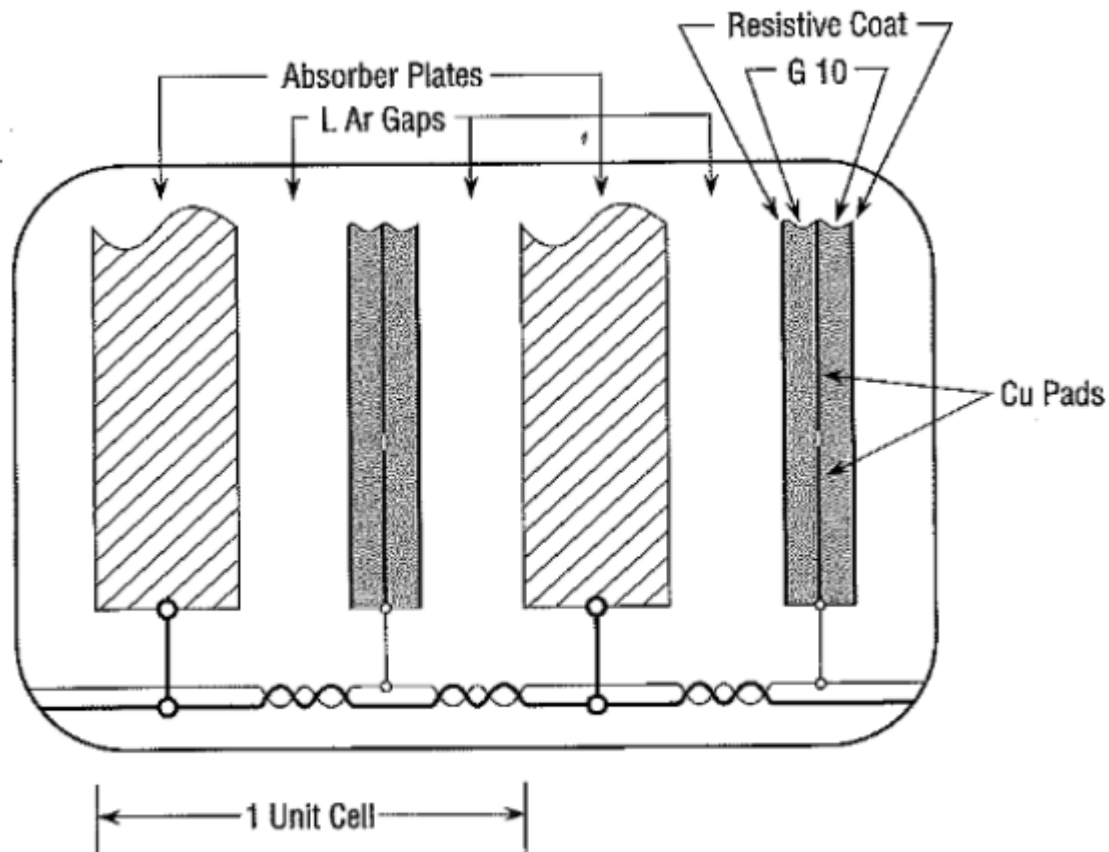


Fig. 27. Schematic view of the liquid argon gap and signal board unit cell.

### Liquid Argon calorimeter:

- no intrinsic amplification
- very stable device
  - argon is pure
  - geometry is stable
  - readout electronics is monitored regularly

### One caveat:

The resistive coat has very high surface resistivity:

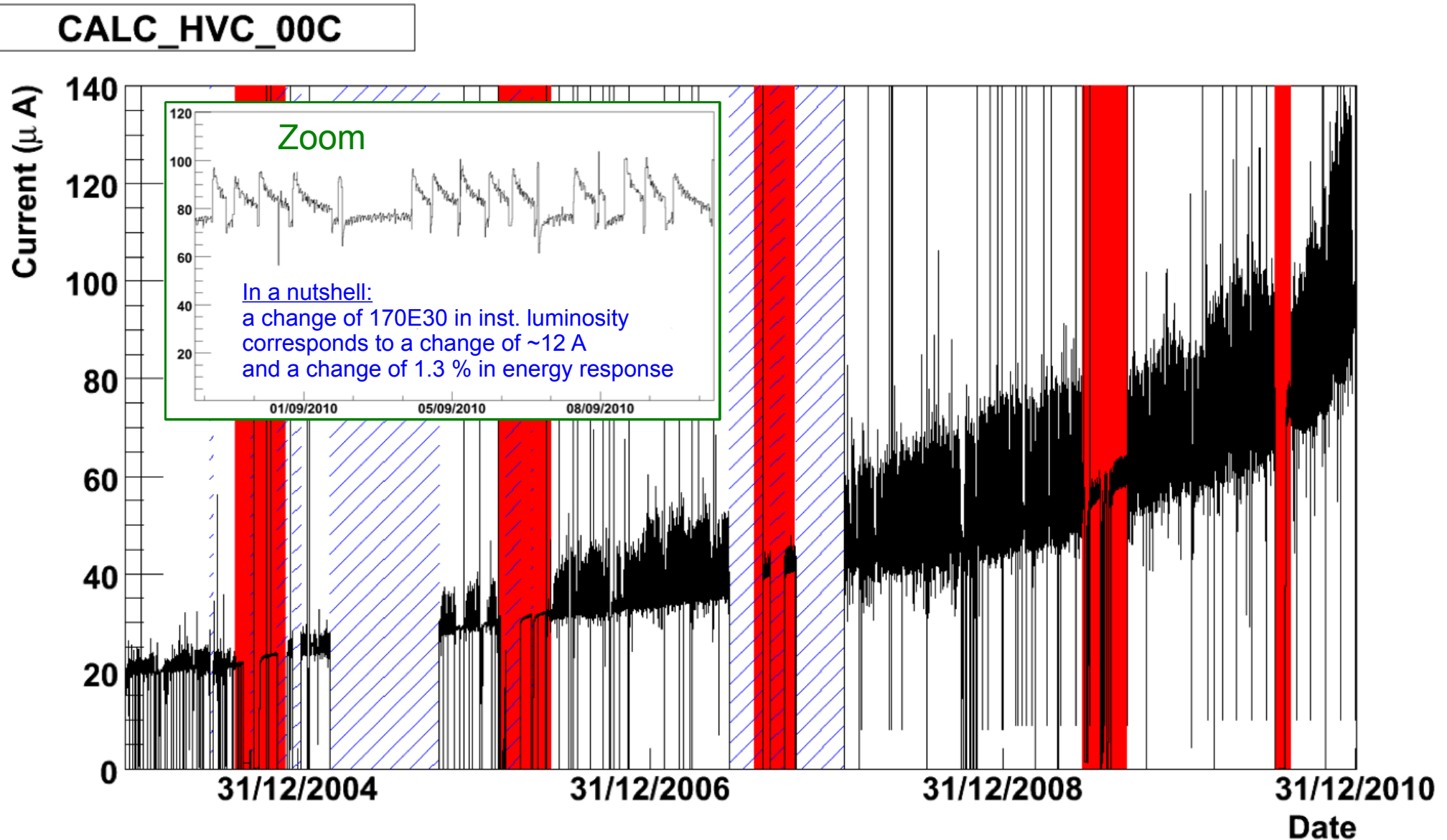
$$\sim 200 \text{ M}\Omega/\square$$

Any significant current will lead to a voltage drop across the resistive coat

- => reduced electric field
- => reduced drift velocity
- => (slightly) reduced energy response

# Calorimeter: currents

This example channel is connected to di-gaps in CC-EM4 readout sections.



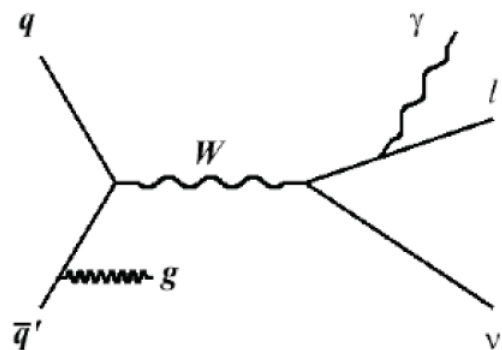


# Measurement strategy

W mass is extracted from transverse mass, transverse momentum and transverse missing momentum:

**Need Monte Carlo simulation to predict shapes of these observables for given mass hypothesis**

NLO event generator with non-perturbative form factor which resums large logarithmic terms from emission of multiple soft gluons:  
DØ uses **ResBos** + **Photos** for W/Z production and decay



+

Parameterised detector model

W mass templates

+

backgrounds

Validated in  
“MC closure test”

Detector calibration

- calorimeter energy scale
- recoil

data

binned likelihood fit

Blind analysis:  
true value of mass hidden from the  
analysers until the analysis was completed

W mass

# Model of W production and decay

Tool	Process	QCD	EW
RESBOS	$W, Z$	NLO	-
WGRAD	$W$	LO	complete $\mathcal{O}(\alpha)$ , Matrix Element, $\leq 1$ photon
ZGRAD	$Z$	LO	complete $\mathcal{O}(\alpha)$ , Matrix Element, $\leq 1$ photon
PHOTOS			QED FSR, $\leq 2$ photons

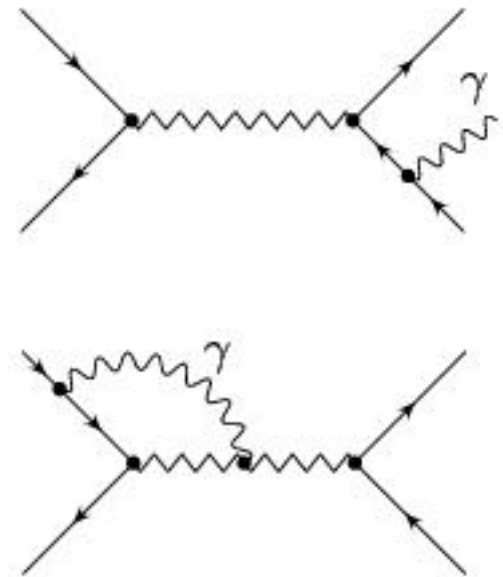
Our main generator is “**ResBos+Photos**”. The NLO QCD in **ResBos** allows us to get a reasonable description of the  $p_T$  of the vector bosons. The two leading EWK effects are the first FSR photon and the second FSR photon. **Photos** gives us a reasonable model for both.

We use **W/ZGRAD** to get a feeling for the effect of the full EWK corrections.

The final “QED” uncertainty we quote is **7/7/9 MeV** ( $m_T, p_T, \text{MET}$ ).

This is the sum of different effects; the two main ones are:

- Effect of full EWK corrections, from comparison of W/ZGRAD in “FSR only” and in “full EWK” modes (**5/5/5 MeV**).
- Very simple estimate of “quality of FSR model”, from comparison of W/ZGRAD in FSR-only mode vs **Photos** (**5/5/5 MeV**).



# Final electron energy scale calibration

**AFTER calorimeter calibration, simulation of effect of inst. luminosity, corrections for dead material, modeling of underlying energy flow:**

final electron energy response calibration, using  $Z \rightarrow e e$ , the known  $Z$  mass value from LEP and the standard “ $f_z$  method”:

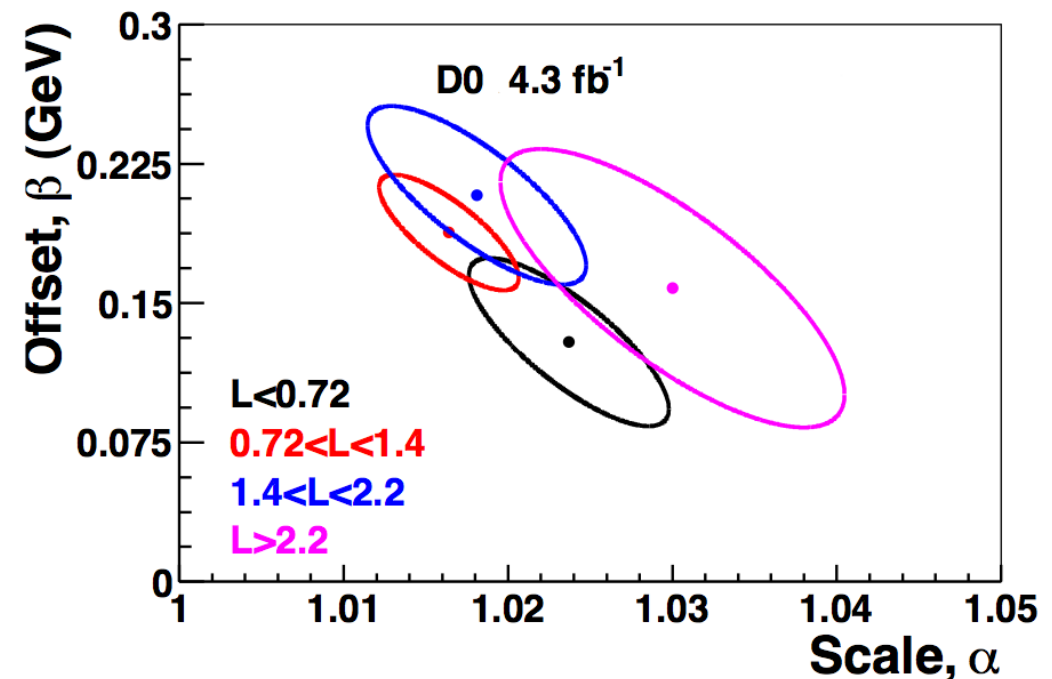
$$E_{\text{measured}} = \text{scale} * (E_{\text{true}} - 43 \text{ GeV}) + \text{offset} + 43 \text{ GeV}$$

We are effectively measuring  $m_W/m_Z$ .

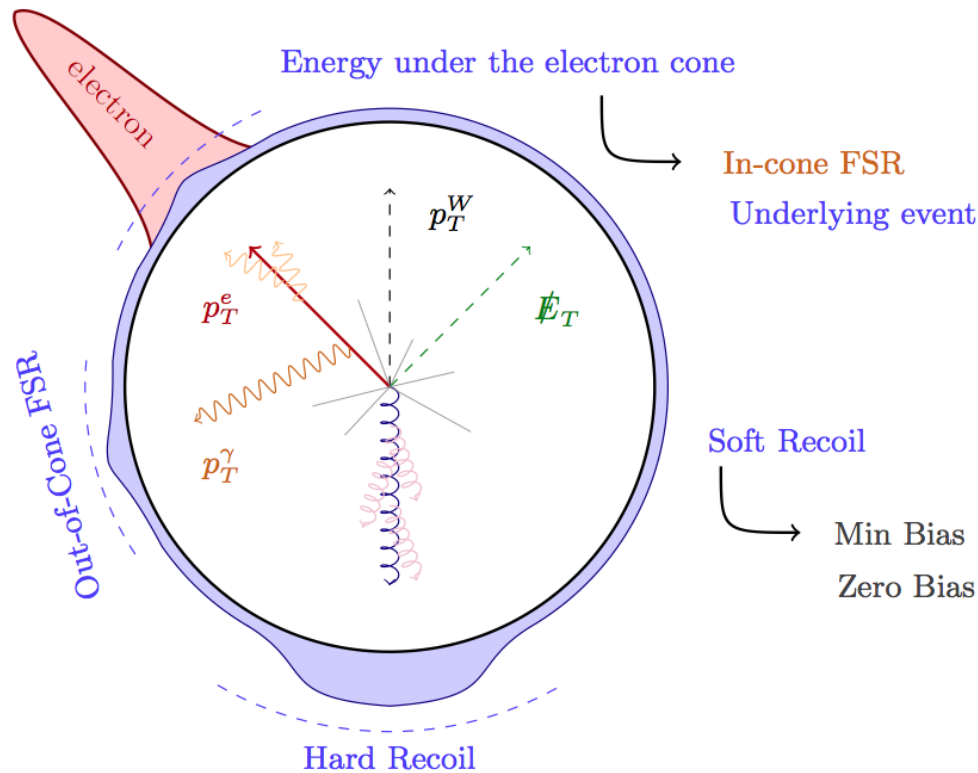
Use energy spread of electrons in  $Z$  decay (e.g. due to  $Z$  boost) to constrain scale *and* offset .

In a nutshell: the  $f_z$  observable allows you to split your sample of electrons from  $Z \rightarrow e e$  into subsamples of different true energy; this way you can “scan” the electron energy response as a function of energy.

In Run IIb we do this separately for four bins of instantaneous luminosity (plot on the right).



# Recoil model



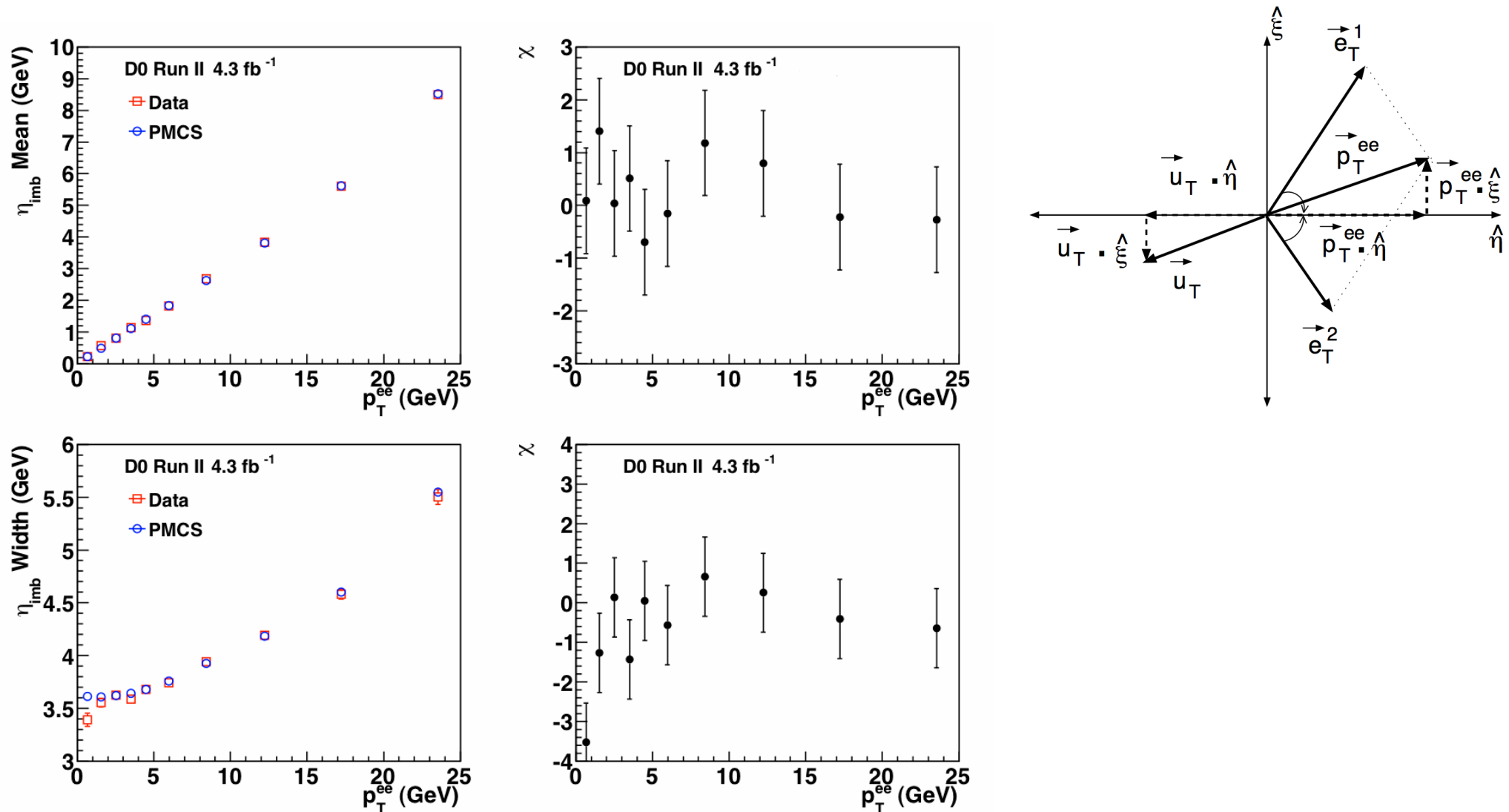
Have five **tunable parameters** in the recoil model that allow us to adjust the response to the hard recoil as well as the resolution (separately for hard and soft components).

$$\vec{u}_T = \vec{u}_T^{\text{HARD}} + \vec{u}_T^{\text{SOFT}} + \vec{u}_T^{\text{ELEC}} + \vec{u}_T^{\text{FSR}}$$

- $\vec{u}_T^{\text{HARD}}$  models the hard hadronic energy from the W recoil.
- $\vec{u}_T^{\text{SOFT}}$  models the soft hadronic activity from zero bias and minimum bias activity.
- $\vec{u}_T^{\text{ELEC}} = -\sum_e \Delta u_{\parallel} \cdot \hat{p}_T(e) + \vec{p}_T^{\text{LEAK}}$  models the recoil energy that was reconstructed under the electron cone, as well as any energy from the electron that leaked outside the cone.
- $\vec{u}_T^{\text{FSR}}$  models the out-of-cone FSR that is reconstructed as hadronic recoil.

# Recoil calibration

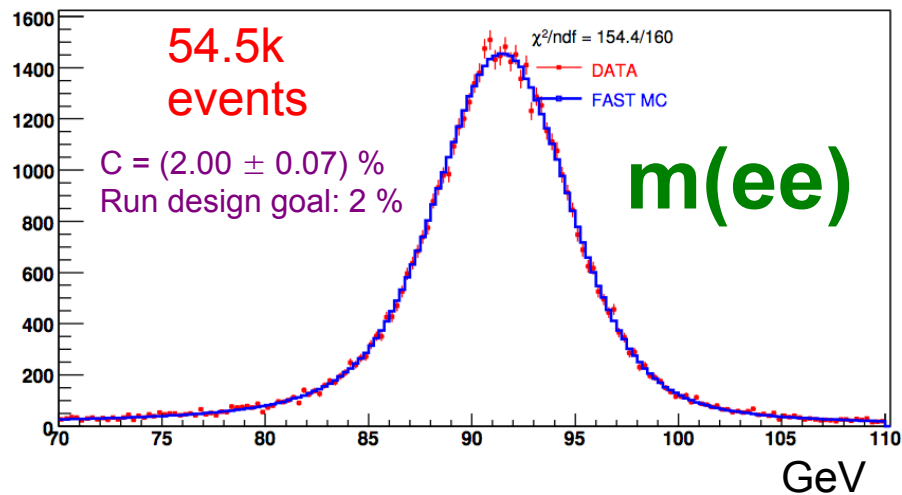
Final adjustment of free parameters in the recoil model is done *in situ* using balancing in  $Z \rightarrow e e$  events and the standard UA2 observables.



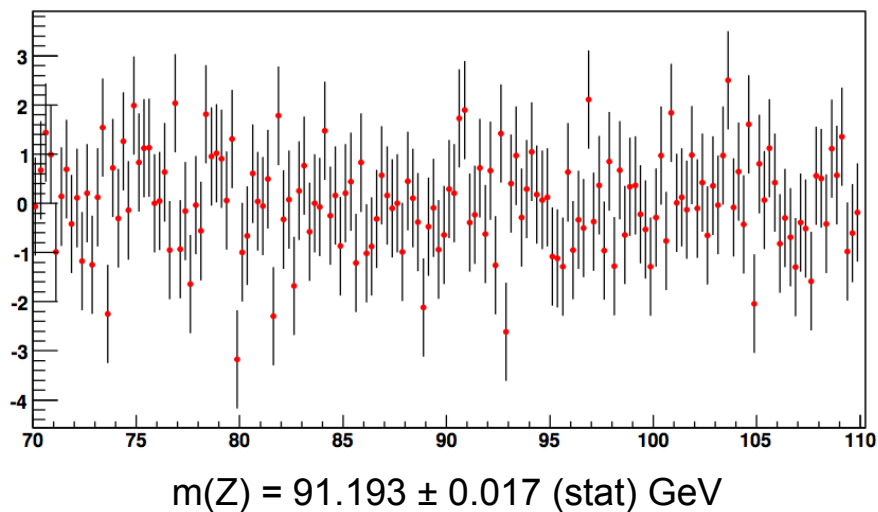


# Z data

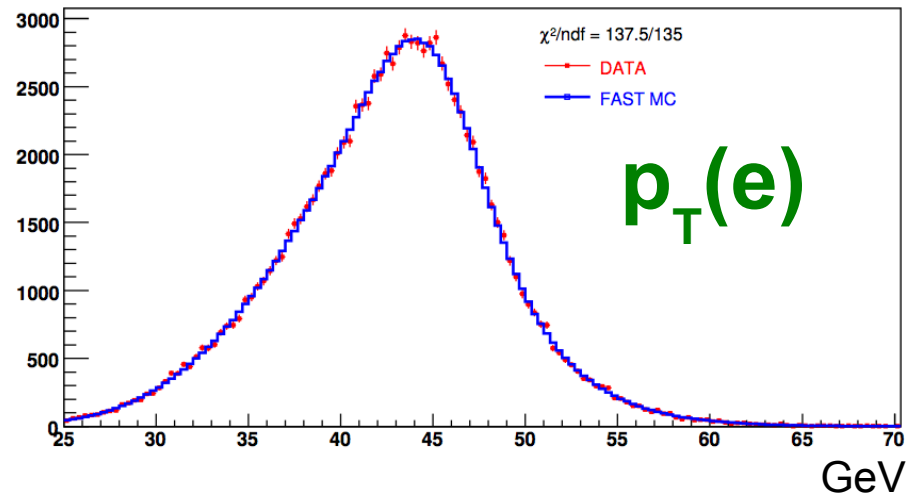
ZCandMass\_CCCC\_Trks



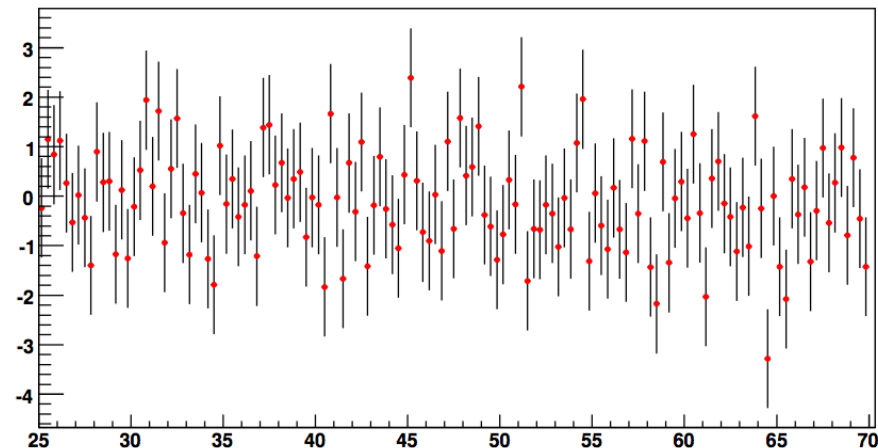
$\chi$  distribution with overall  $\chi^2 = 154.4$  for 160 bins



ZCandElecPt\_0



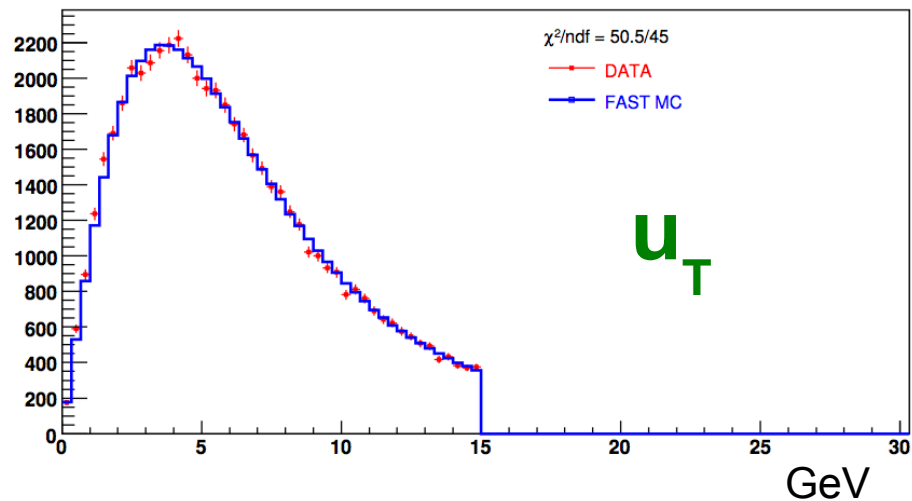
$\chi$  distribution with overall  $\chi^2 = 137.5$  for 135 bins



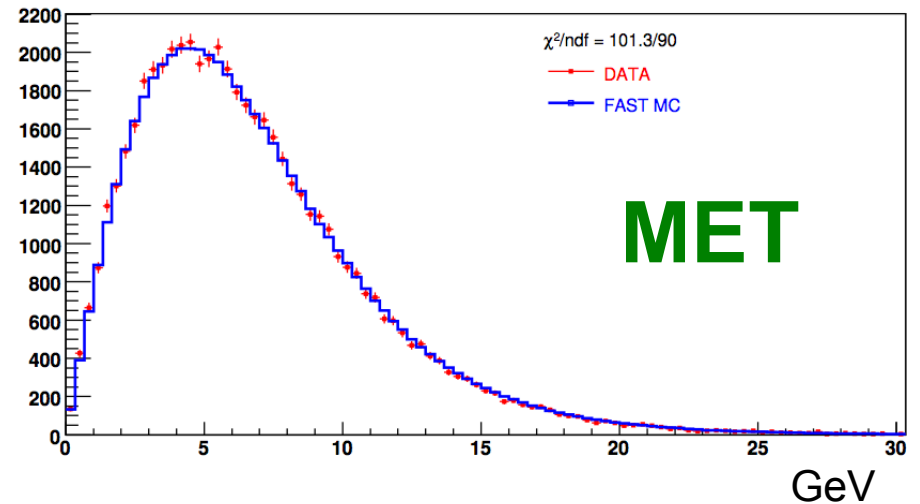
Good agreement between data and parameterised Monte Carlo.

# Z data

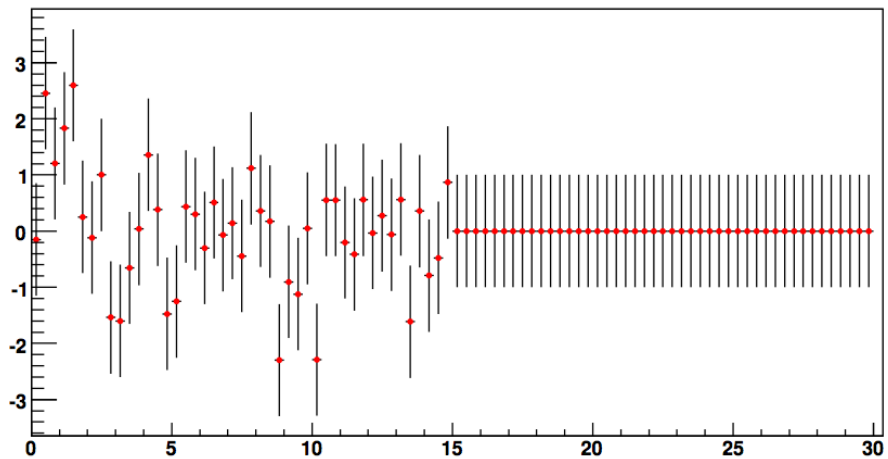
ZCandRecoilPt\_0



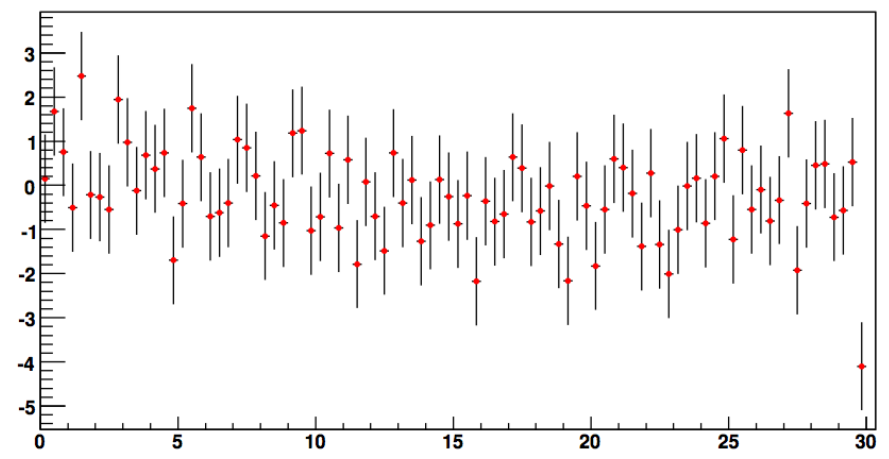
ZCandMet\_0



$\chi$  distribution with overall  $\chi^2 = 50.5$  for 45 bins



$\chi$  distribution with overall  $\chi^2 = 101.3$  for 90 bins

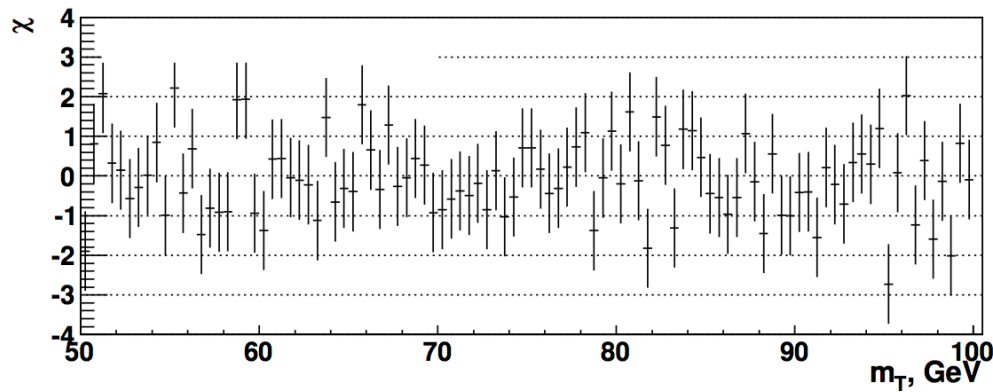
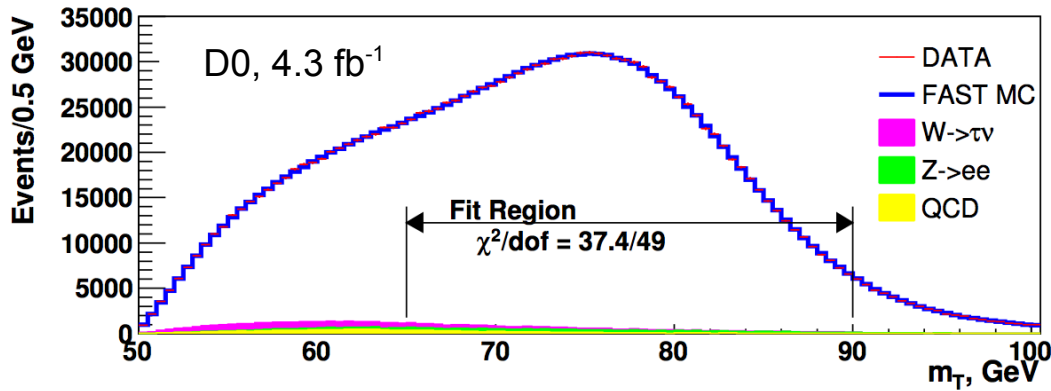


Good agreement between data and parameterised Monte Carlo.

1.68M events  
central electrons ( $|\eta| < 1.05$ )

# W data

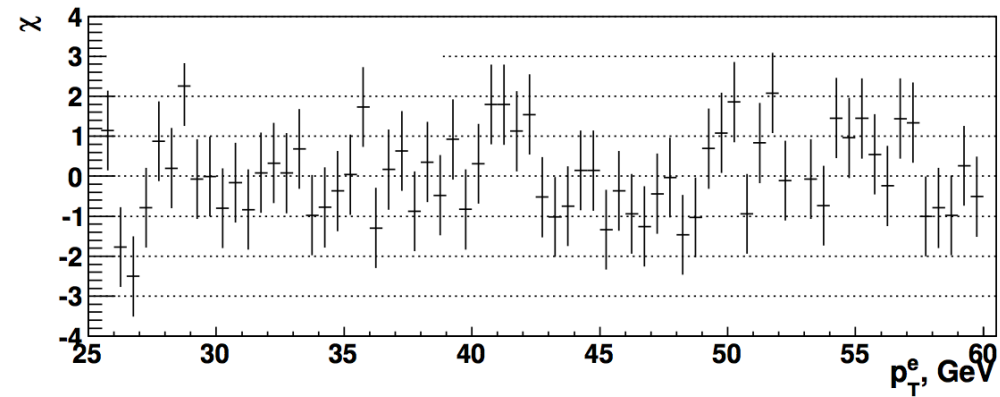
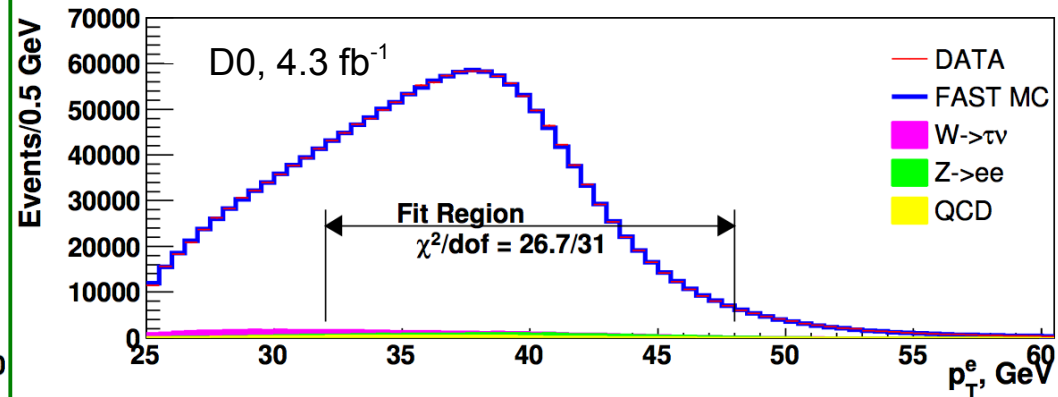
$m_T$



Fit results:

$$m(W) = 80371 \pm 13 \text{ MeV (stat)}$$

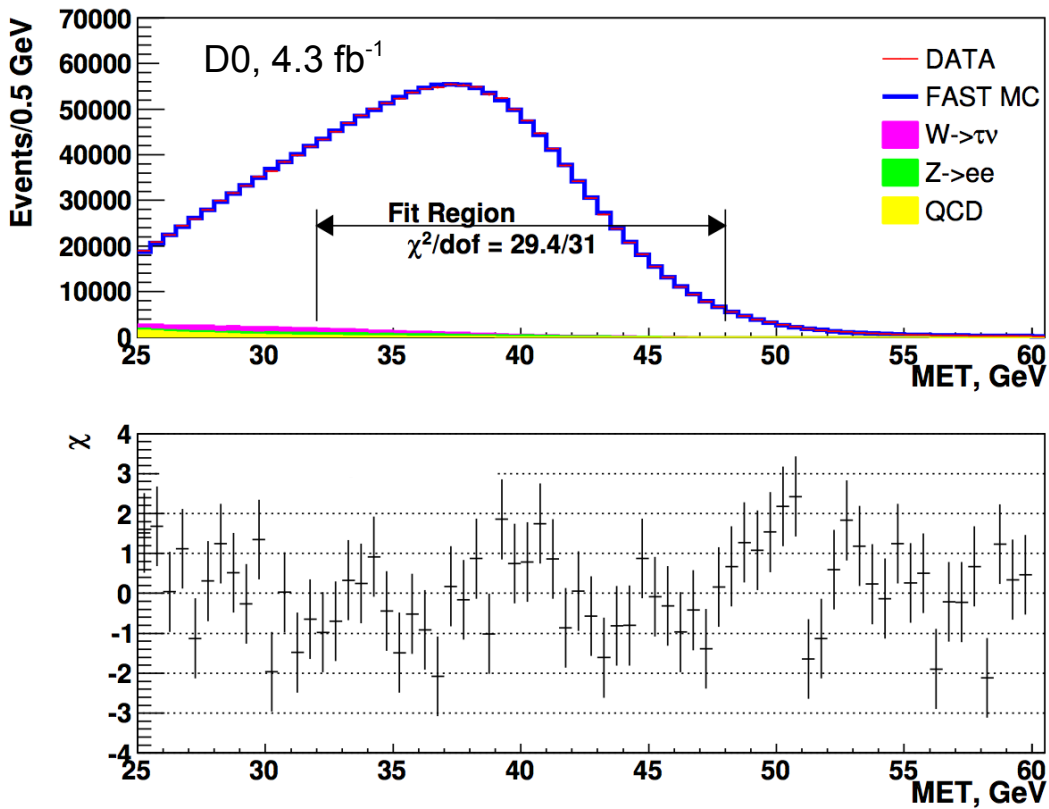
$p_T(e)$



$$m(W) = 80343 \pm 14 \text{ MeV (stat)}$$

# W data

## MET



Fit results:

$$m(W) = 80355 \pm 15 \text{ MeV (stat)}$$

# Summary of uncertainties

systematic uncertainties	Source	$\sigma(m_W)$ MeV $m_T$	$\sigma(m_W)$ MeV $p_T(e)$	$\sigma(m_W)$ MeV $E_T$
	<b>Experimental</b>			
	Electron Energy Scale	16	17	16
	Electron Energy Resolution	2	2	3
	Electron Energy Nonlinearity	4	6	7
	$W$ and $Z$ Electron energy loss differences	4	4	4
	Recoil Model	5	6	14
	Electron Efficiencies	1	3	5
	Backgrounds	2	2	2
	<b>Experimental Total</b>	18	20	24
	<b>W production and decay model</b>			
	PDF	11	11	14
	QED	7	7	9
	Boson $p_T$	2	5	2
	<b>W model Total</b>	13	14	17
	<b>Total</b>	22	24	29
<b>statistical</b>		13	14	15
<b>total</b>		26	28	33

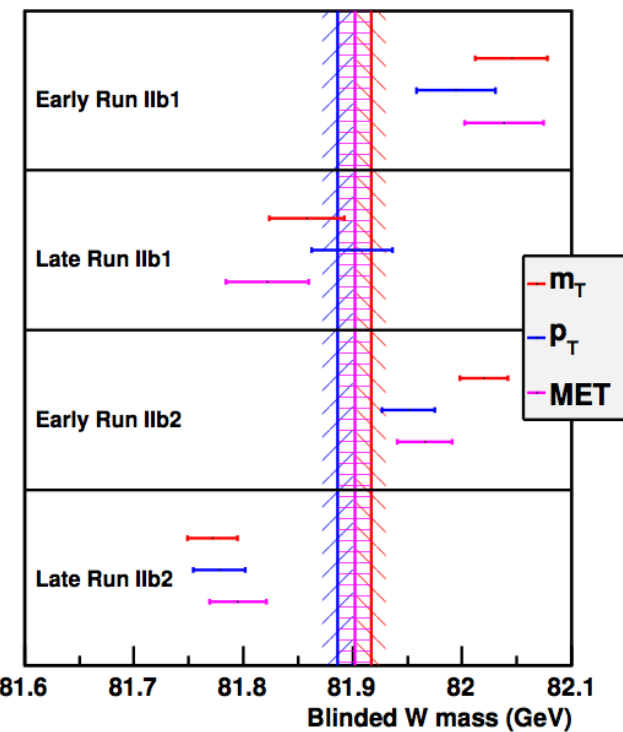
Keep in mind that this analysis uses *only* Run IIb data, *i.e.* it is intended to be combined with our Run IIa result.  
23 MeV uncertainty for the combination with Run IIa.



# Consistency checks

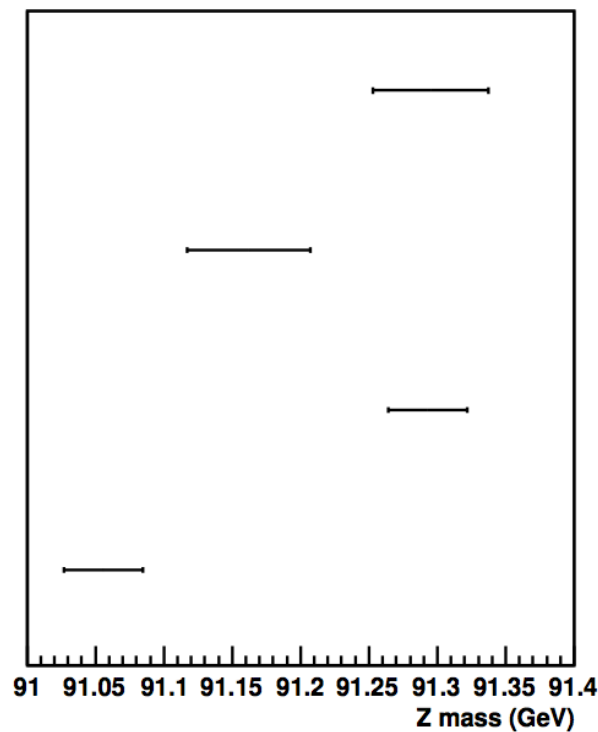
Split data sample into four data taking periods and measure W mass separately for each period:

W

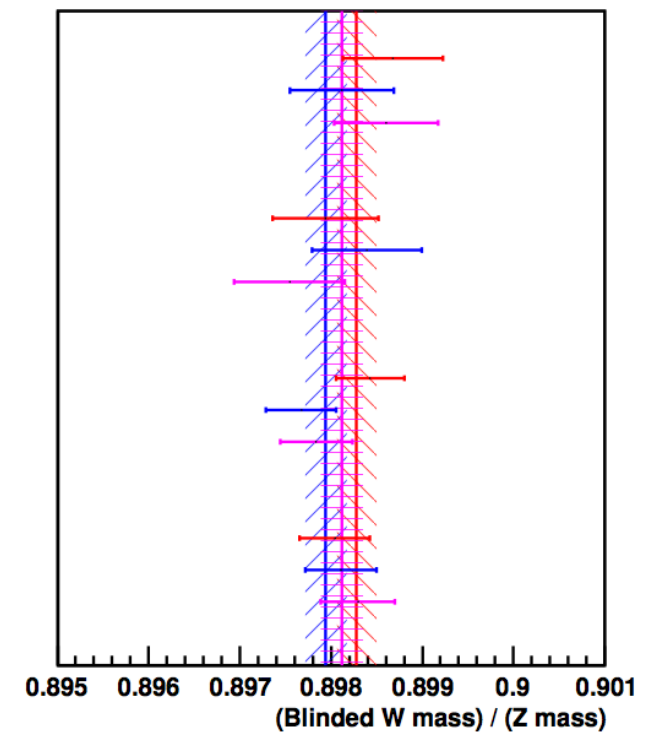


Error bars represent W statistics.

Z



“W/Z”

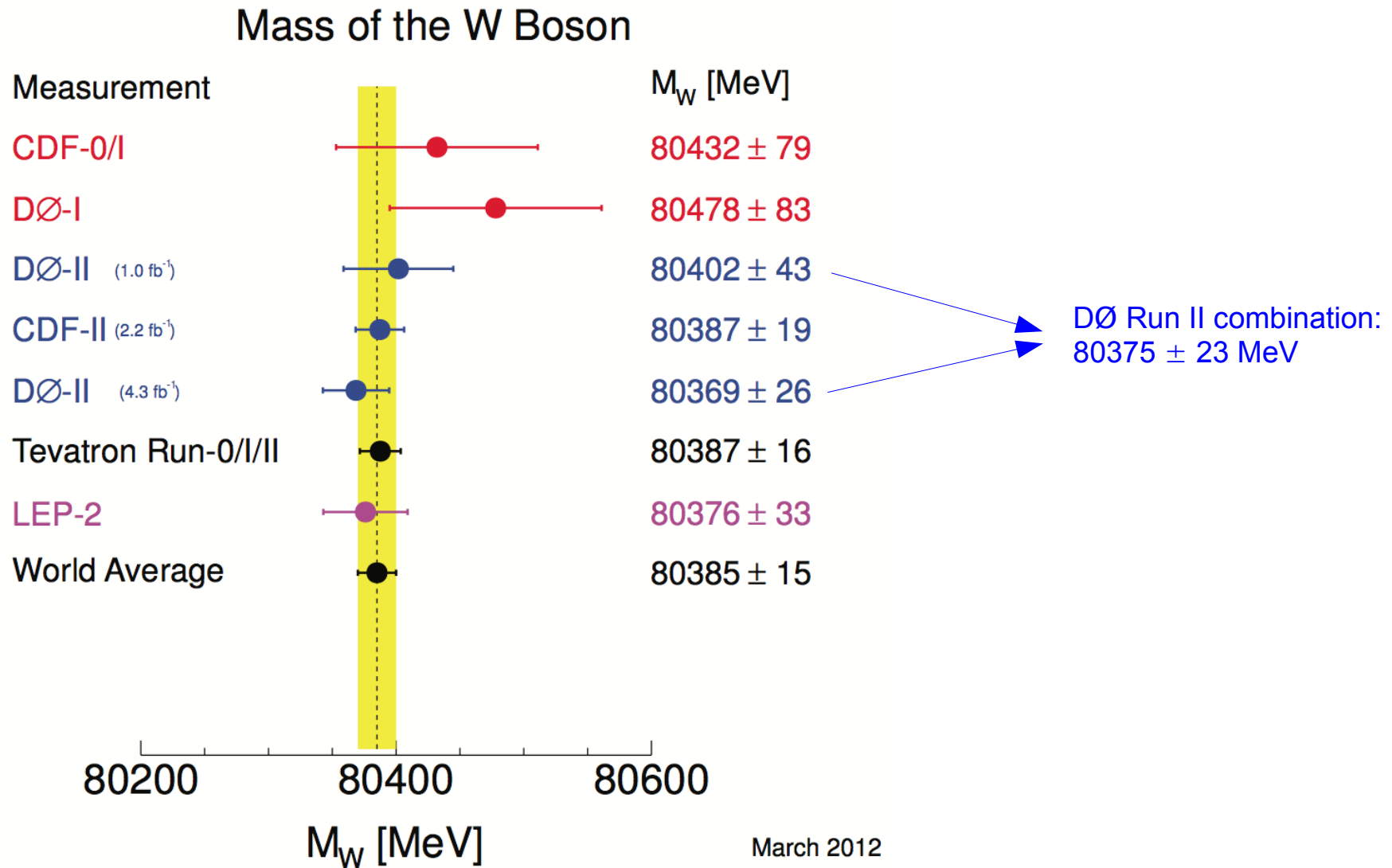


Error bars represent  
W and Z statistics.

Mass ratio is stable over time.

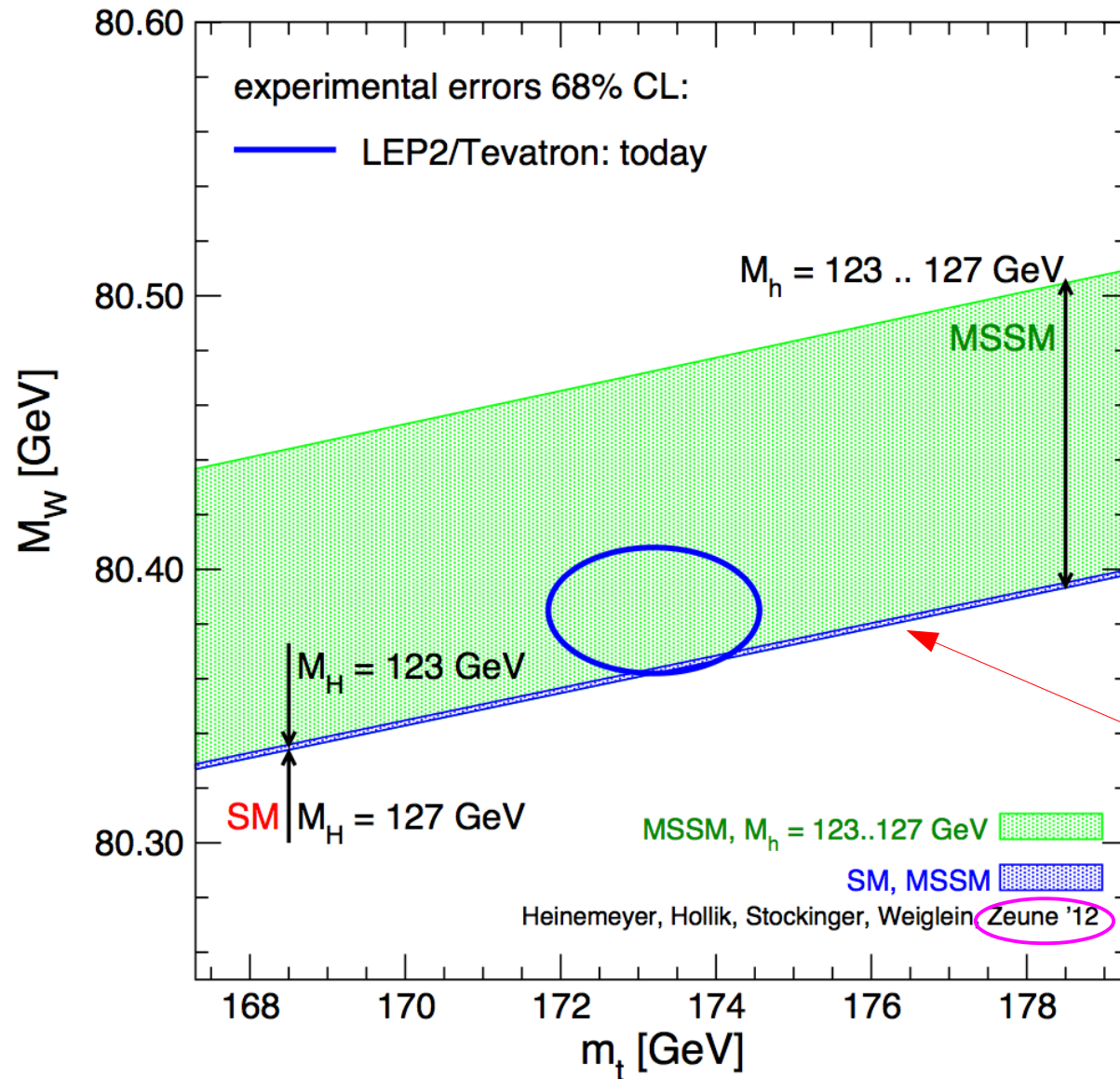
These are just a few examples. Many more cross-checks have been performed.

# Comparison with previous results; New averages



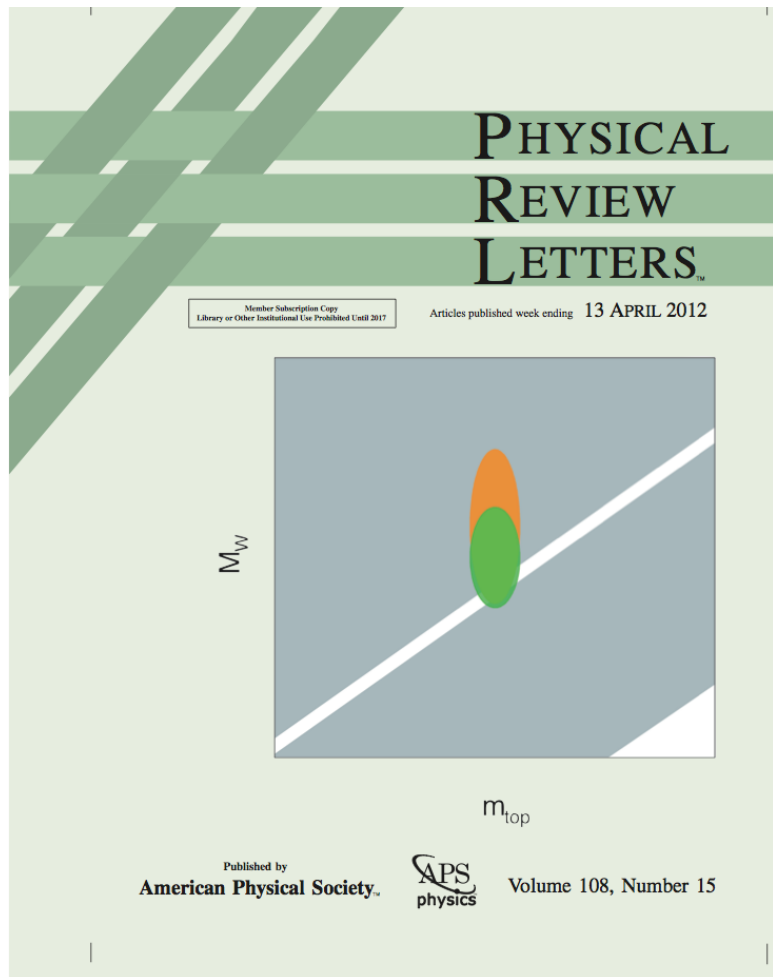
[arXiv:1204.0042 \[hep-ex\]](https://arxiv.org/abs/1204.0042)

# New summary graph

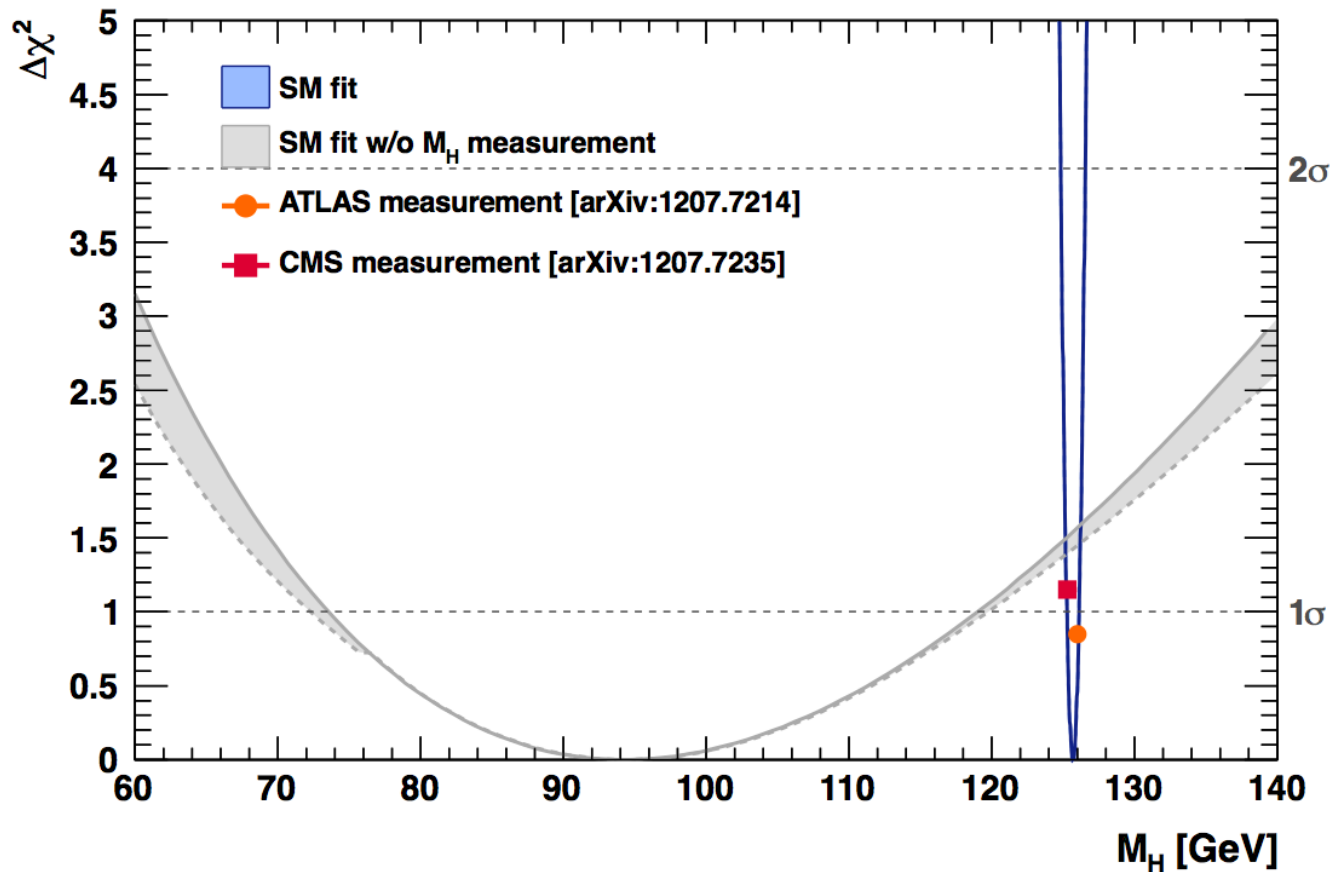


In the context of the Standard Model (SM), the mass of the new boson discovered at CERN is inside this blue band.

# Results



# Constraints on the Higgs boson mass



Indirect constraint  
on Higgs mass:

$$M_H = 94^{+25}_{-22} \text{ GeV}$$

Consistent ( $1.3 \sigma$ ) with direct measurements the mass of the new boson discovered at CERN.

Gfitter group,  
arXiv:1209.2716 [hep-ph]

Alternatively, this test can be “turned around”: use electroweak fit, including measurement of Higgs boson mass, to predict the W boson mass:

$$\begin{aligned} M_W &= 80.3593 \pm 0.0056_{m_t} \pm 0.0026_{M_Z} \pm 0.0018_{\Delta\alpha_{\text{had}}} \\ &\quad \pm 0.0017_{\alpha_S} \pm 0.0002_{M_H} \pm 0.0040_{\text{theo}} \\ &= 80.359 \pm 0.011_{\text{tot}} \end{aligned}$$

Direct measurement:  
 $M_W = 80.385 \pm 0.015$



# Projections

Source	Public. 2009 (1.0 fb <sup>-1</sup> )	Public. 2012 (4.3 fb <sup>-1</sup> )	Proj. 10 fb <sup>-1</sup>	Proj. 10 fb <sup>-1</sup> improv.	Proj. 10 fb <sup>-1</sup> improv. + EC
<b>Statistical</b>	23	13	9	9	8
<b>Experimental syst.</b>					
Electron energy scale	34	16	11	11	10
Electron energy resolution	2	2	2	2	2
EM shower model	4	4	4	2	2
Electron energy loss	4	4	4	2	2
Hadronic recoil	6	5	3	3	2
Electron ID efficiency	5	1	1	1	1
Backgrounds	2	2	2	2	2
Subtotal experimental syst.	35	18	13	12	11
<b>W production and decay model</b>					
PDF	9	11	11	11	5
QED	7	7	7	3	3
boson $p_T$	2	2	2	2	2
Subtotal W model	12	13	13	12	6
Total systematic uncert.	37	22	19	17	13
<b>Total</b>	<b>44</b>	<b>26</b>	<b>21</b>	<b>19</b>	<b>15</b>

combination: 23

# Conclusions

Attempted to briefly summarise my research programme of the last ~10 years.

## « Mise au point de la calorimétrie au Run II de l'expérience DØ »

“Overhaul of the calorimetry for Run II of the DØ experiment”

- Poor calorimeter performance at the start of Run II – **unexpected, reasons unknown**.
- “*With the current calorimeter performance we are not going to measure the  $W$  mass with DØ*” (DØ electroweak convener in 2003).
- **After long and diverse studies** of issues like bugs in the readout electronics, *in situ* gain calibrations, uninstrumented material, shower simulations and “dark currents”, **we now have decent, well-understood performance**.
- Results of these studies can be seen in many of the published results from DØ.

## « Mesure de la masse du boson $W$ »

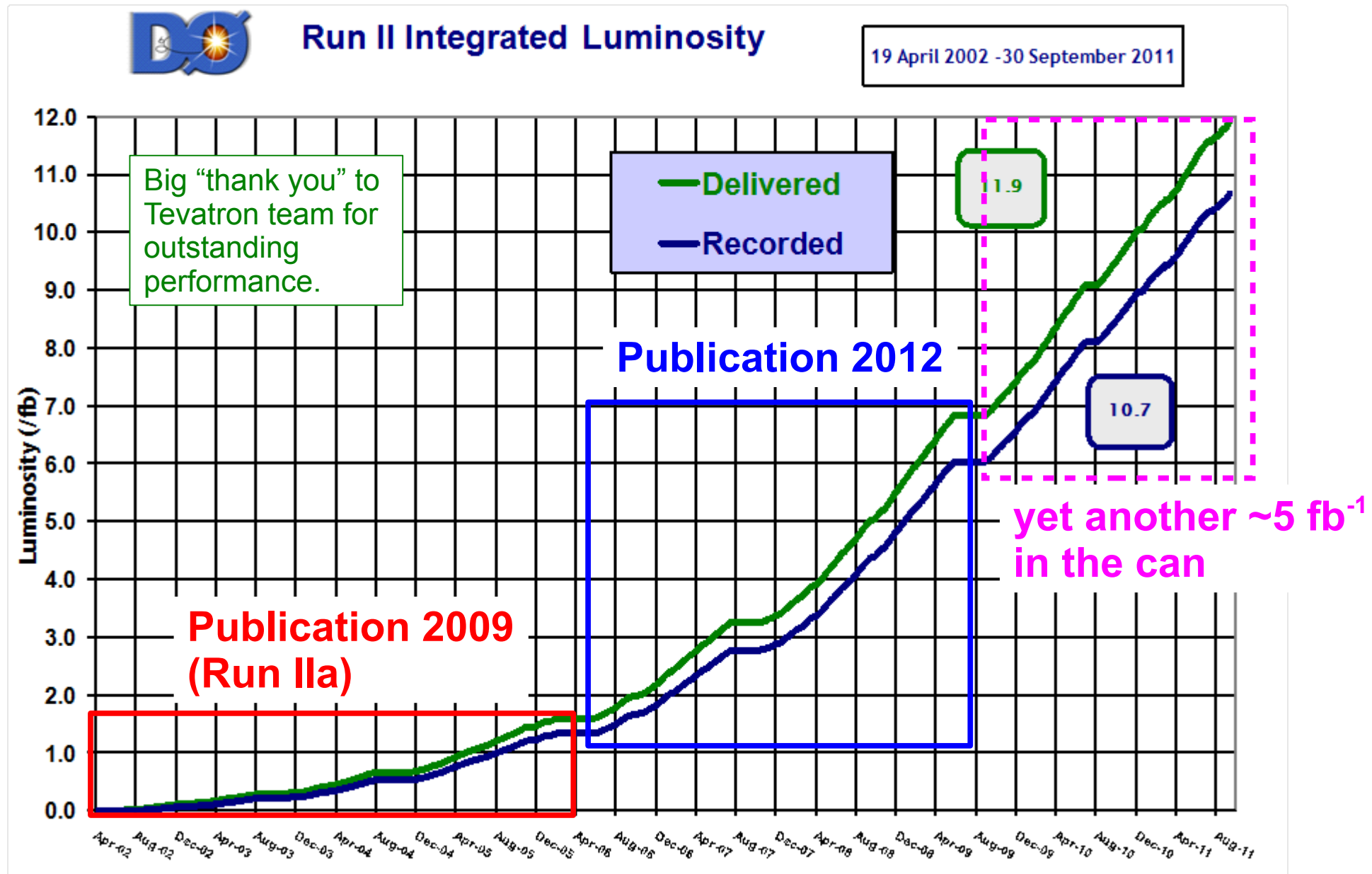
“Measurement of the  $W$  boson mass”

- Together with our friends across the ring, we have reduced the uncertainty in the  $W$  boson mass from **33 MeV (LEP) to 15 MeV**.
- This improvement became available just at the right time, because it is a key ingredient that is needed **to check if the new boson discovered at CERN has the properties of the standard model Higgs boson**.

This programme is a team effort. Many thanks to all the colleagues and friends who I had the privilege to work with.

# Backup Slides

# Data periods and analysis iterations



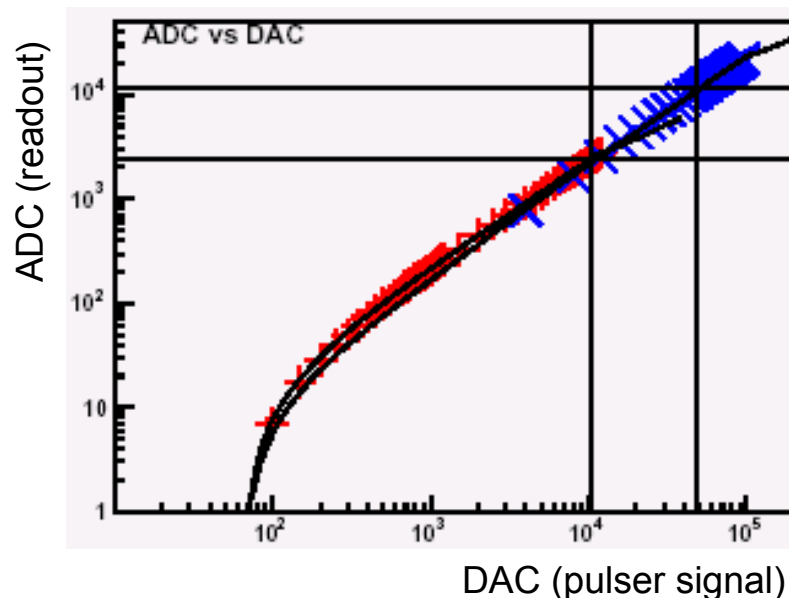
# Electronics calibration

**Aim:** correct for channel-by-channel differences in electronics response.

**Principle:**

inject known signal into preamplifier and see what the electronics measures.

Do this separately for gains x8 and x1, possibly also separately for the two L1 SCAs per channel.



**Major improvements to electronics calibration in d0reco p17:**

- use database for up-to-date calibration constants (pedestals, gains, non-linearities)
- smarter pulser patterns, improved parameterisation of measured response
- improved timing corrections
- improved corrections for pulser/physics response differences

# Phi intercalibration

Qiang Zhu, “*Measurement of the  $W$  boson mass in  $p\bar{p}$  collisions at  $\sqrt{s} = 1.8 \text{ TeV}$ ”, PhD thesis, April 1994, available from the D0 web server, and references therein.*

$p\bar{p}$  beams in the Tevatron are not polarised.

→ Energy flow in the direction transverse to the beams should not have any azimuthal dependence. Any  $\Phi$  dependence must be the result of instrumental effects.

## Energy flow method:

Consider a given  $\eta$  bin of the calorimeter. Measure the density of calorimeter objects above a given  $E_T$  threshold as a function of  $\Phi$ . With a perfect detector, this density would be flat in  $\Phi$ .

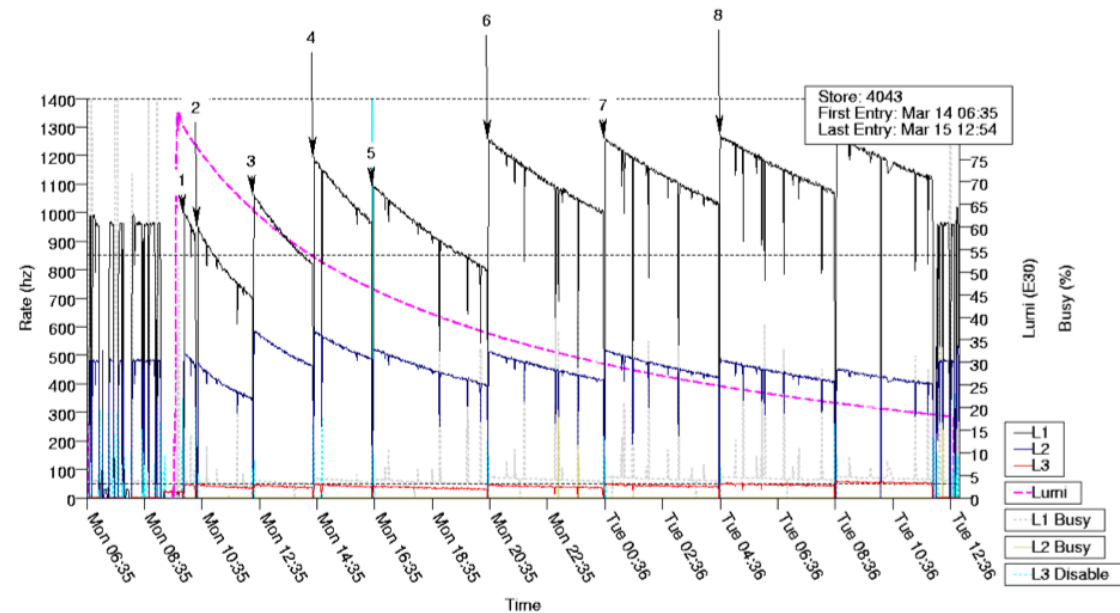
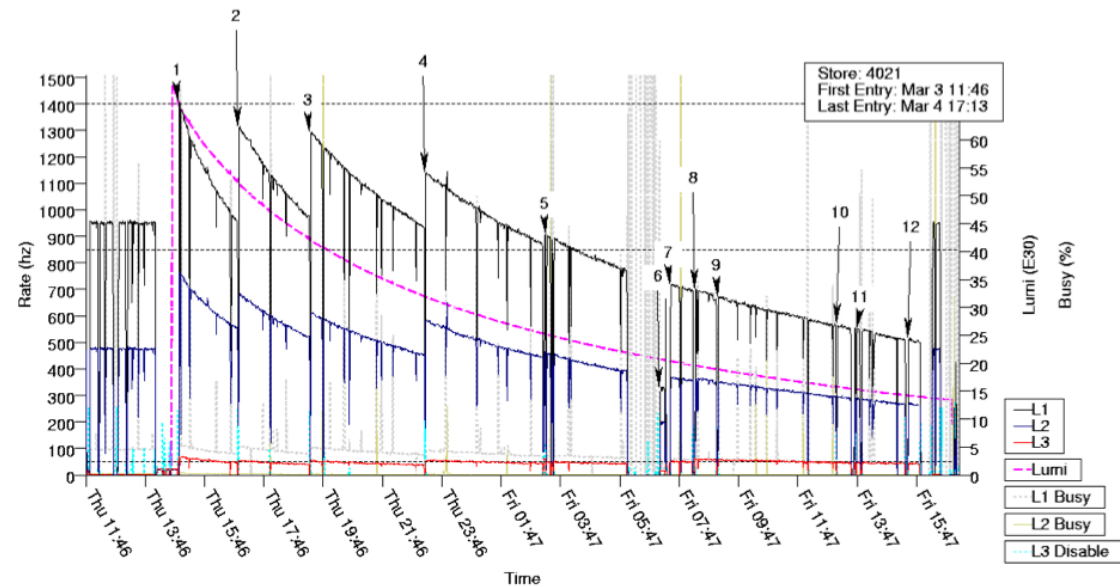
Assuming that any  $\Phi$ -non-uniformities are due to energy scale variations, the uniformity of the detector can be improved by applying multiplicative calibration factors to the energies of calorimeter objects in each  $\Phi$  region in such a way that the candidate density becomes flat in  $\Phi$  (“ $\Phi$  intercalibration”).

Subtleties:

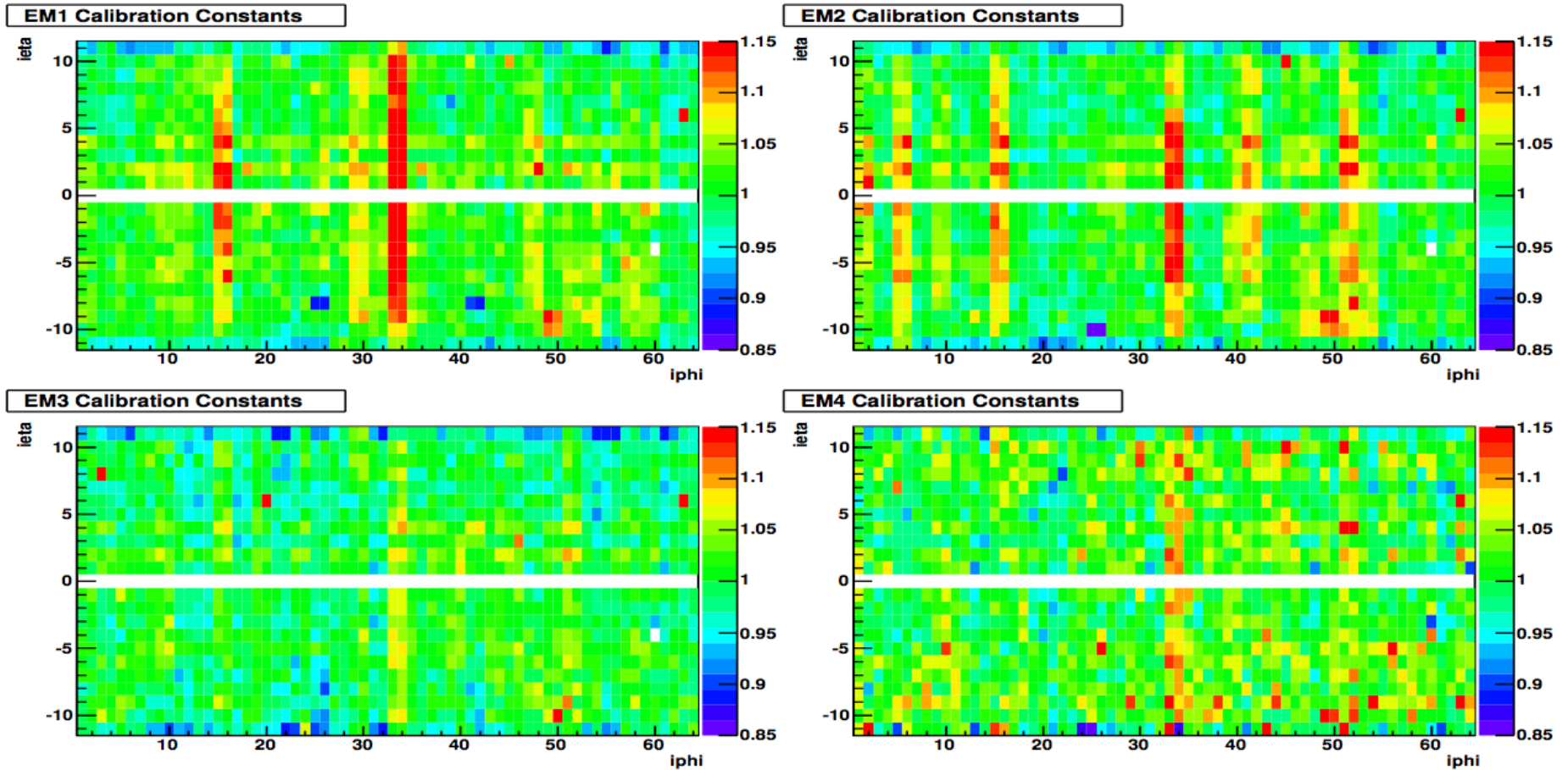
- distribution of primary vertices not necessarily centred on the centre of the calorimeter,
- beams possibly titled w.r.t. axis of the calorimeter,
- in addition to scale variations, a calorimeter can have other problems (non-linearities, ...),
- ...



# Phi intercalibration



# Phi intercalibration



# Eta-dependent absolute scale

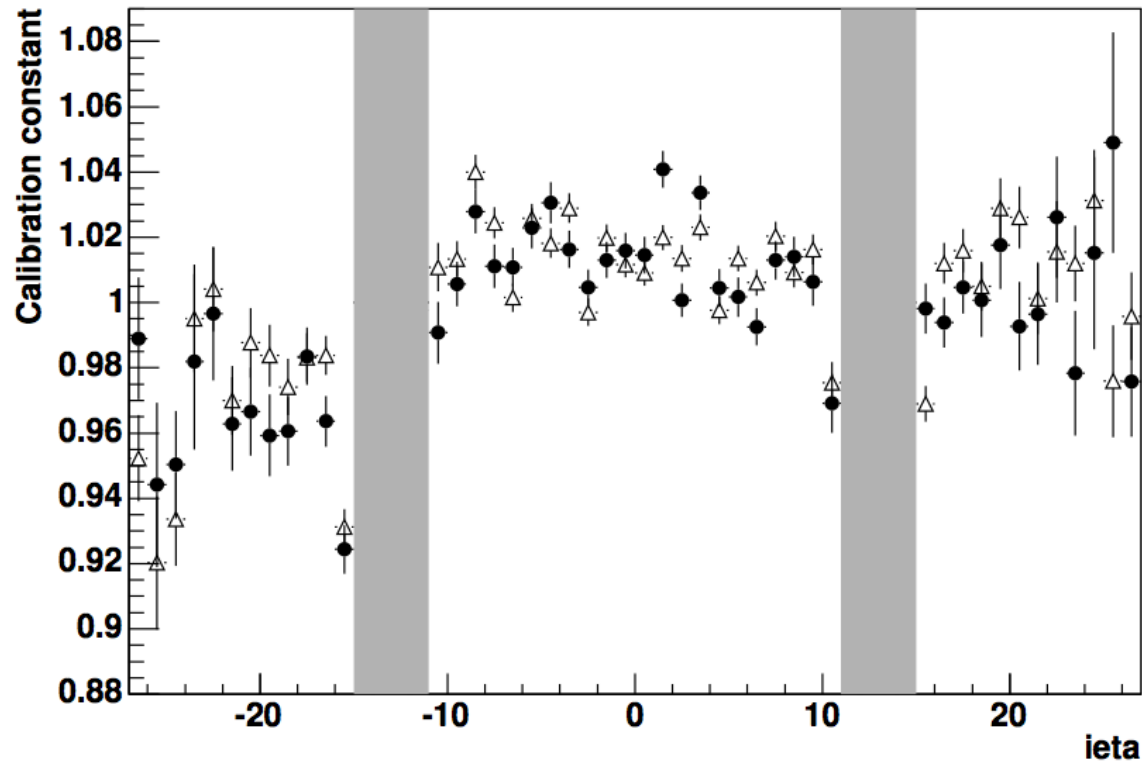
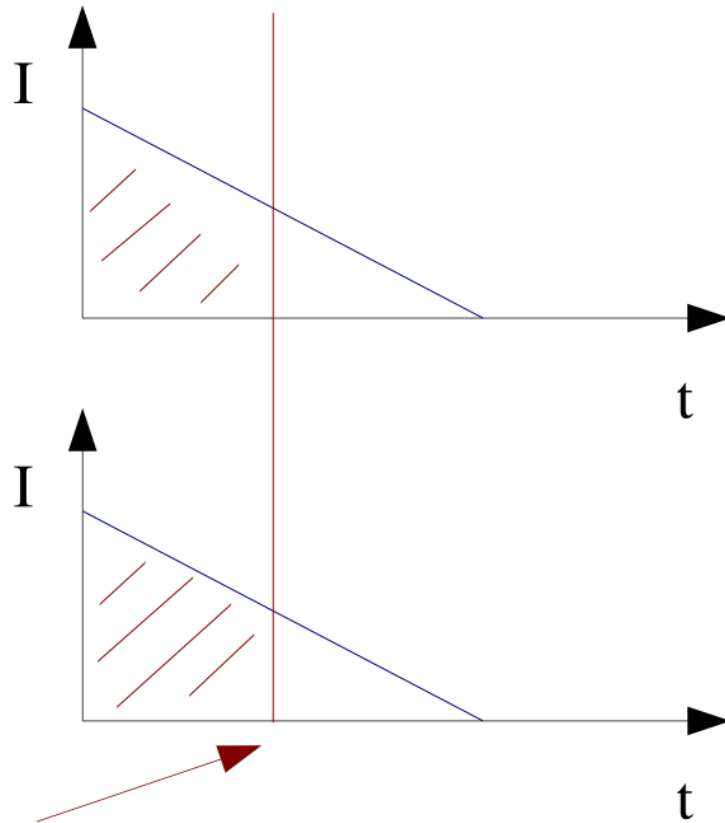


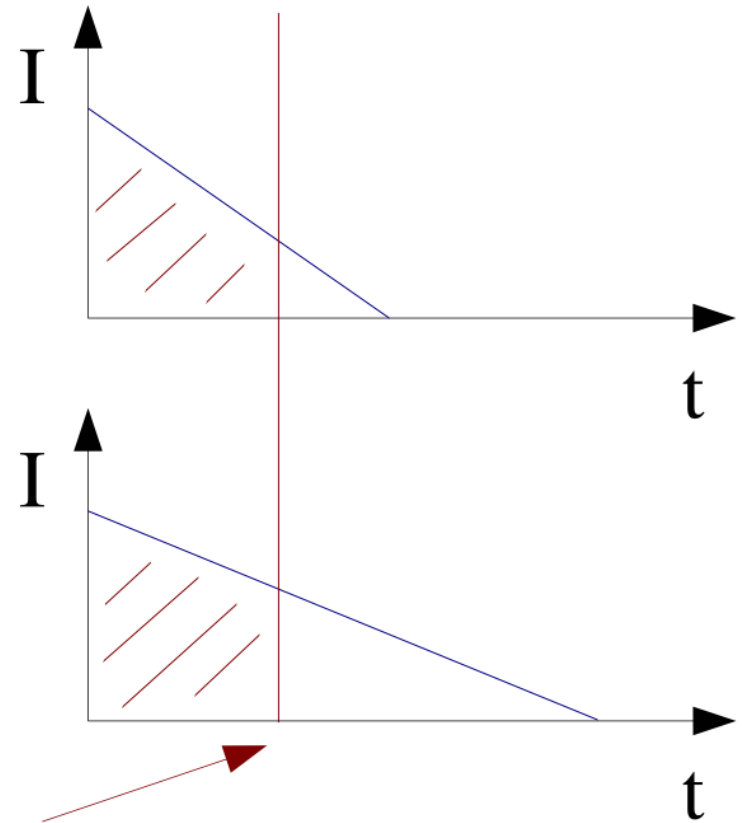
FIGURE 4.7 – Résultat de la détermination de l'échelle absolue en énergie, séparément pour chaque anneau à  $\eta$  (*ieta*) donné. Les zones grises indiquent les zones de transition entre les cryostats (elles ne sont pas prises en compte dans l'ajustement des constantes de calibration à l'aide de l'échantillon  $Z \rightarrow ee$ ). Le point à *ieta* = -27 représente la constante commune qui est définie pour les anneaux à  $-37 \leq \text{ieta} \leq -27$ , *idem* pour *ieta* = +27. Les triangles représentent les résultats obtenus pour les données enregistrées avant la période d'arrêt en sept/nov 2003, les points représentent ceux pour les données prises juste après cette période d'arrêt.

# Finite integration time



finite integration time

(a) géométrie parfaite du « *di-gap* »



finite integration time

(b) la carte de lecture ne se trouve pas exactement au centre du « *di-gap* »

# Event selection

## Event selection

- CAL only trigger (single EM)
- vertex  $z < 60\text{ cm}$

## Electron selection

- $p_T > 25\text{GeV}$
- $\text{HMatrix7} < 12$ ,  $\text{emf} > 0.9$  and  $\text{iso} < 0.15$
- $\eta_{\text{det}} < 1.05$  in the calorimeter fiducial region
- In the calorimeter  $\phi$  fiducial region, as determined from the track
- Spatial track match, track with  $p_T > 10\text{GeV}$  and at least one SMT hit

## $Z \rightarrow ee$ selection

- At least two good electrons
- Hadronic recoil transverse momentum  $u_T < 15 \text{ GeV}$
- Invariant mass  $70 < m_{ee} < 110 \text{ GeV}$

## $W \rightarrow e\nu$ selection

- At least one good electron
- Hadronic recoil transverse momentum  $u_T < 15 \text{ GeV}$
- Transverse mass  $50 < m_T < 200 \text{ GeV}$
- $\cancel{E}_T > 25 \text{ GeV}$

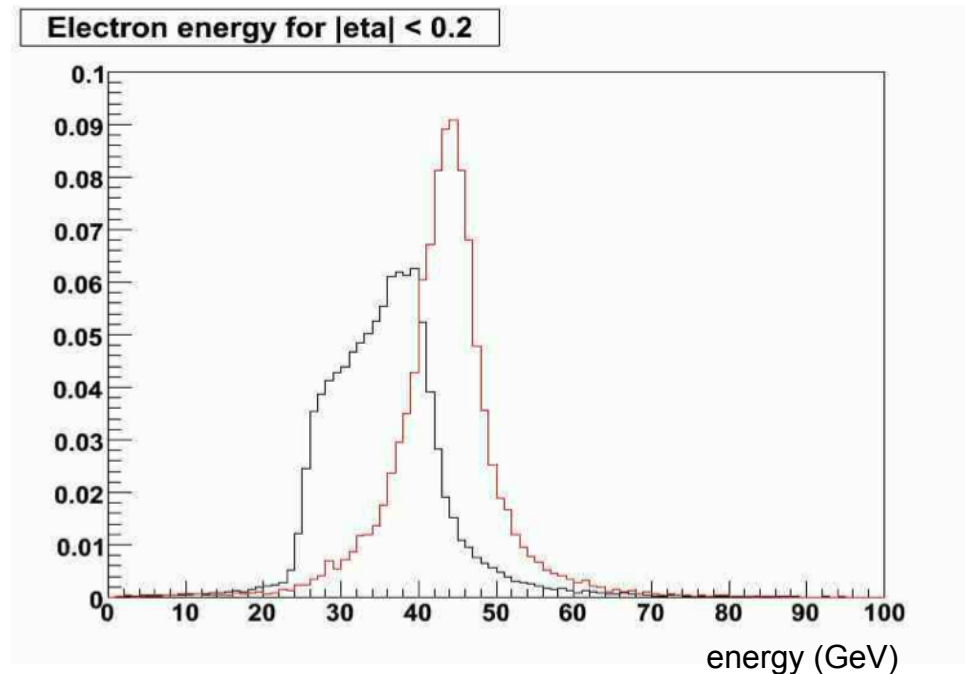
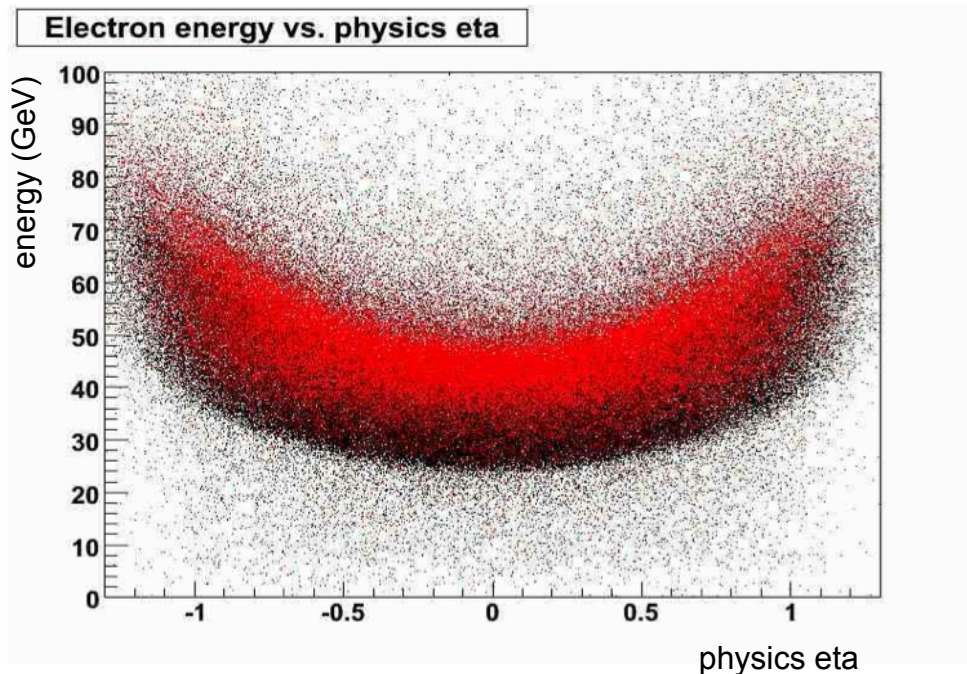
Number of candidates after selection:

	54,512 ( $Z \rightarrow e e$ )
	1,677,394 ( $W \rightarrow e \nu$ )

# Electrons from $Z \rightarrow e e$ and $W \rightarrow e \nu$

Black:  $W \rightarrow e \nu$

Red:  $Z \rightarrow e e$



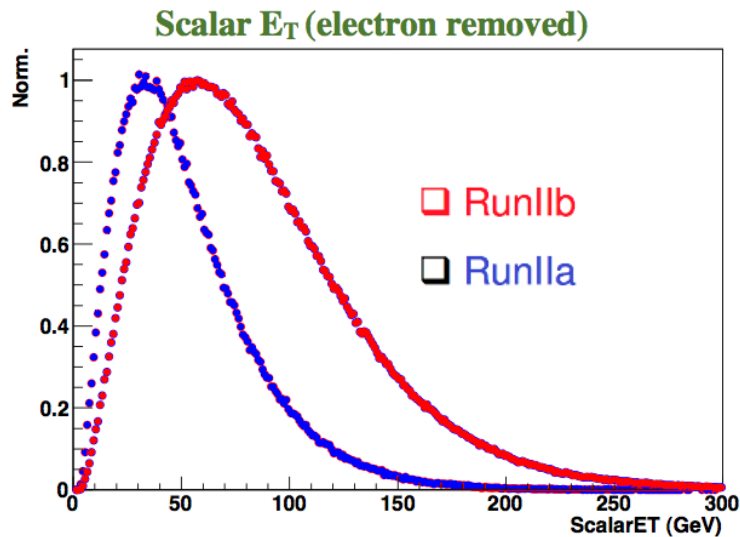
At a given physics eta, the spread in energy of electrons from  $Z \rightarrow e e$  is small. Also, the overlap with the energy spectrum of electrons from  $W \rightarrow e \nu$  is limited.

NB: overlap can be increased by including Z events in the CC-EC configuration (at the cost of understanding the EC).



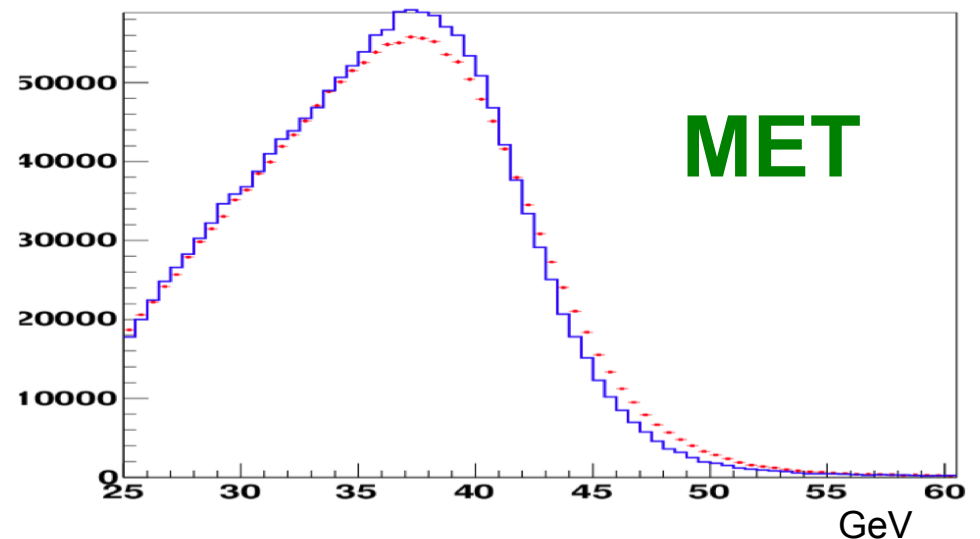
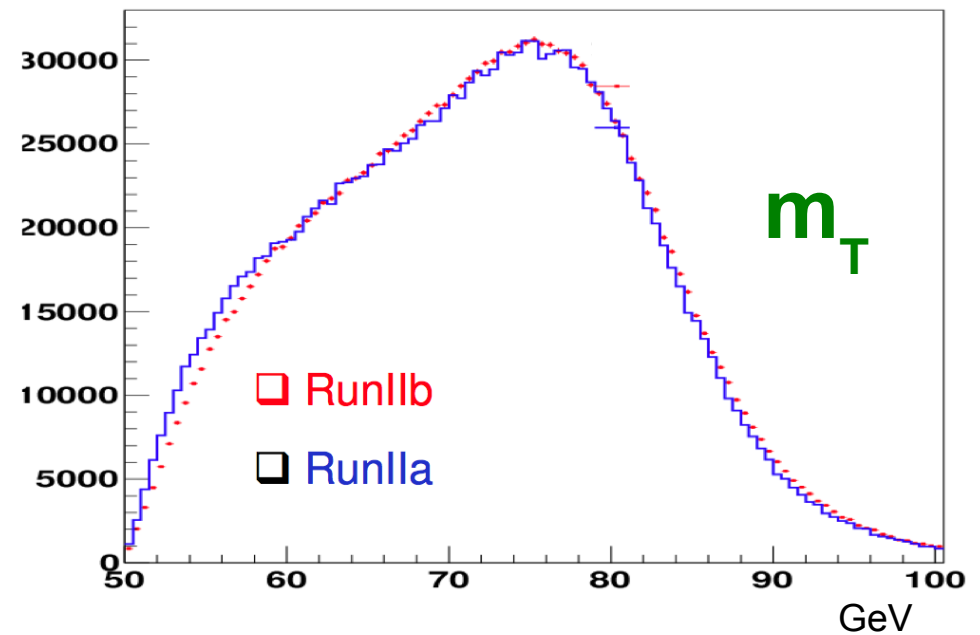
# Run IIb-specific challenges

Higher lumi, hence “way more activity in the detector”:



Does have quite an impact on the observables of interest (as shown on the right).

This is why we had to do significant additional R&D (w.r.t. to Run IIa analysis). No additional R&D is expected for the final  $5 \text{ fb}^{-1}$  (similar lumi spectrum as in current analysis).



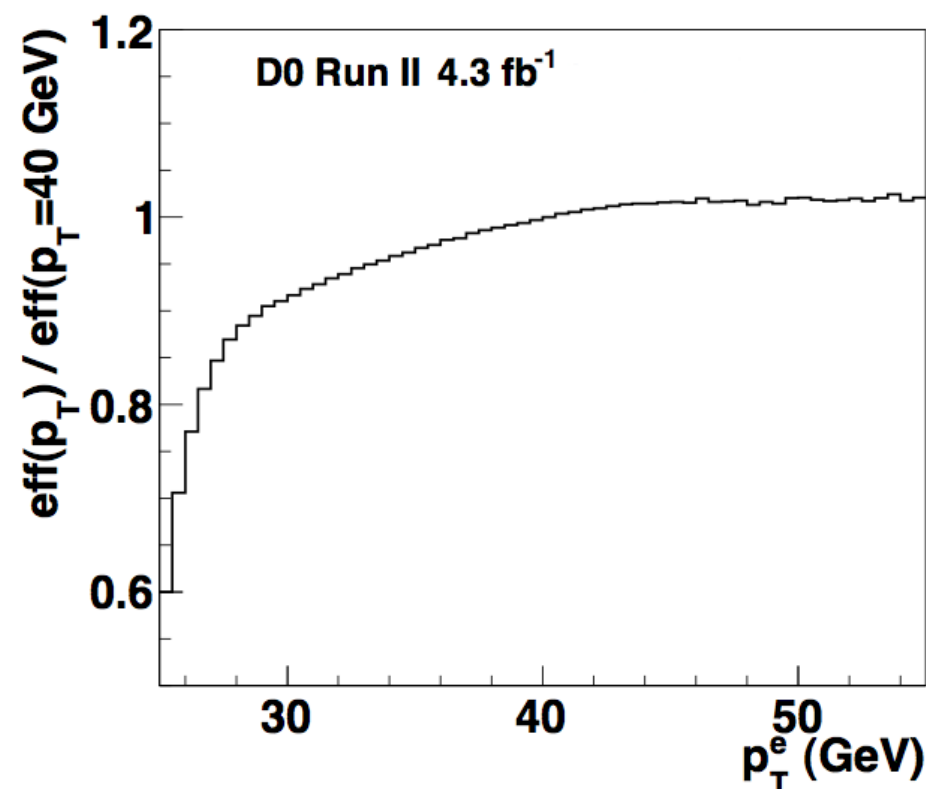
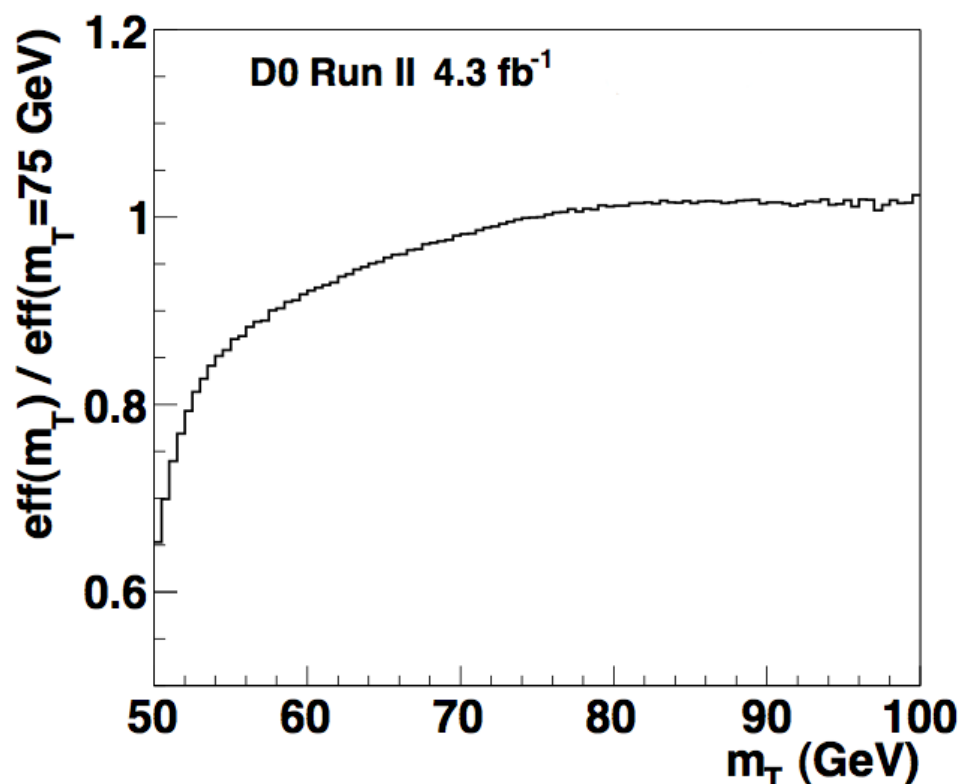
# Electron efficiency model

Detailed model of electron reconstruction/identification efficiency in the busy Run IIb environment:

- dependence on electron kinematics ( $p_T$ , rapidity)
- effect of the hard recoil
- effect of pileup

Two critical control samples:

- W and Z events from detailed simulation, with “overlay” of collider data (trigger on random bunch crossing)
- $Z \rightarrow e e$  (can be selected with minimal electron requirements)



# Recoil model

Have five **tunable parameters** in the recoil model that allow us to adjust the response to the hard recoil as well as the resolution (separately for hard and soft components):

$$\vec{u}_{T,smear}^{soft} = \sqrt{\alpha_{MB}} \vec{u}_T^{MB} + \vec{u}_T^{ZB}$$

model of spectator partons  
(based on soft collisions  
in collider data)

model of pileup/noise  
(from collider data, random trigger)

$$u_{T,smear}^{\parallel,hard} = \left( R_A + R_B \cdot e^{-p_T^Z / \tau_{HAD}} \right) p_T^Z \left\langle \frac{u_T}{p_T^Z} \right\rangle^{\parallel} + S_A \left( u_T^{\parallel} - p_T^Z \left\langle \frac{u_T}{p_T^Z} \right\rangle^{\parallel} \right)$$

model of hard recoil response  
(from detailed first-principles simulation)

# Combination of the three observables

We take the results from the three observables (with their correlations) and combine them:

$$m_{\tau}: 80.371 \pm 0.013 \text{ (stat)} \pm 0.022 \text{ (syst)}$$

$$p_{\tau}^e: 80.343 \pm 0.014 \text{ (stat)} \pm 0.024 \text{ (syst)}$$

$$\text{MET: } 80.355 \pm 0.015 \text{ (stat)} \pm 0.029 \text{ (syst)}$$

$$\rho = \begin{pmatrix} \rho_{m_{\tau}m_{\tau}} & \rho_{m_{\tau}p_{\tau}^e} & \rho_{m_{\tau}\cancel{E}_T} \\ \rho_{m_{\tau}p_{\tau}^e} & \rho_{p_{\tau}^ep_{\tau}^e} & \rho_{p_{\tau}^e\cancel{E}_T} \\ \rho_{m_{\tau}\cancel{E}_T} & \rho_{p_{\tau}^e\cancel{E}_T} & \rho_{\cancel{E}_T\cancel{E}_T} \end{pmatrix} = \begin{pmatrix} 1.0 & 0.89 & 0.86 \\ 0.89 & 1.0 & 0.75 \\ 0.86 & 0.75 & 1.0 \end{pmatrix}$$

When considering only the uncertainties which are allowed to decrease in the combination (i.e. *not* QED and PDF), we find that the MET measurement has negligible weight. We therefore only retain  $p_{\tau}^e$  and  $m_{\tau}$  for the combination.

The combined result is:

$$\begin{aligned} M_W &= 80.367 \pm 0.013 \text{ (stat)} \pm 0.022 \text{ (syst)} \text{ GeV} \\ &= 80.367 \pm 0.026 \text{ GeV.} \end{aligned}$$

The probability to observe a larger spread between the three measurements than in the data is 5 %.

We further combine with our earlier Run II result ( $1 \text{ fb}^{-1}$ ) to obtain the new D0 Run II result:

$$\begin{aligned} M_W &= 80.375 \pm 0.011 \text{ (stat)} \pm 0.020 \text{ (syst)} \text{ GeV} \\ &= 80.375 \pm 0.023 \text{ GeV.} \end{aligned}$$

# PDF uncertainties

## In principle:

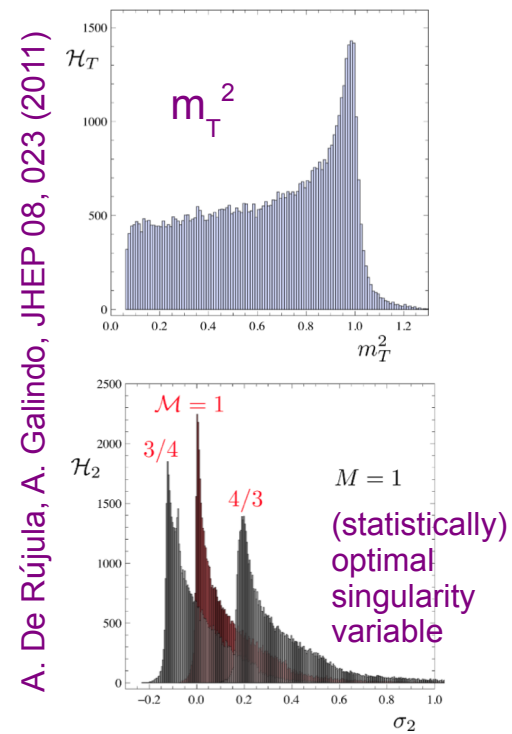
transverse observables (e.g.  $m_T$ ) are insensitive to the uncertainties in the (longitudinal) parton distribution functions (PDFs)

## In practice:

the uncertainties are to some extent reintroduced via the limited  $\eta$  coverage of experiments, which are not invariant under longitudinal boosts

## How to reduce the impact of the PDF uncertainties in measurements of the W boson mass ?

- Reduce the uncertainties in the PDFs  
e.g. via measurements of the W charge asymmetry at the Tevatron and the LHC (complementarity of the two colliders)
- Reduce the impact of the PDF uncertainties on W boson mass  
by extending the  $\eta$  coverage as much as possible  
(challenging: understanding lepton energy scale and pile-up and backgrounds in the forward detectors)
- Possibly reduce the impact of the PDF uncertainties on W boson mass  
by exploring even more robust observables  
("single out events with small longitudinal momentum") to replace/complement  $m_T$



These three approaches are not mutually exclusive, *i.e.* they can be pursued at the same time and gains should “add up”.

# Future PDF sets

Our theory friends are also active on improvements to PDF sets.

An example:

MSUHEP-100707, SMU-HEP-10-10, arXiv:1007.2241[hep-ph]

## New parton distributions for collider physics

Hung-Liang Lai,<sup>1,2</sup> Marco Guzzi,<sup>3</sup> Joey Huston,<sup>1</sup> Zhao Li,<sup>1</sup> Pavel M. Nadolsky,<sup>3</sup> Jon Pumplin,<sup>1</sup> and C.-P. Yuan<sup>1</sup>

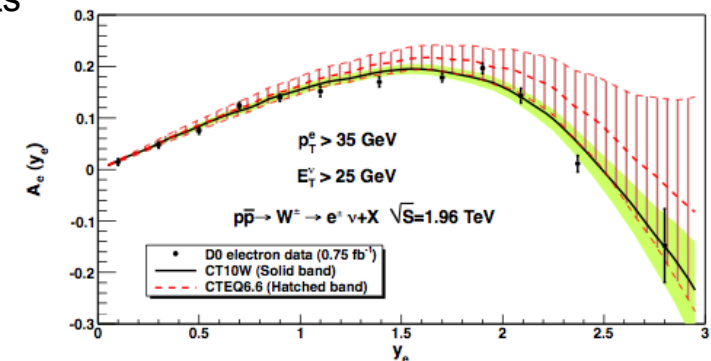
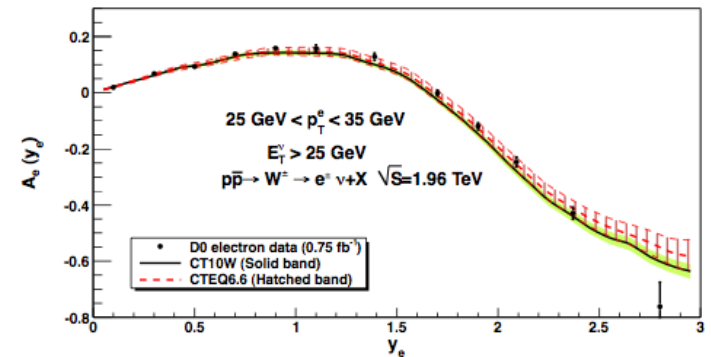
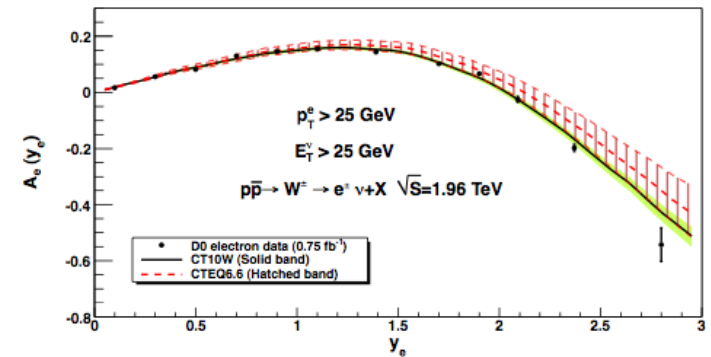
<sup>1</sup>*Department of Physics and Astronomy,  
Michigan State University, East Lansing, MI 48824-1116, U.S.A.*

<sup>2</sup>*Taipei Municipal University of Education, Taipei, Taiwan*

<sup>3</sup>*Department of Physics, Southern Methodist University, Dallas, TX 75275-0175, U.S.A.*

The PDF set “CT10W” is an important step towards including new results on W (lepton) charge asymmetry from the Tevatron into PDF sets. Critical to further constrain the u/d ratio !

Not quite “production quality” yet, but this is going into the right direction.





# Global electroweak fit

Sept 12 version of Gfitter standard model fit includes, in addition to the latest theory calculations, the LEP/SLD precision legacy, ..., various updates:

- latest top quark combination from Tevatron,
- latest world average W boson mass,
- measurements of the “Higgs boson mass” from the LHC.

Parameter	Input value	Free in fit	Fit result incl. $M_H$	Fit result not incl. $M_H$	Fit result incl. $M_H$ but not exp. input in row
$M_H$ [GeV] <sup>(o)</sup>	$125.7 \pm 0.4$	yes	$125.7 \pm 0.4$	$94^{+25}_{-22}$	$94^{+25}_{-22}$
$M_W$ [GeV]	$80.385 \pm 0.015$	–	$80.367 \pm 0.007$	$80.380 \pm 0.012$	$80.359 \pm 0.011$
$\Gamma_W$ [GeV]	$2.085 \pm 0.042$	–	$2.091 \pm 0.001$	$2.092 \pm 0.001$	$2.091 \pm 0.001$
$M_Z$ [GeV]	$91.1875 \pm 0.0021$	yes	$91.1878 \pm 0.0021$	$91.1874 \pm 0.0021$	$91.1983 \pm 0.0116$
$\Gamma_Z$ [GeV]	$2.4952 \pm 0.0023$	–	$2.4954 \pm 0.0014$	$2.4958 \pm 0.0015$	$2.4951 \pm 0.0017$
$\sigma_{\text{had}}^0$ [nb]	$41.540 \pm 0.037$	–	$41.479 \pm 0.014$	$41.478 \pm 0.014$	$41.470 \pm 0.015$
$R_\ell^0$	$20.767 \pm 0.025$	–	$20.740 \pm 0.017$	$20.743 \pm 0.018$	$20.716 \pm 0.026$
$A_{\text{FB}}^{0,\ell}$	$0.0171 \pm 0.0010$	–	$0.01627 \pm 0.0002$	$0.01637 \pm 0.0002$	$0.01624 \pm 0.0002$
$A_\ell$ (*)	$0.1499 \pm 0.0018$	–	$0.1473^{+0.0006}_{-0.0008}$	$0.1477 \pm 0.0009$	$0.1468 \pm 0.0005^{(\dagger)}$
$\sin^2\theta_{\text{eff}}^\ell(Q_{\text{FB}})$	$0.2324 \pm 0.0012$	–	$0.23148^{+0.00011}_{-0.00007}$	$0.23143^{+0.00010}_{-0.00012}$	$0.23150 \pm 0.00009$
$A_c$	$0.670 \pm 0.027$	–	$0.6680^{+0.00025}_{-0.00038}$	$0.6682^{+0.00042}_{-0.00035}$	$0.6680 \pm 0.00031$
$A_b$	$0.923 \pm 0.020$	–	$0.93464^{+0.00004}_{-0.00007}$	$0.93468 \pm 0.00008$	$0.93463 \pm 0.00006$
$A_{\text{FB}}^{0,c}$	$0.0707 \pm 0.0035$	–	$0.0739^{+0.0003}_{-0.0005}$	$0.0740 \pm 0.0005$	$0.0738 \pm 0.0004$
$A_{\text{FB}}^{0,b}$	$0.0992 \pm 0.0016$	–	$0.1032^{+0.0004}_{-0.0006}$	$0.1036 \pm 0.0007$	$0.1034 \pm 0.0004$
$R_c^0$	$0.1721 \pm 0.0030$	–	$0.17223 \pm 0.00006$	$0.17223 \pm 0.00006$	$0.17223 \pm 0.00006$
$R_b^0$	$0.21629 \pm 0.00066$	–	$0.21474 \pm 0.00003$	$0.21475 \pm 0.00003$	$0.21473 \pm 0.00003$
$\bar{m}_c$ [GeV]	$1.27^{+0.07}_{-0.11}$	yes	$1.27^{+0.07}_{-0.11}$	$1.27^{+0.07}_{-0.11}$	–
$\bar{m}_b$ [GeV]	$4.20^{+0.17}_{-0.07}$	yes	$4.20^{+0.17}_{-0.07}$	$4.20^{+0.17}_{-0.07}$	–
$m_t$ [GeV]	$173.18 \pm 0.94$	yes	$173.52 \pm 0.88$	$173.14 \pm 0.93$	$175.8^{+2.7}_{-2.4}$
$\Delta\alpha_{\text{had}}^{(5)}(M_Z^2)$ ( $\Delta\nabla$ )	$2757 \pm 10$	yes	$2755 \pm 11$	$2757 \pm 11$	$2716^{+49}_{-43}$
$\alpha_s(M_Z^2)$	–	yes	$0.1191 \pm 0.0028$	$0.1192 \pm 0.0028$	$0.1191 \pm 0.0028$
$\delta_{\text{th}} M_W$ [MeV]	$[-4, 4]_{\text{theo}}$	yes	4	4	–
$\delta_{\text{th}} \sin^2\theta_{\text{eff}}^\ell$ ( $\Delta$ )	$[-4.7, 4.7]_{\text{theo}}$	yes	–1.4	4.7	–

<sup>(o)</sup> Average of ATLAS ( $M_H = 126.0 \pm 0.4$  (stat)  $\pm 0.4$  (sys)) and CMS ( $M_H = 125.3 \pm 0.4$  (stat)  $\pm 0.5$  (sys)) measurements assuming no correlation of the systematic uncertainties (see discussion in Sect. 2). <sup>(\*)</sup> Average of LEP ( $A_\ell = 0.1465 \pm 0.0033$ ) and SLD ( $A_\ell = 0.1513 \pm 0.0021$ ) measurements, used as two measurements in the fit.

<sup>(†)</sup> The fit w/o the LEP (SLD) measurement gives  $A_\ell = 0.1474^{+0.0005}_{-0.0009}$  ( $A_\ell = 0.1467^{+0.0006}_{-0.0004}$ ).

<sup>(Δ)</sup> In units of  $10^{-5}$ . <sup>(∇)</sup> Rescaled due to  $\alpha_s$  dependency.

# Global electroweak fit

Complete fit:

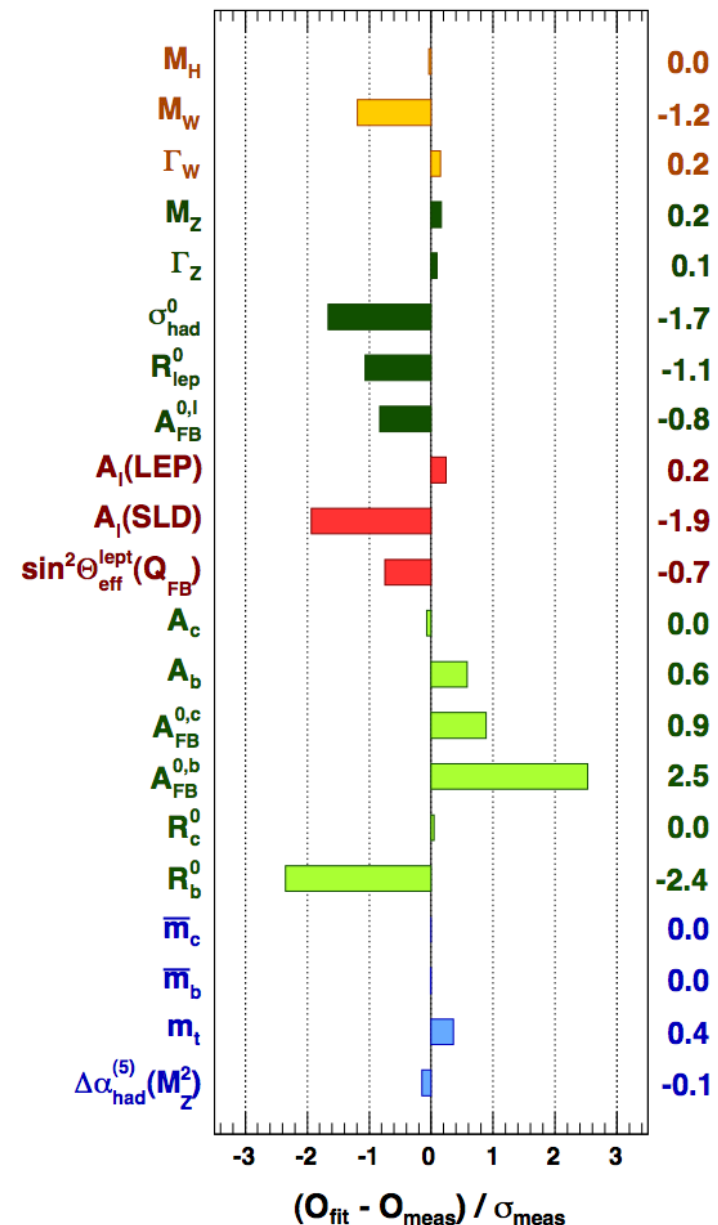
$\chi^2_{\min} = 21.8$  for 14 degrees of freedom.

Pull values for the different observables are shown on the right.

- no value exceeds 3 sigma
- largest individual contribution to  $\chi^2$  from FB asymmetry of bottom quarks.

Overall good agreement between precision data and standard model.

As is well known, some tension between  $A_l(\text{SLD})$  and  $A_{\text{FB}}^{0,b}$  from LEP.



# Global electroweak fit

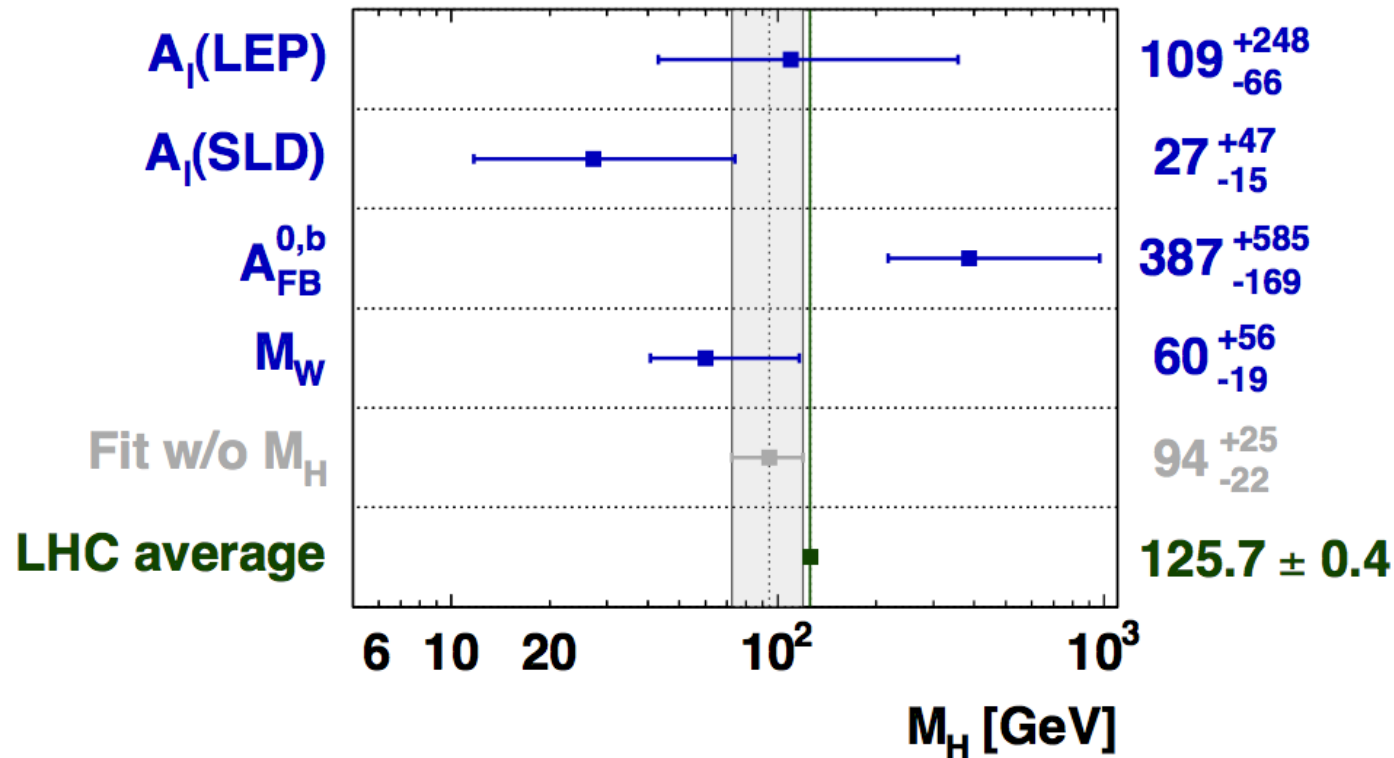


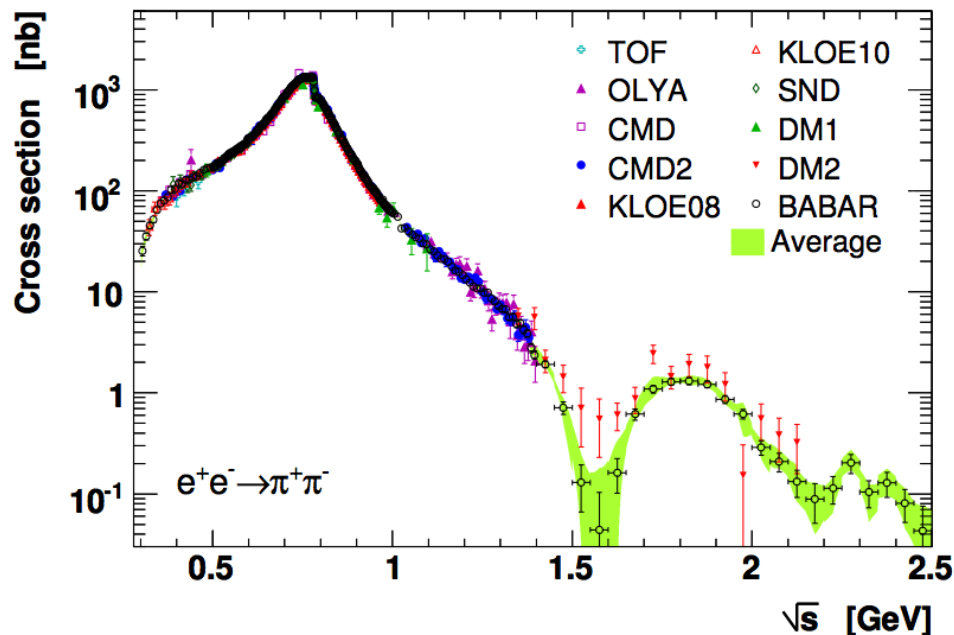
Figure 2: Left: pull comparison of the fit results with the direct measurements in units of the experimental uncertainty. Right: determination of  $M_H$  excluding the direct  $M_H$  measurements and all the sensitive observables from the fit, except the one given. Note that the fit results shown are not independent.

# Hadronic contributions to $\alpha(M_Z^2)$

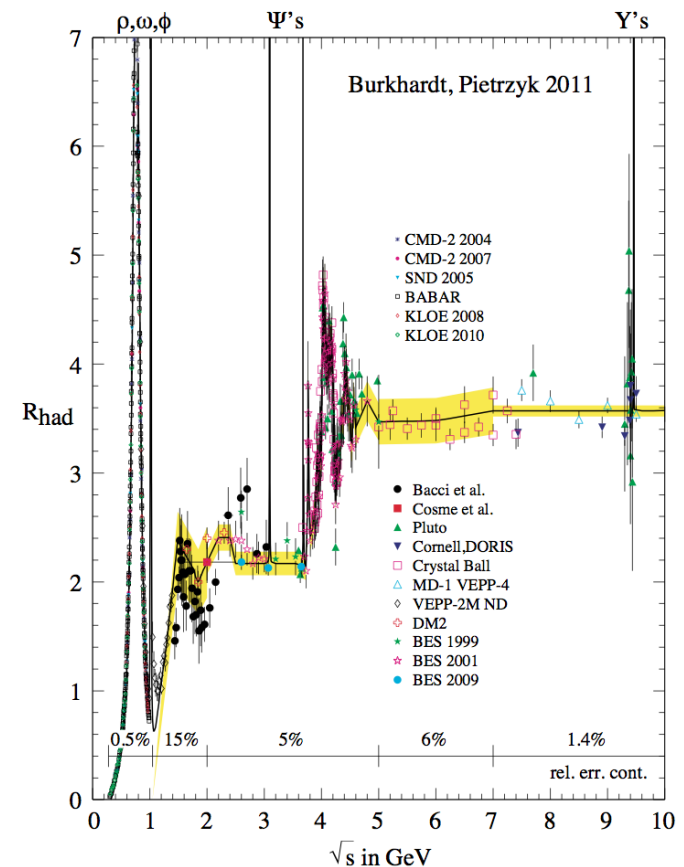
Electroweak fit requires the knowledge of the **electromagnetic coupling strength at the Z mass scale** to an accuracy of 1% or better.

**Hadronic contribution for quarks with masses smaller than  $M_Z$**  cannot be obtained from perturbative QCD alone (low energy scale).

Constrain photon vacuum polarisation function using measured total cross section for  **$e^+e^-$  annihilation to hadrons** above the two-pion threshold.

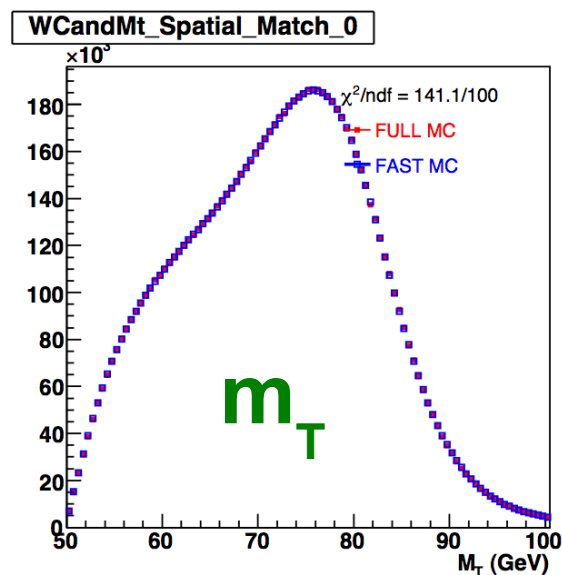


Davier *et al.*, Eur. Phys. J. C71, 1515 (2011)

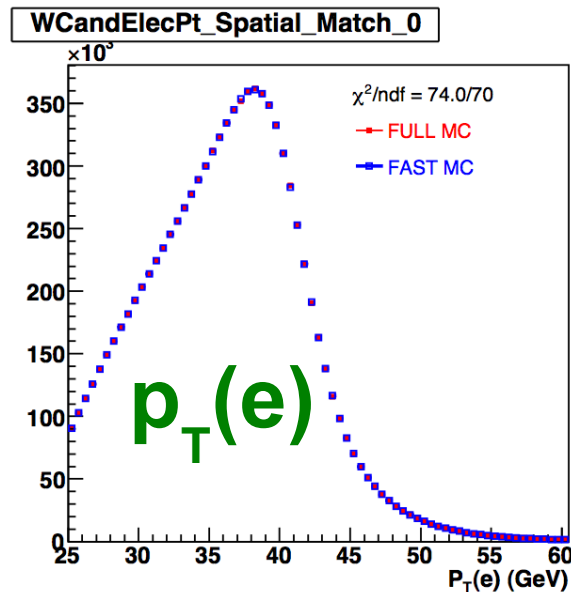
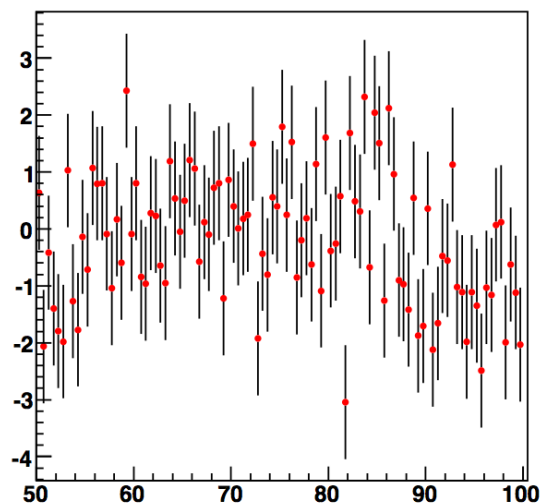


Burkhardt and Pietrzyk, Phys. Rev. D 84, 037502 (2011)

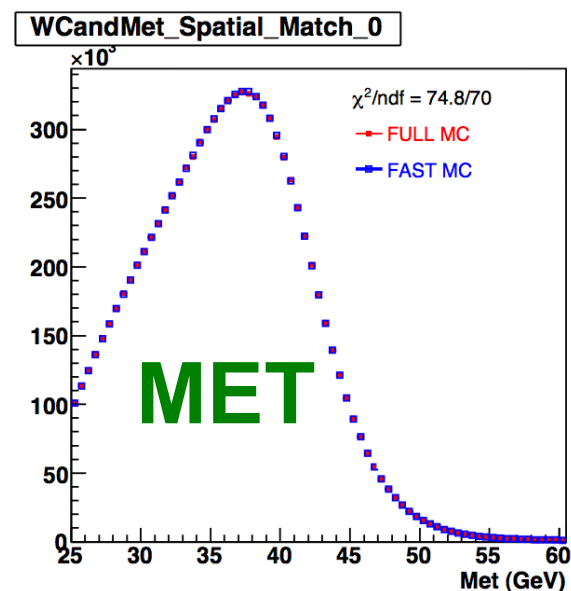
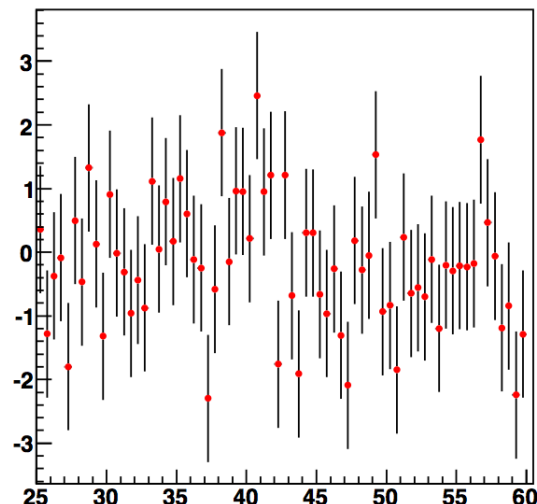
# MC closure test



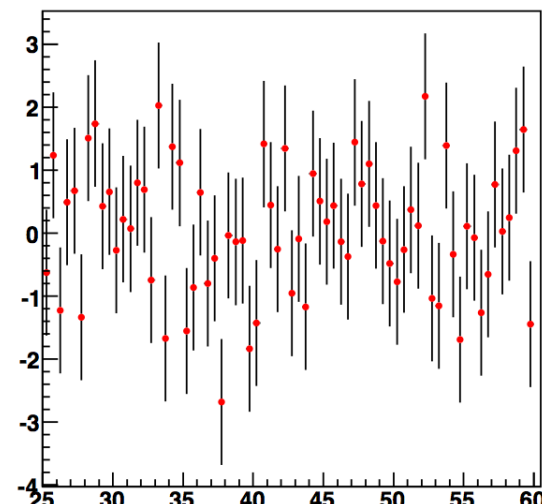
$\chi$  distribution with overall  $\chi^2 = 141.1$  for 100 bins



$\chi$  distribution with overall  $\chi^2 = 74.0$  for 70 bins

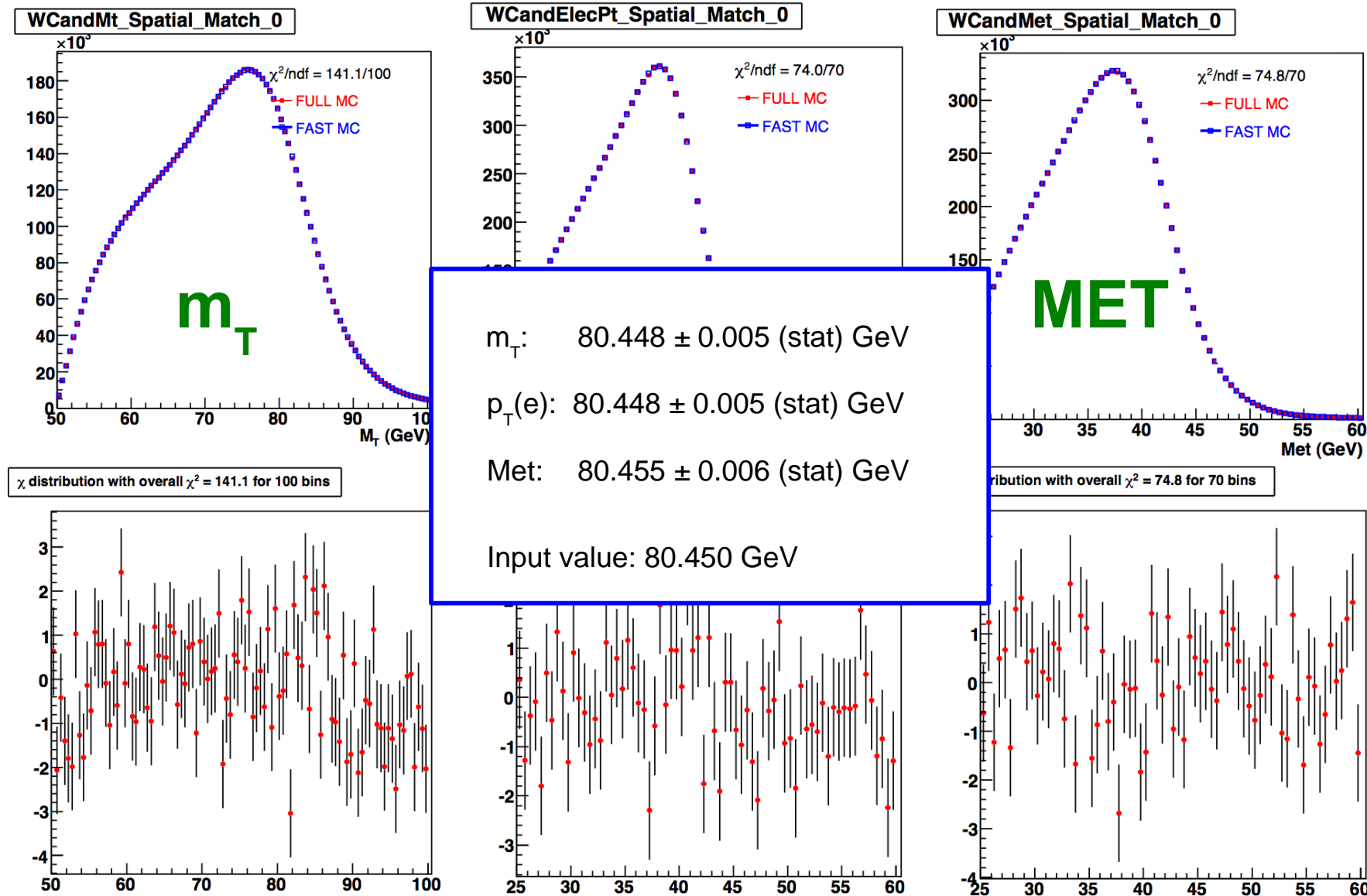


$\chi$  distribution with overall  $\chi^2 = 74.8$  for 70 bins



Very good agreement between fast and full MC.  
Fitted W mass within one sigma of generated mass for all three observables.

# MC closure test



Very good agreement between fast and full MC.  
Fitted W mass within one sigma of generated mass for all three observables.

Full MC  $W \rightarrow e \nu$  62M events simulated, 9.8M events after selection



# Definition of $f_Z$

To determine  $\alpha$  and  $\beta$  we use the following strategy. Suppose  $R_{EM}(E_0) = \alpha' E_0 + \beta'$ , then:

$$M(Z) = \sqrt{2E(e_1)E(e_2)(1 - \cos \omega)} \Rightarrow M(Z) \simeq \alpha' \times M_{true}(Z) + f_Z \beta' + \mathcal{O}(\beta'^2)$$

where

$$f_Z(true) = \frac{(E_0(e_1) + E_0(e_2))(1 - \cos \omega)}{M_{true}(Z)}$$

Inspired by this observation, we fit templates of  $m_{ee} \times f_Z$  for varying  $\alpha$  and  $\beta$  against our  $Z$  sample.

# Electron energy resolution

Electron energy resolution is driven by two components:

sampling fluctuations and constant term

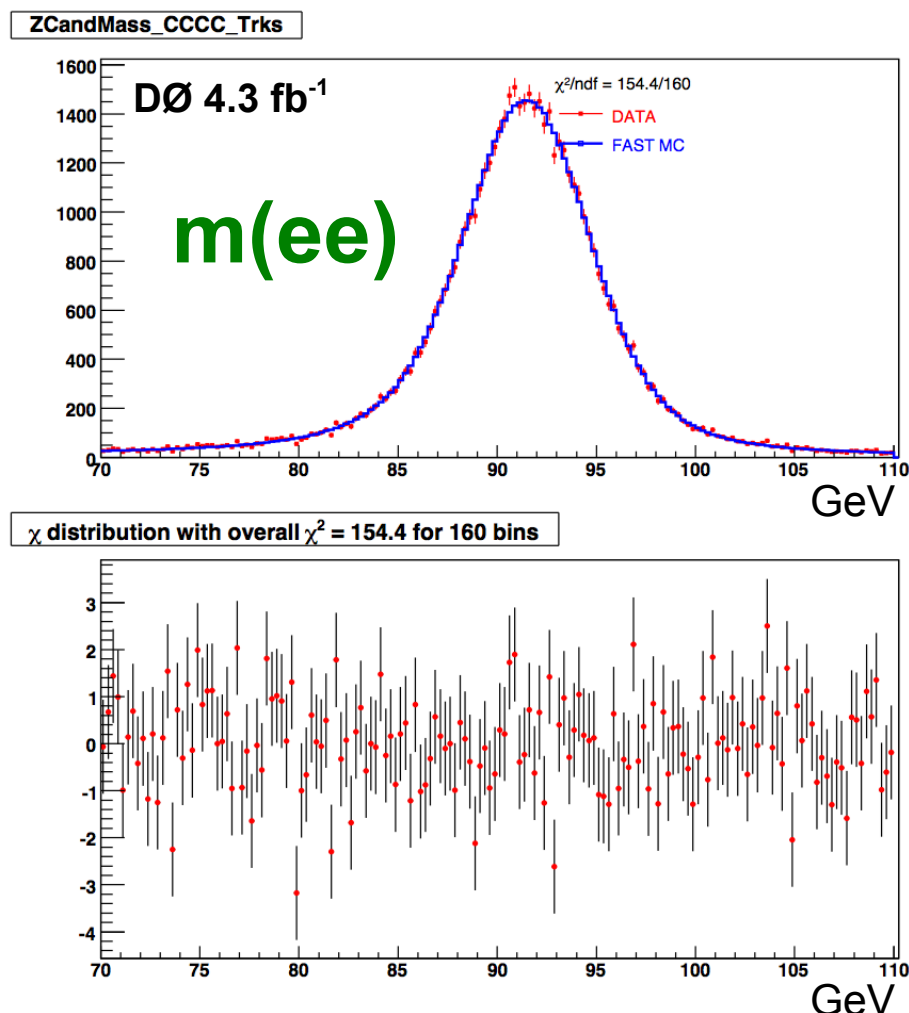
**Sampling fluctuations** are driven by sampling fraction of CAL modules (well known from simulation and testbeam) and by uninstrumented material. As discussed before, amount of material has been quantified with good precision.

**Constant term** is extracted from  $Z \rightarrow e e$  data (essentially fit to observed width of Z peak).

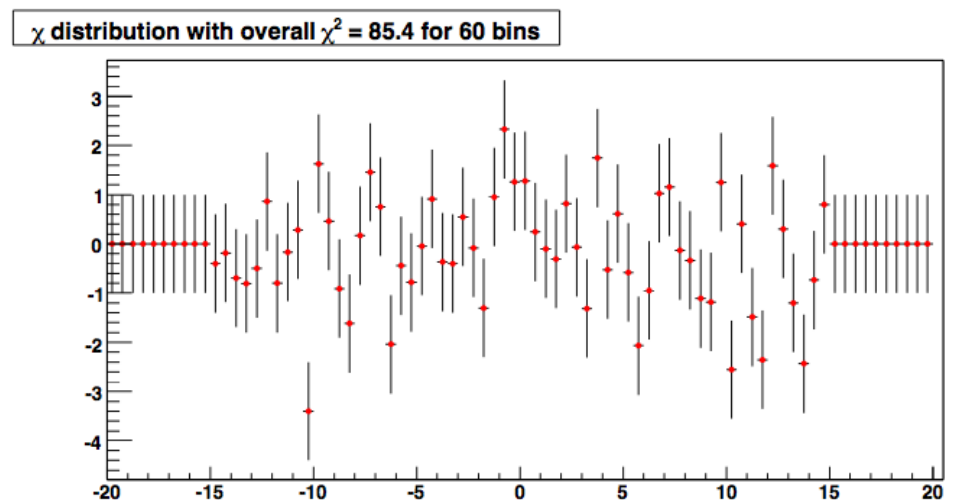
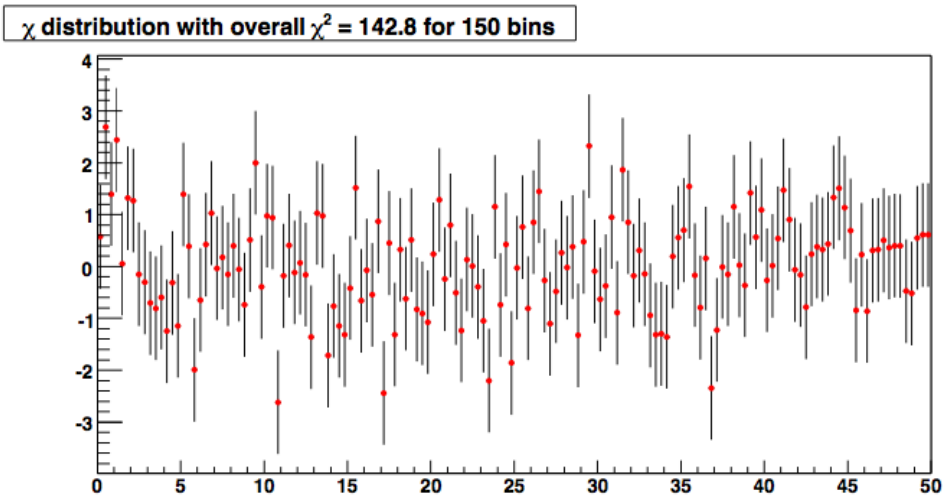
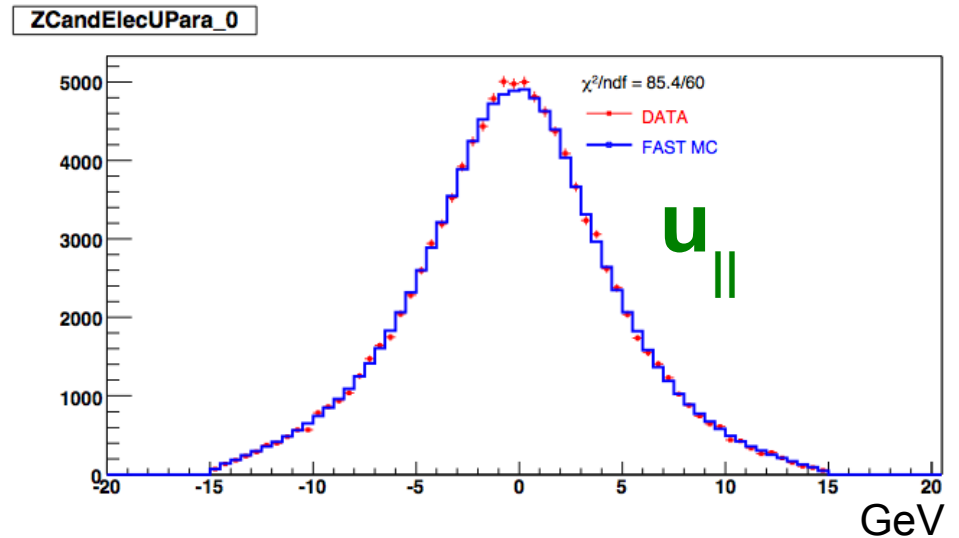
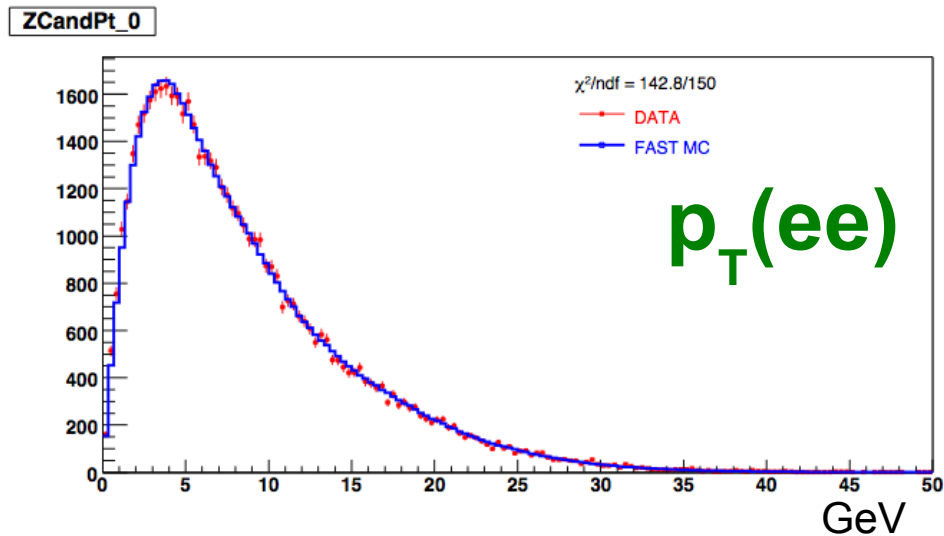
**Result:**

$$C = (2.00 \pm 0.07) \%$$

in excellent agreement with Run II design goal (2%)



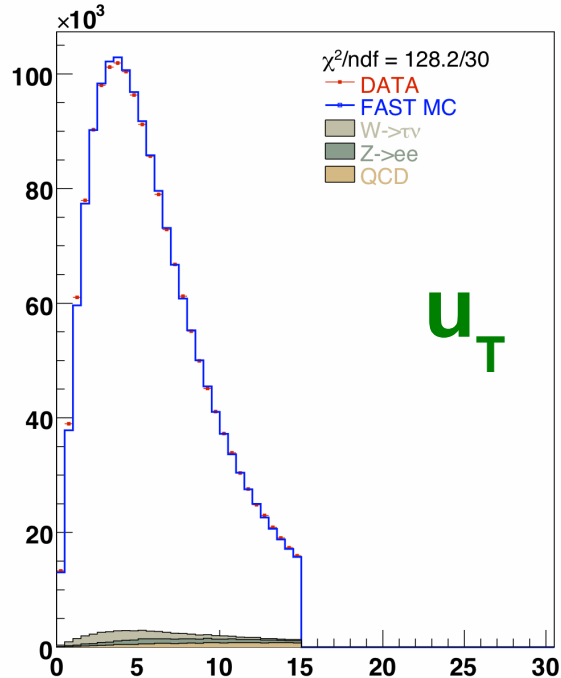
# Z data



Good agreement between data and parameterised Monte Carlo.

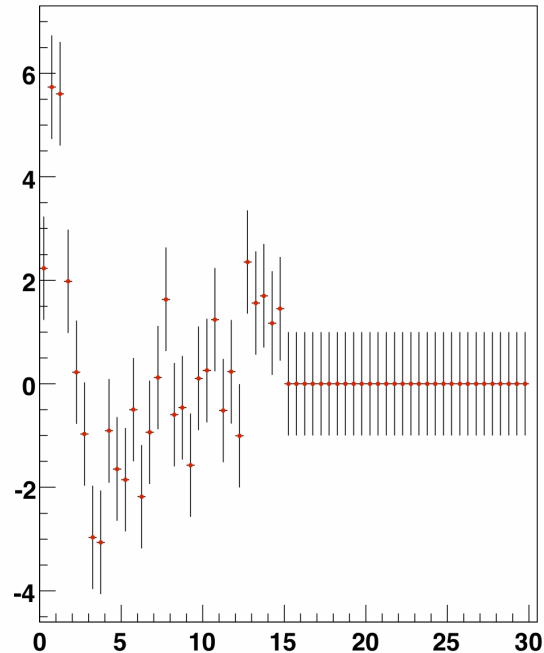
# W data

WCandRecoilPt\_Spatial\_Match\_0

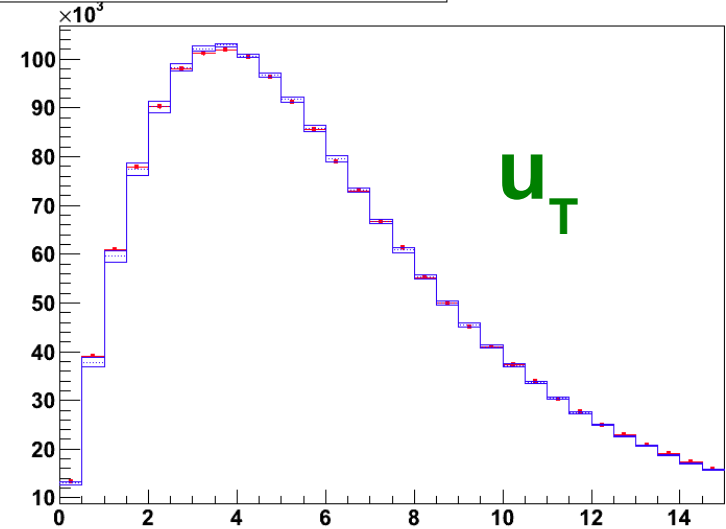


Here the error bars only reflect the finite statistics of the  $W$  candidate sample.

$\chi$  distribution with overall  $\chi^2 = 128.2$  for 30 bins



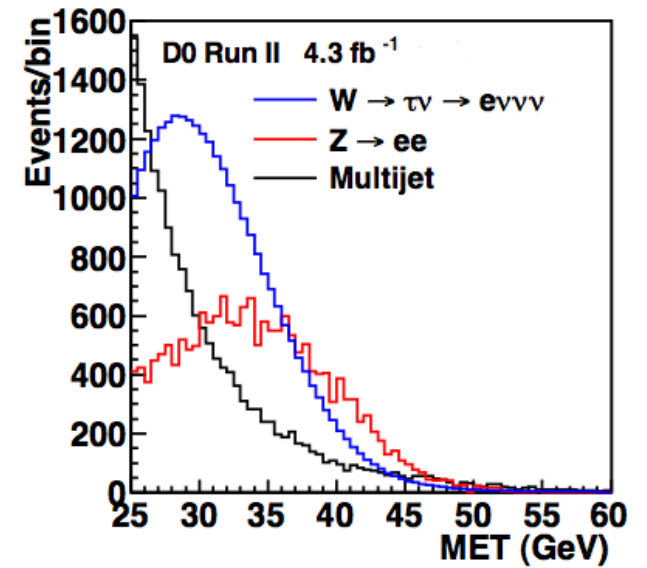
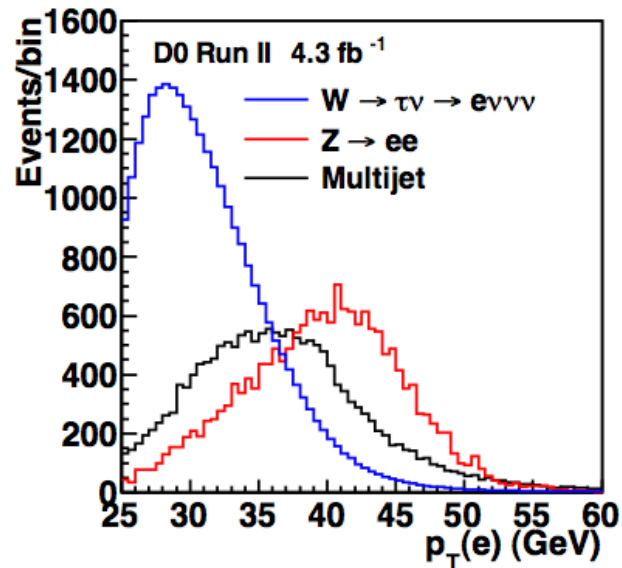
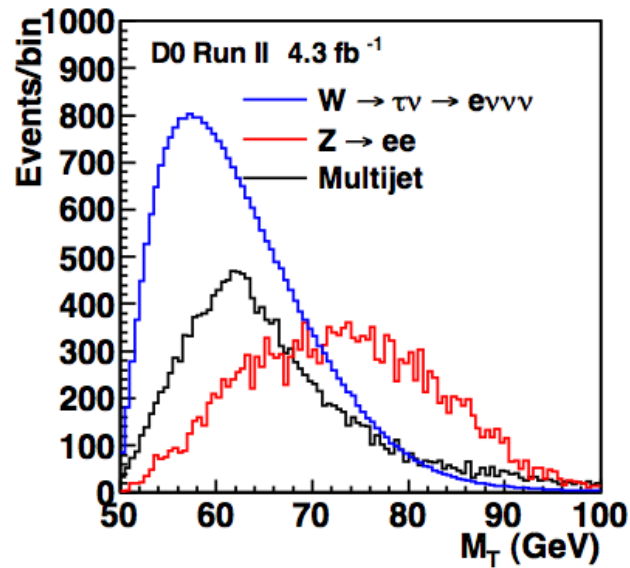
WCandRecoilPt\_Spatial\_Match\_0



These are the same  $W$  candidates in the data. The blue band represents the uncertainties in the fast MC prediction due to the uncertainties in the recoil tune from the finite  $Z$  statistics.

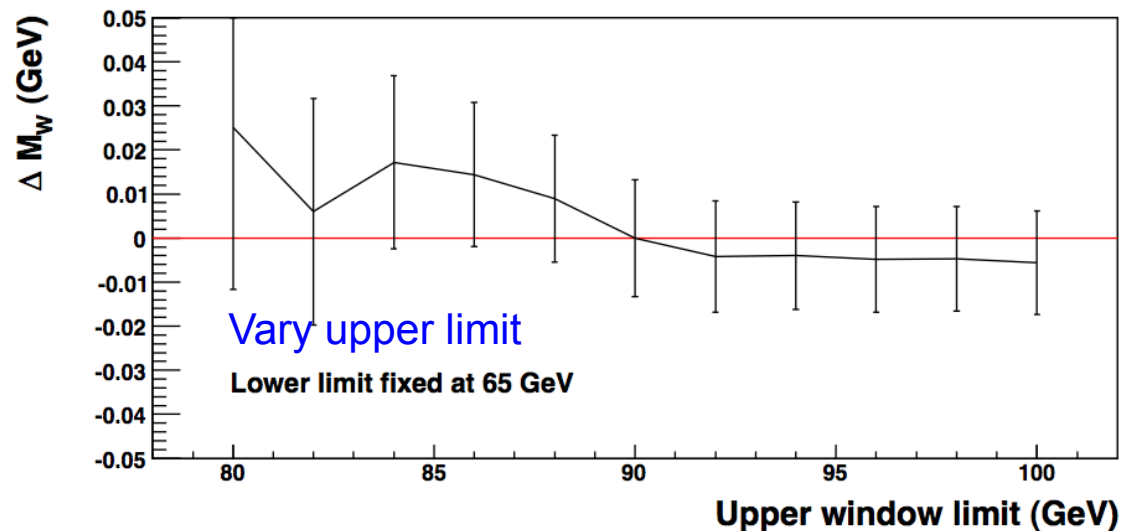
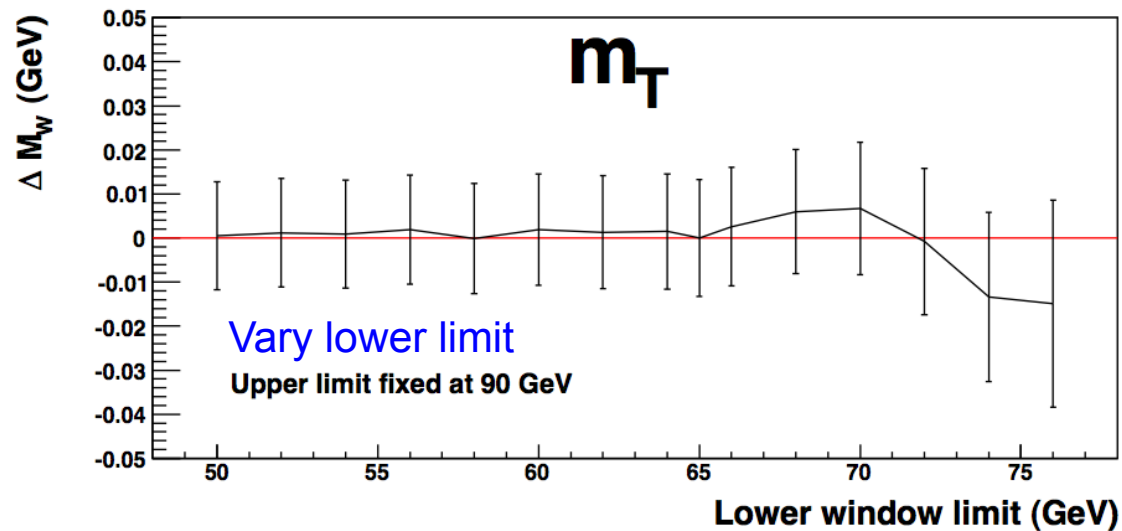
Good agreement between data and parameterised Monte Carlo.

# Backgrounds



# Consistency checks

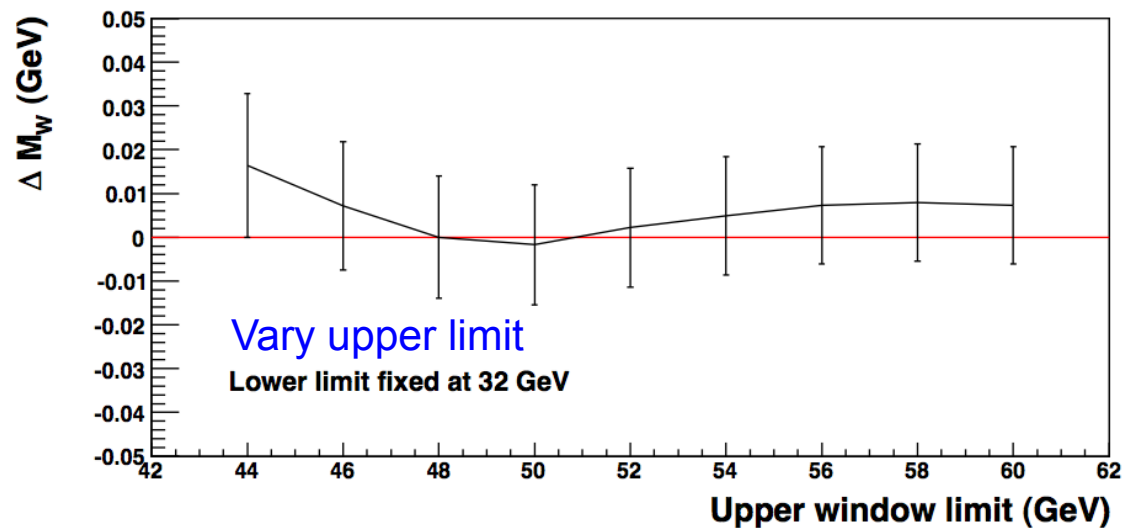
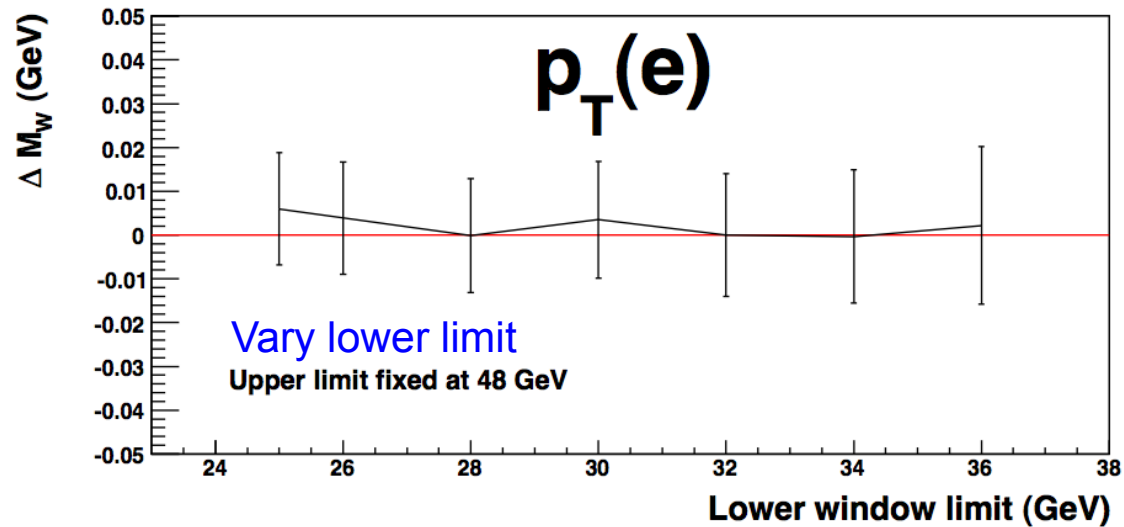
Vary the range used in the  $m_T$  fit:



Measurement is stable

# Consistency checks

Vary the range used in the  $p_T(e)$  fit:

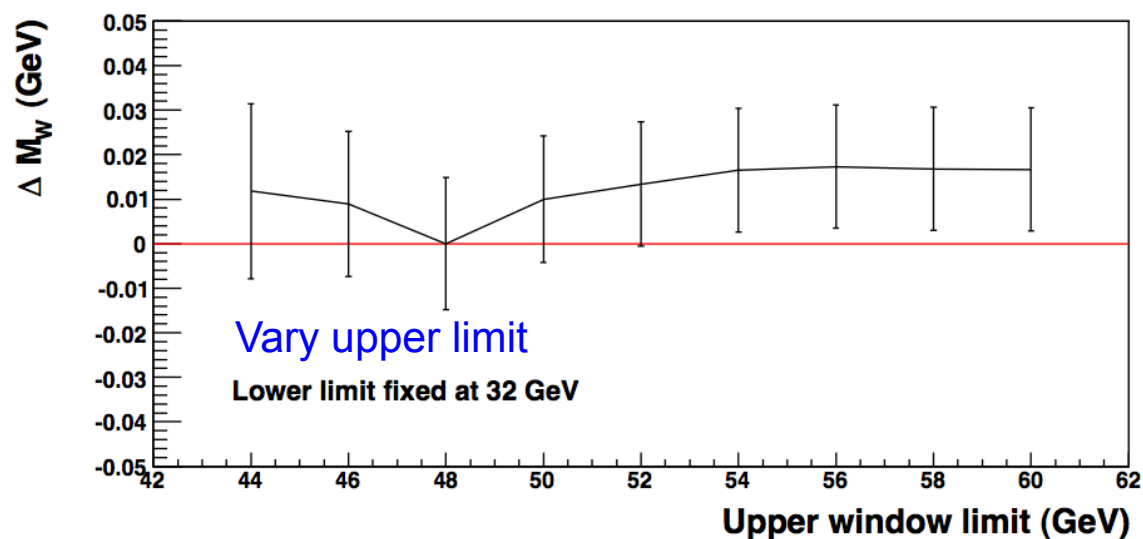
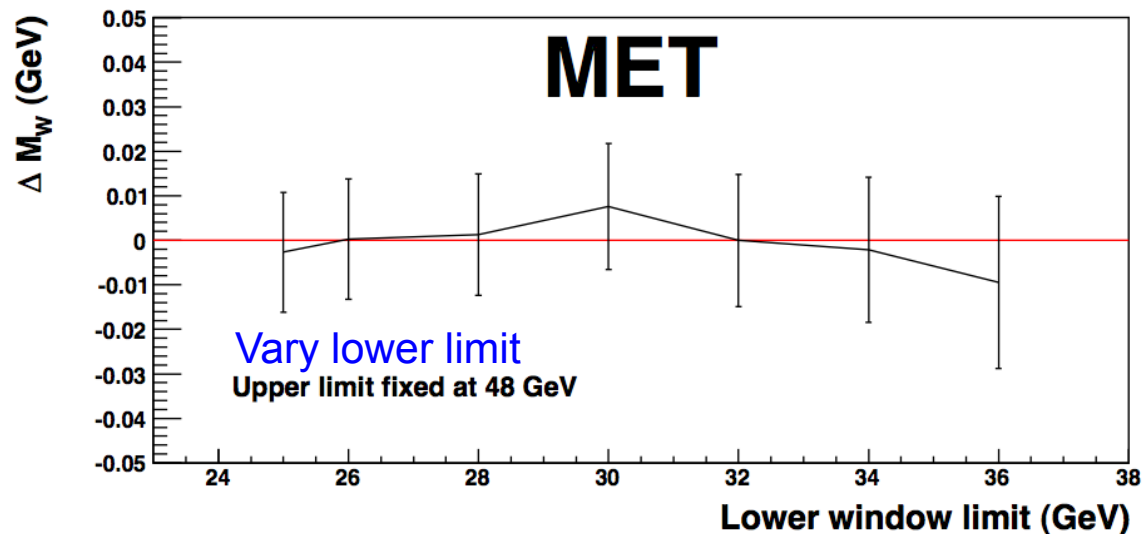


Measurement is stable



# Consistency checks

Vary the range used in the MET fit:

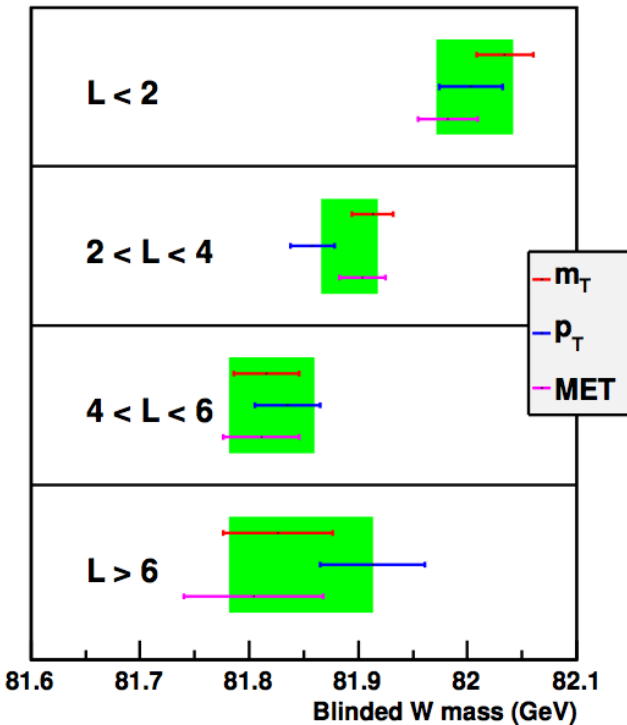


Measurement is stable

# Consistency checks

Split data sample into four bins of instantaneous luminosity and measure W mass separately for each bin:

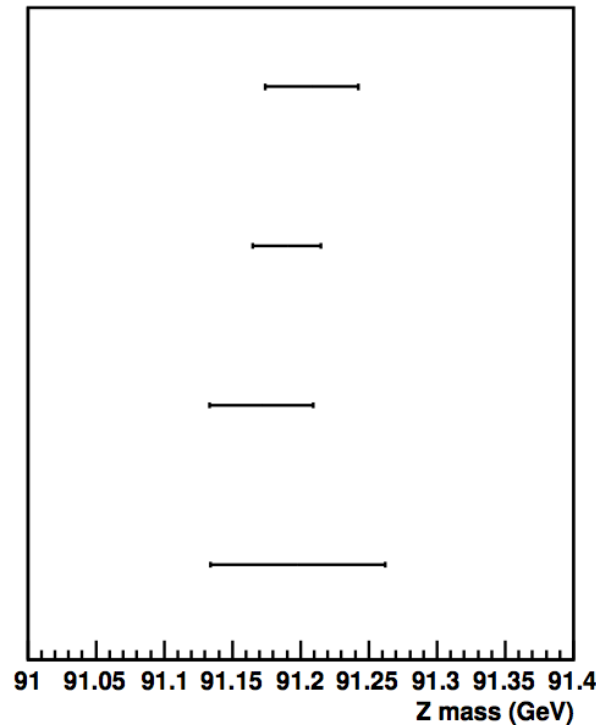
**W**



Error bars represent W statistics.

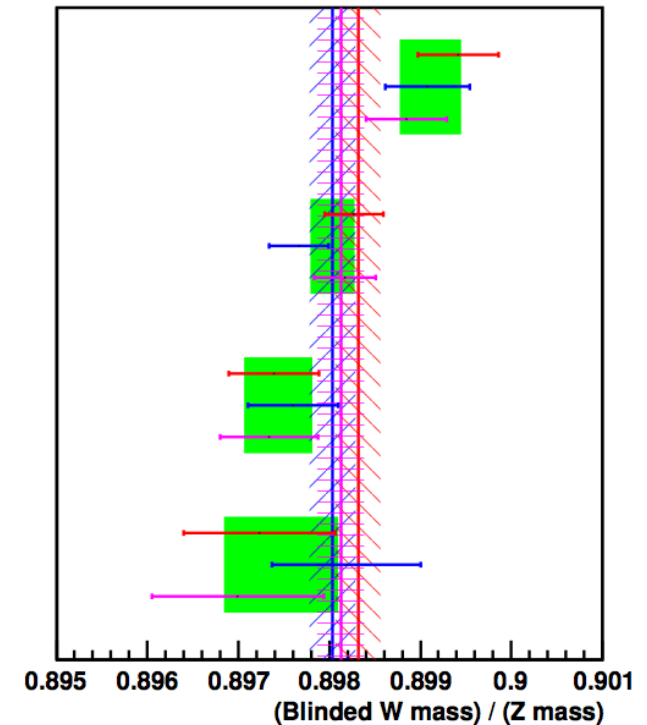
Green bands represent EM scale uncertainty (100 % correlated for  $m_T$ ,  $p_T$  and MET).

**Z**



Sorry, still using blinded mass in these plots.  
But it does not matter here ...  
differences between observables and subsamples  
are preserved by the blinding.

**“W/Z”**



Error bars represent W and Z statistics.

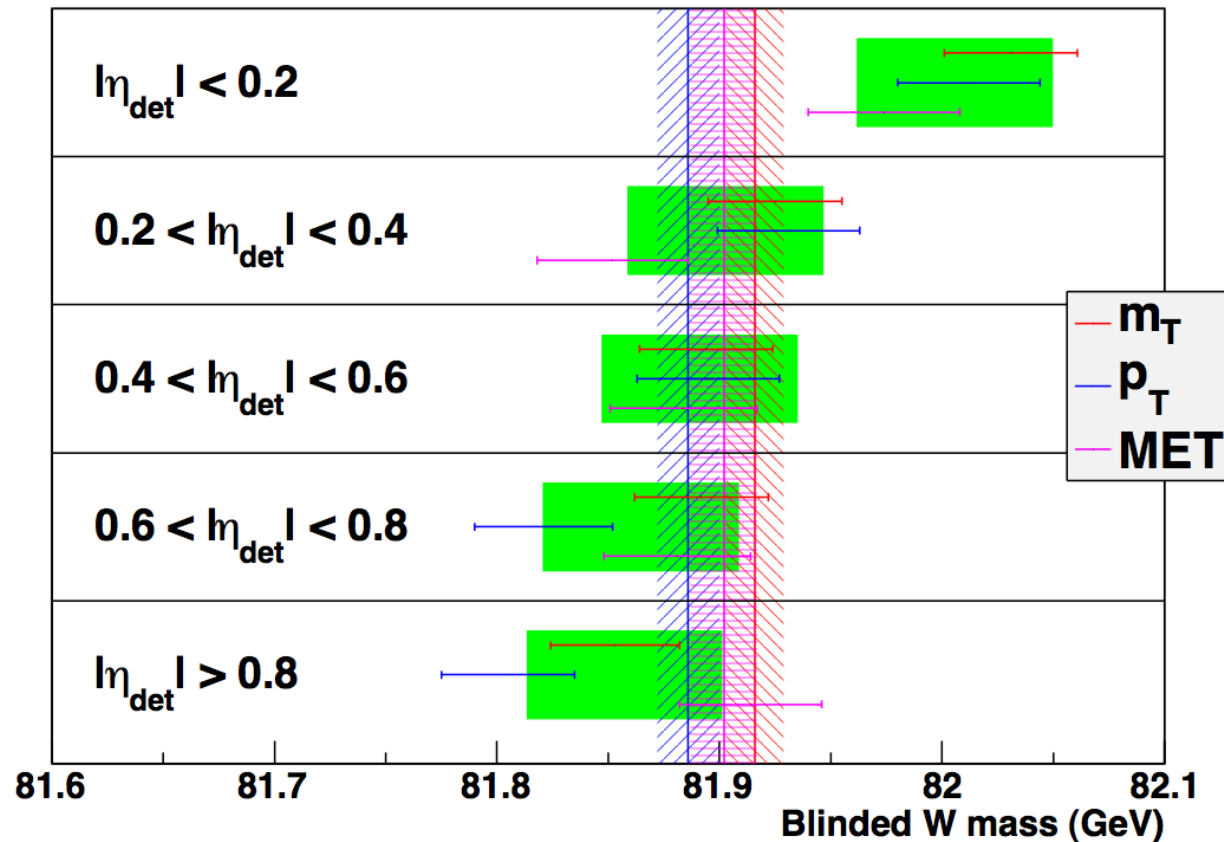
Green bands represent contribution from Z alone (100 % correlated for  $m_T$ ,  $p_T$  and MET).

Mass ratio is stable with lumi.

# Consistency checks

Split data sample into five bins of detector eta and measure W mass separately for each bin:

**W**



Error bars represent W statistics.

Green bands represent the part of the EM scale uncertainty that is uncorrelated from one eta bin to another (100 % correlated for  $m_T$ ,  $p_T$  and MET).

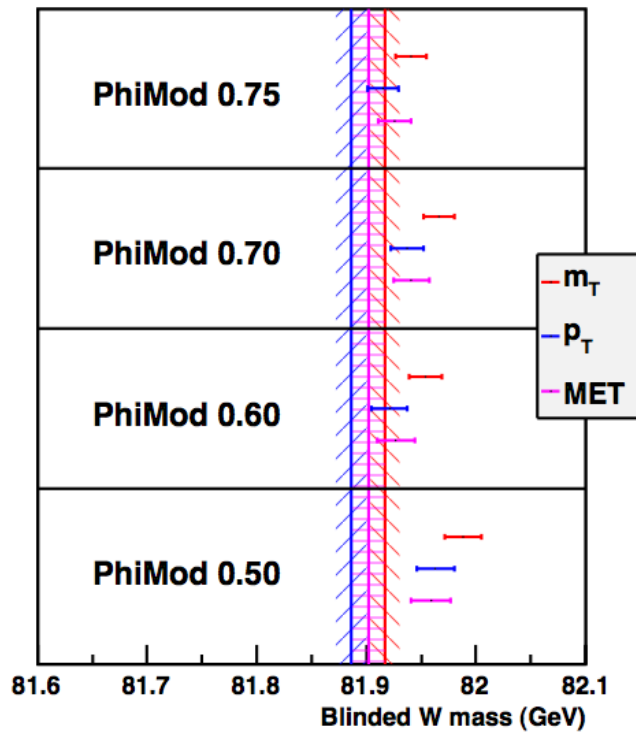
Sorry, still using blinded mass in these plots. But it does not matter here ... differences between observables and subsamples are preserved by the blinding.

Mass is stable with eta.

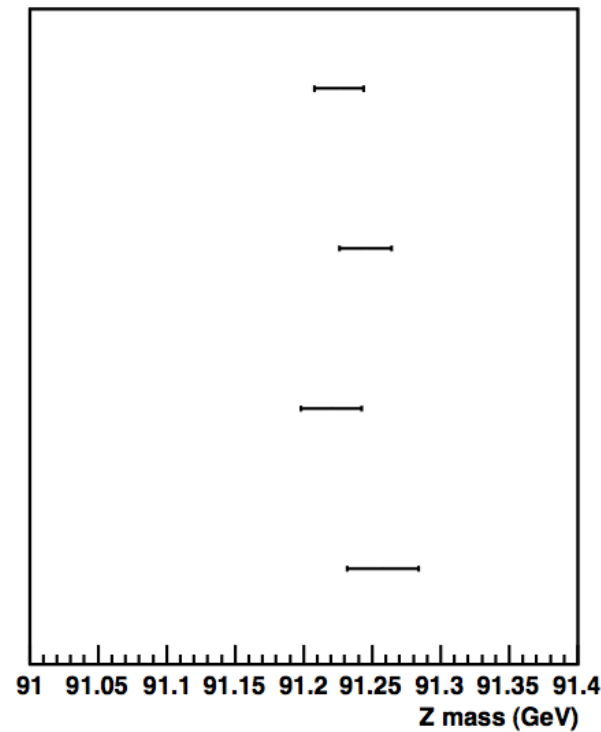
# Consistency checks

Vary phi fiducial cut. In default analysis, keep 80 % of acceptance. Here we test four tighter requirements.

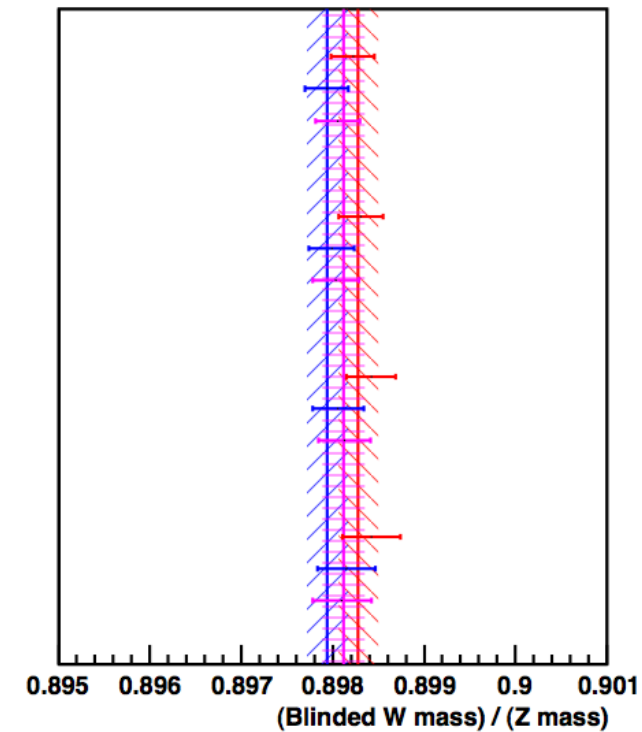
**W**



**Z**



**“W/Z”**



Error bars represent W statistics.

Error bars represent W and Z statistics.

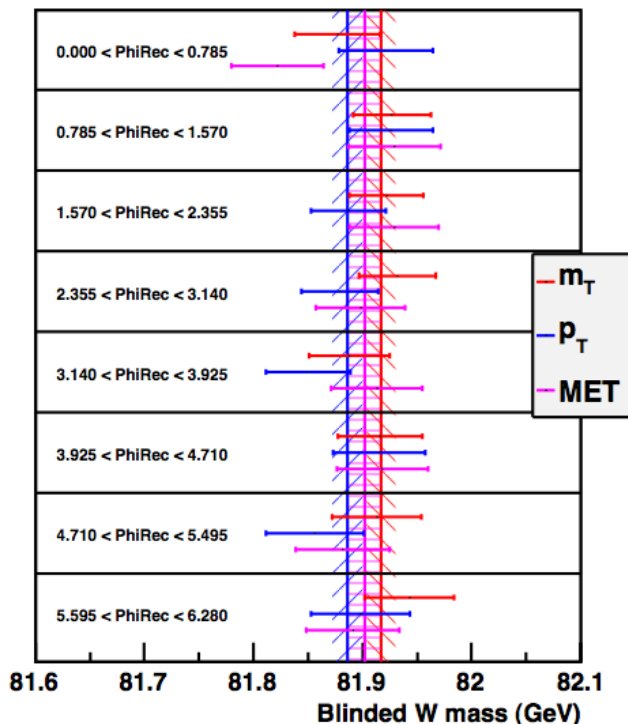
Sorry, still using blinded mass in these plots.  
But it does not matter here ...  
differences between observables and subsamples  
are preserved by the blinding.

Mass ratio is stable with fiducial requirement

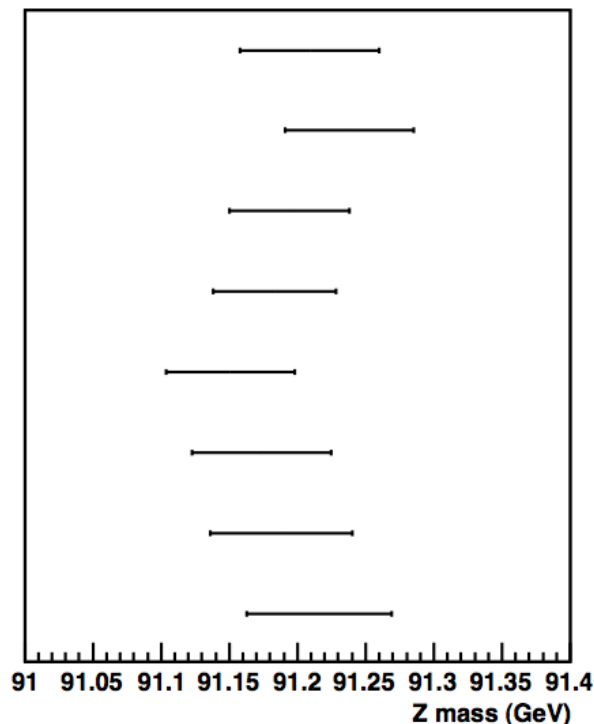
# Consistency checks

Split data sample into eight bins according to the direction in phi of the measured recoil vector, and measure W boson mass separately in each bin.

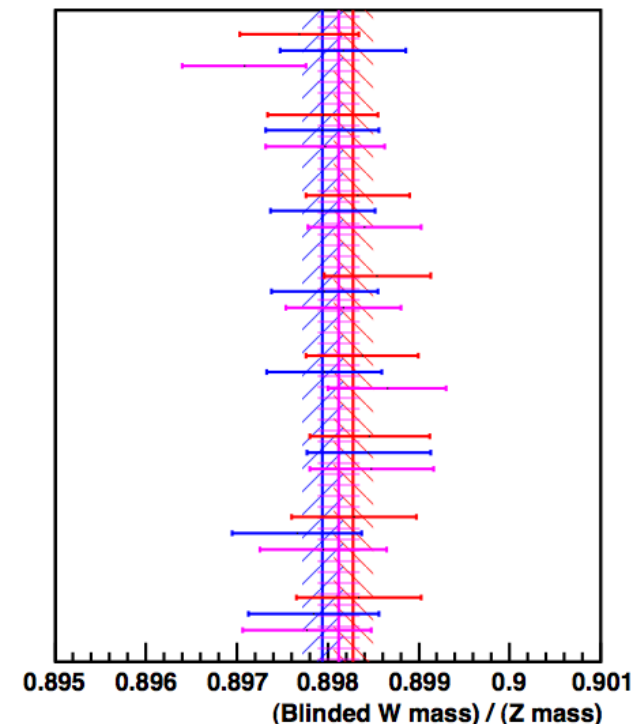
W



Z



“W/Z”



Error bars represent W statistics.

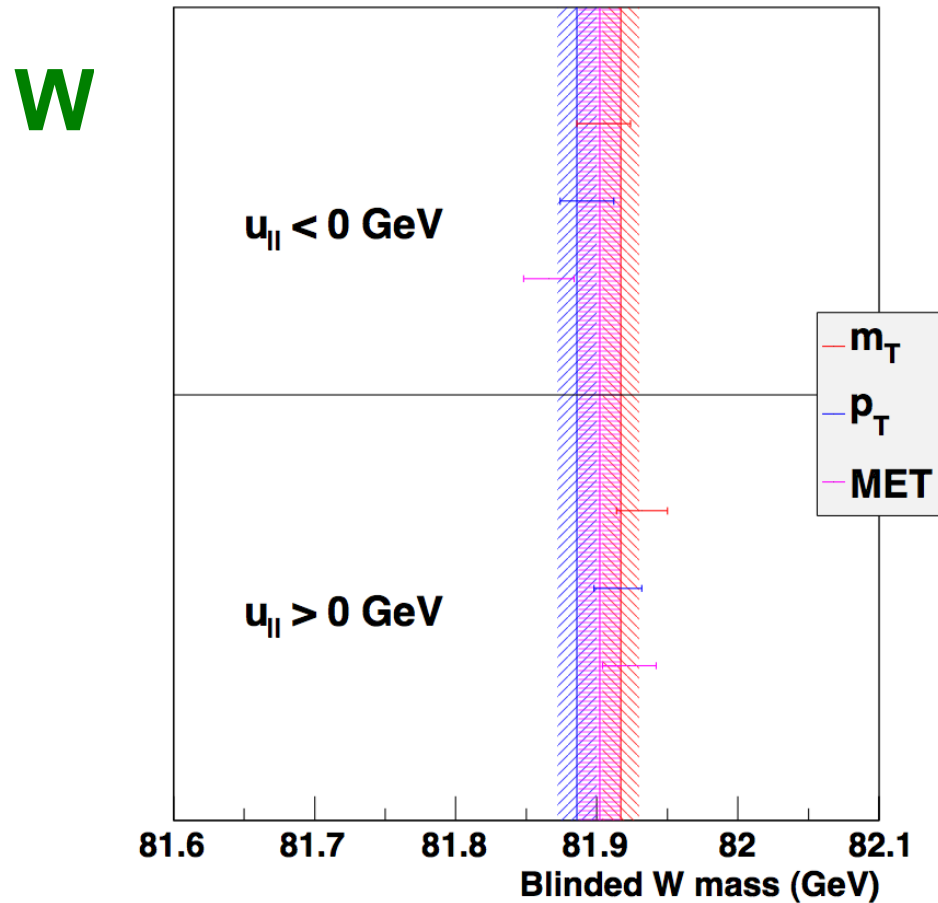
Error bars represent W and Z statistics.

Sorry, still using blinded mass in these plots.  
But it does not matter here ...  
differences between observables and subsamples  
are preserved by the blinding.

Mass ratio is stable with recoil phi.

# Consistency checks

Split data sample into two bins of  $u_{||}$  and measure  $W$  mass separately for each bin:



Error bars represent  $W$  statistics.

Sorry, still using blinded mass in these plots.  
But it does not matter here ...  
differences between observables and subsamples  
are preserved by the blinding.

Mass is stable with  $u_{||}$ .